UNIVERSITY OF OKLAHOMA

GRADUATE COLLEGE

THE LIGAND BINDING PROPERTIES OF THE OXYSTEROL-BINDING PROTEIN FAMILY SUBFAMILY-I

A DISSERTATION

SUBMITTED TO THE GRADUATE FACULTY

in partial fulfillment of the requirements for the

Degree of

DOCTOR OF PHILOSOPHY

By

JUAN IGNACIO VIERA NUÑEZ
Norman, Oklahoma
2018

THE LIGAND BINDING PROPERTIES OF OXYSTEROL-BINDING PROTEIN FAMILY SUBFAMILY-I

A DISSERTATION APPROVED FOR THE
DEPARTMENT OF CHEMISTRY AND BIOCHEMISTRY

BY THE COMMITTEE CONSISTING OF

Dr. Anthony Burgett, Chair

Dr. Helen Zgurskaya

Dr. Christina Bourne

Dr. Robert Cichewicz

Dr. Laura Bartley

Dr. Michael Ihnat

I dedicate this my mom, who raised me and was my first role model.

I dedicated this to my family, especially to my sister and my brother, I keep you in my heart. To my nephew, and future generations, I hope my accomplishments inspire you and allow you to succeed.

Acknowledgments

I want to acknowledge the members of the Burgett Lab who are my friends, colleagues and my second family.

Thank you, Dr. Sims, Dr. Zgurskaya, Dr. Cichewicz, and Dr. Bourne, who allowed me to use instruments in their labs, which let me accomplish my research.

Thank you OU Department of Electronics Shop for helping me keep the scintillation counter alive.

Table of Contents

List of Tables

List of Figures

Abstract

The oxysterol-binding protein/OSBP-related proteins (OSBP/ORPs) are a family of proteins conserved in all eukaryotes that have complex biological activities connected to lipid transport and lipid regulation. OSBP is ubiquitously expressed in tissues and is required in the replication of a broad array of pathogenic Enterovirus species. Alternatively, ORP4L is only expressed in a few select tissues and plays an important role in the proliferation and viability of certain cancers. Although the OSBP/ORPs have been reported to interact with an array of ligands, including various sterols, phospholipid compounds, and natural product compounds, the comprehensive characterization of ligand binding to the OSBP/ORP proteins has not been performed. Additionally, this is the first binding study on human OSBP and ORP4L, an important step for designing ligands for therapeutic targeting of the ORPs. The goal of this research is to characterize the ligand binding of human OSBP and ORP4. We utilized two experimental approaches to understand the small molecule ligand binding ability of OSBP and ORP4L. The first experimental approach was to determine binding affinities of multiple classes of potential ligands for OSBP and ORP4L, which was accomplished through the implementation of a high-throughput ligand binding assay using cloned and expressed human OSBP and ORP4L proteins. Through screening oxysterols for ligand binding, specific sites of oxysterol side chain oxidation were identified as being critical for high-affinity interaction with OSBP and ORP4. Specifically, oxysterols that show high-affinity binding with OSBP and ORP4L have hydroxyls at the C20, C24, C25, C26 or C27 positions, but not at the C22. The importance of the side chain in oxysterol binding was further determined by testing a series of 20-hydroxycholesterol analogs produced in our

lab. The second experimental approach employed was to construct and test a structural model of how OSBP interacts with its small molecule ligands, specifically the natural product compound OSW-1. Using the existing partial OSBP/ORP structures from yeast orthologs, we constructed a model for OSW-1-OSBP interactions. The tentative model was used to identify OSBP potentially critical residues that are essential for OSW-1 binding, and the identified amino acids were selected for mutation. One OSBP point mutant was successfully cloned, expressed and tested for ligand binding. The OSBP H522A mutant negatively affects OSW-1 binding while not affecting oxysterol binding, which supports our interaction model. The results of these projects inform us of how small molecule ligands bind OSBP and ORP4L, and perhaps by analogy the other OSBP/ORPs. These research accomplishments will aid in the design of new generations of OSBP/ORP binding small molecules, including potentially novel anti-cancer and anti-viral compounds for therapeutic development to selectively target only OSBP or only ORP4.

Chapter 1: OSBP and OSBP-Related Proteins (ORPs)

1.1 Overview

Oxysterol binding protein (OSBP) and OSBP-related proteins (ORPs) are expressed in eukaryotes.[1] These proteins have conserved ligand-binding domains, and the different OSBP/ORP members appear to undertake separate biological functions.[2] Recently, this protein family has become the focus of drug development projects.[2] The research in this dissertation is focused on characterizing the small molecule ligand binding to individual OSBP/ORPs, specifically OSBP and ORP4L, and how ligand binding modulates the biological activity of the OSBP/ORPs. The introduction will cover OSBP/ORP protein biochemistry, cellular function, known ligand binding, and connections to disease biology.

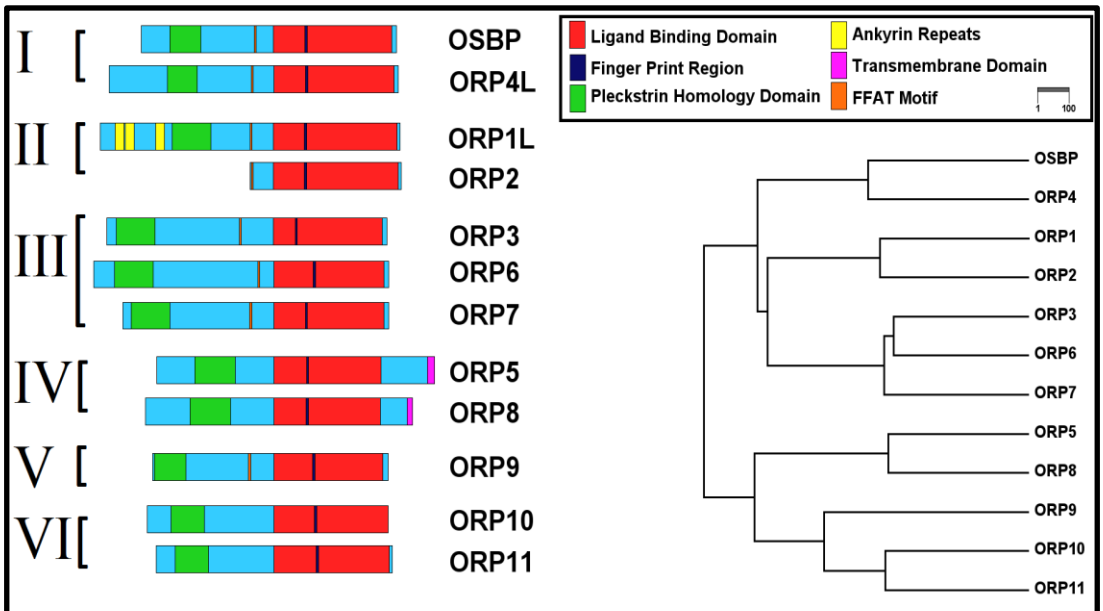

Figure 1: OSBP/ORP Family divided by subfamilies
Domain graphs were based off full-length Oxysterol Binding Protein (OSBP) and the OSBP-related protein (ORP). The graphs were generated and aligned at the beginning of their ligand domain, using DOG2.0. The tree was generated using amino acid percent identity of OSBP/ORP ligand binding domains using Jalview bioinformatics software.

1.2 Overview of the OSBP/ORPs

1.2.1 Overview

Most of the OSBP/ORP proteins are cytosolic lipid binding proteins.[3] Humans have 12 ORP genes, and through alternative splicing, at least, 16 protein variants are expressed.[4,5] The proteins can be grouped, based on their amino acid sequence, into six distinct subfamilies (**Figure 1**).[4–7] In humans, cellular expression, and tissue distribution vary depending on the ORP. We are beginning to learn the function and molecular interaction of many of these proteins, but there is still much that is unknown.

1.2.2 History of the OSBP and ORPS

In 1981, OSBP was discovered in the search for the major regulator in cholesterol synthesis.[8–10] Its most notable feature was its ability to bind 25-OHC.[8] OSBP was not the influential oxysterol-mediated regulator of cholesterol biosynthesis; SREBP was discovered to be responsible for this function.[11] These initial experiments involved purifying cellular OSBP and testing its binding against sterols.[12,13] The first attempts to understand the properties of OSBP, involved recombinant rabbit OSBP and revealed that deleting amino acids 455 to 809 eliminated binding.[14] In the mid-1990s, the first yeast genes that are paralogs of the OSBP were identified.[15,16] ORP4 was first identified as OSBP2 and cloned of monkey retinal cells.[17] Then by 2000, the remaining human ORPs were documented.[4,18] The first indications that OSBP/ORPs were potentially druggable

targets came in 2011 when OSBP and ORP4L were shown to be the targets of antiproliferative compounds.[19]

1.2.3 Properties of OSBP/ORPs

The OSBP/ORPs have come in varying lengths but overall have a standard organization. The OSBP/ORPs have localizing domains and motifs on their N-terminal halves. The most common feature of OSBP/ORP is the large ~50KDa ligand binding domain (LBD) which is located on the C-terminal end of the protein.[4,18] The second most common domain for this family of proteins is the pleckstrin homology (PH) domain.[4] The PH domain is generally known for its ability to bind to phospholipid on membranes.[20] The PH domains for different OSBP/ORPs are still not fully understood, as the localization sites vary depending on the protein.[21] There seem to be other factors that affect cellular localization.[22] All the OSBP/ORPs, except for ORP2, possess this domain. ORP2 is the smallest OSBP/ORP containing only an LBD.[23] The third most common feature of the OSBP/ORPs is the diphenylalanine in an acidic tract (FFAT), its consensus sequence is EFFDAxE.[24] This motif allows for proteins to associate with the endoplasmic reticulum (ER) by binding vesical associate proteins (VAP). Additionally, ORP3 possess an FFAT-like motif, which also helps it associate with VAP proteins.[25] Two of the human OSBP/ORP proteins that do not have FFAT motifs, ORP5 and ORP8, instead contain transmembrane (TM) domains that keep them tethered to the ER.[26,27] By possessing the FFAT or the ER-bound TM, OSBP/ORPs appear to have near universal interaction with ER. ORP10 and ORP11 do not have FFAT motif or TM domains and do not appear to interact with the ER directly. The dual membrane subcellular regions that ORPs localize too are referred to a membrane contact sites (MCS). The rarest feature found in the human

ORP family is the ankyrin repeat domain (ANK) found in the long version of ORP1 allowing it to associate with late endosomes (LE).[28–30]

1.2.4 Structural Biology of the Anchoring Domains and Motifs

The PH domain is 100 – 120 amino acid long domain that has been associated with phosphoinositide binding. The only determined structures of human OSBP/ORP PH domains are from ORP8 and ORP11 (**Figure 2**).[31,32] The general structure of this domain is two seven stranded anti-parallel beta sheets sandwiched together and C-terminal amphipathic helix.[33] The beta sheets are connected through various loops that are essential for binding phosphates. The PH domain is electrostatically polarized, where the bottom of the beta sheets and the connecting loops have a net positive charge, which

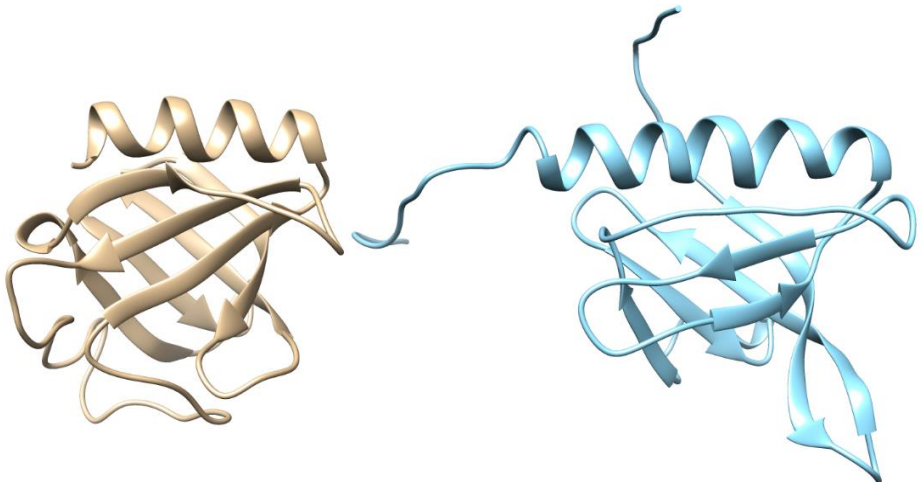

Figure 2: PH Domains of ORP8 and ORP11

Structures of two human OSBP/ORP PH domains that have been solved. The structure of ORP8 has been solved through X-ray crystallography (PDB: 5U77, DOI: 10.2210/pdb5U77/pdb).[31] The structure of ORP11 was solved through NMR (PDB: 2D9X, DOI: 10.2210/pdb2D9X/pdb).[32] Molecular graphics were generated with UCSF Chimera.

allows it to bind negatively charged groups likes phosphates.[33]

FFAT is a seven amino acid sequence that is known for binding VAP proteins. The general consensus sequence of EFFDAxE. So far, the only human OSBP/ORP FFAT motifs that have been determined has been of OSBP.[34] These studies show that the VAP-FFAT interactions are held together through hydrogen bonding and that the first phenylalanine locks into a hydrophobic pocket in VAP.[34]

ORP1L is unique among the human OSBP/ORP family for having an N-terminal Ankryin repeating domain (ANK). This domain composes the first 237 residues of ORP1L. Currently, the only ORP ANK that has its structure solved is of the yeast homolog Osh1.[35] However, the Osh1 ANK has low sequence homology to the ORP1 ANK and are also known to have different interacting partners.[35] The general structure of ANK domains is a composite of two alpha-helical subunits that form a hairpin loop (**Figure 3**).[35,36]

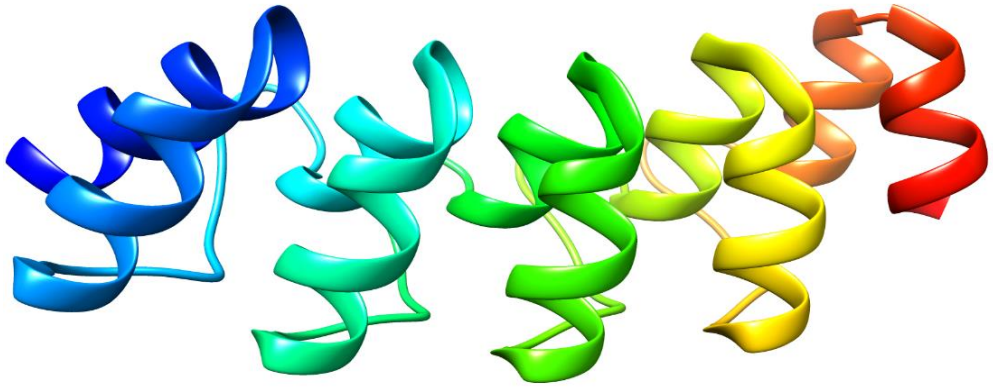

Figure 3: Example of Ankyrin Repeat (PDB: 5GIK)
An artificial ankyrin repeat protein represented in a rainbow color pattern to emphasize the connected alpha-helical subunits of this domain (PDB: 5GIK, DOI: 10.2210/pdb5GIK/pdb).[36] Molecular graphics were generated with UCSF Chimera.

ORP5 and ORP8 are the only two human OSBP/ORPs that contain TM domains, instead of FFAT motifs. The TM domain is a fatty alpha-helix that is 18-19 residues in length.[21] There is no crystal structure for this domain.

1.2.5 Structural Biology of the Ligand Binding Domain

The OSBP-related domain (ORD), also known as the ligand binding domain (LBD), is a highly conserved and defining feature that all OSBP/ORP proteins possess. In the literature, ORD, and LBD are used interchangeably, and for this dissertation, LBD will be used. Unfortunately, to date, no human LBD structure has been determined. There are LBD crystal structures that have been determined are from the yeast OSBP homologue (Osh) proteins (**Figure 4**), which are from *S. cerevisiae* Os3, Osh4, and Osh6, and *K. Lactis* Osh1.[35,37–39] A generic LBD ranges from 300 - 400 amino acids and contains the highly conserved sequence motif EQVSHHP.[5] Also, the LBD is large around 50 kDa and is a dynamic domain with many flexible segments that allow it to bind a diverse number of ligands. Despite these similarities, some differences lead to some specificity in ligand binding.

The full-length Osh3 protein is very large and composed of multiple domains, but the LBD is so narrow that it can only bind phospholipids, like PI4P.[39] On the other hand, Osh4 is a short protein that is only composed of the LBD, which is wide enough to bind sterols or phospholipids.[37,40] Through X-ray crystallography Osh1 and Osh4 have been shown to bind cholesterol and a wide range of oxysterols. Osh6 has only been shown to bind PI4P and phosphatidylserine (PS).[38]

The LBD begins with a small semi-flexible N-terminal lid region, part of this region can be used to interact with certain ligands, like PI4P. The lid then proceeds into two alpha helices, which are inside the domain. Both the helices and the β-barrel-like structures contribute to the interior aliphatic binding tunnel, that can fit in the acyl chains of phospholipids or an entire steroidal compound. The domain ends with a flexible C-

terminal sub-domain, which forms a flexible hinge and loops back opening of the domain

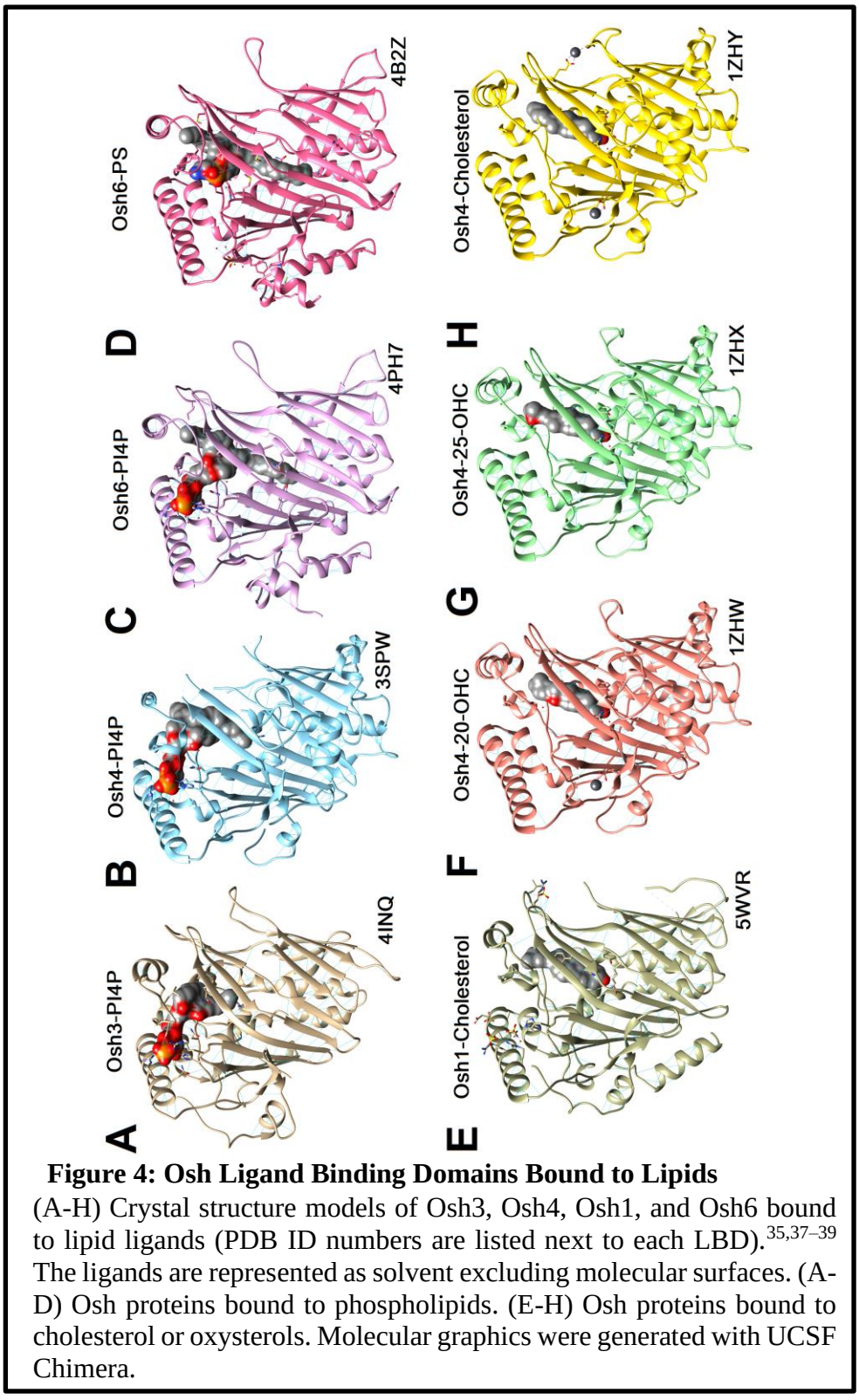

Figure 4: Osh Ligand Binding Domains Bound to Lipids

(A-H) Crystal structure models of Osh3, Osh4, Osh1, and Osh6 bound to lipid ligands (PDB ID numbers are listed next to each LBD).[35,37–39] The ligands are represented as solvent excluding molecular surfaces. (A-D) Osh proteins bound to phospholipids. (E-H) Osh proteins bound to cholesterol or oxysterols. Molecular graphics were generated with UCSF Chimera.

to function as cover alongside the lid.

The lid in Osh3 is fixed in place with the binding motif of (R/K)-(R/K)-X-X-I-(P/D) which is conserved in OSBP, ORP2, ORP3, ORP4, ORP6, and ORP7.[39] In the lid, the amide backbone of M660 forms a hydrogen bond with the 1-phosphate of PI4P (**Figure 5**). The methionine is not conserved, but the ligand-backbone interaction is maintained in Os4 and Osh6.[39] The PI4P head group binds at the entrance of the hydrophobic ligand binding tunnel where a cluster of highly conserved basic residues interact keep it in place.[39,40] For Osh3, the 4-phosphate group of PI4P form direct hydrogen binding with the residues H745, R746 (β-barrel like structure) and R949 (C-terminal subdomain).[39] Residues H745, R746 are part of the conserved fingerprint motif of the LBD that is normally two histidines in all human ORPs.[41] Residues K717 and N720, which are highly conserved in all human and yeast OSBP/ORPs, form part of the end of the central helices and are involved in hydrogen bonding the 1-phosphate of PI4P.[38–40] E945 and R949 are involved in water-mediated hydrogen bond interactions.[39] E945 and R949, along with K941 and R952 form direct interactions with the phosphoinositol head group (**Figure 5**).[39] As for the inositol, the 3-hydroxyl forms a water-mediated hydrogen bond with the backbone carbonyl of E945, and 4-hydroxyl forms a direct hydrogen bond with E945. [39] The long acyl chains of PI4P is housed down the hydrophobic binding tunnel.[39,40]

For ORP-steroid binding, the promiscuity comes in the LBD's ability to pack the sterol head down, through the hydrophobic binding tunnel, onto a cluster of polar residues to accommodate the 3-hydroxyl and for water molecules to lock in the acyl chain hydroxyl.[35,37,42] Despite having an essential function in the steroidal binding, the polar

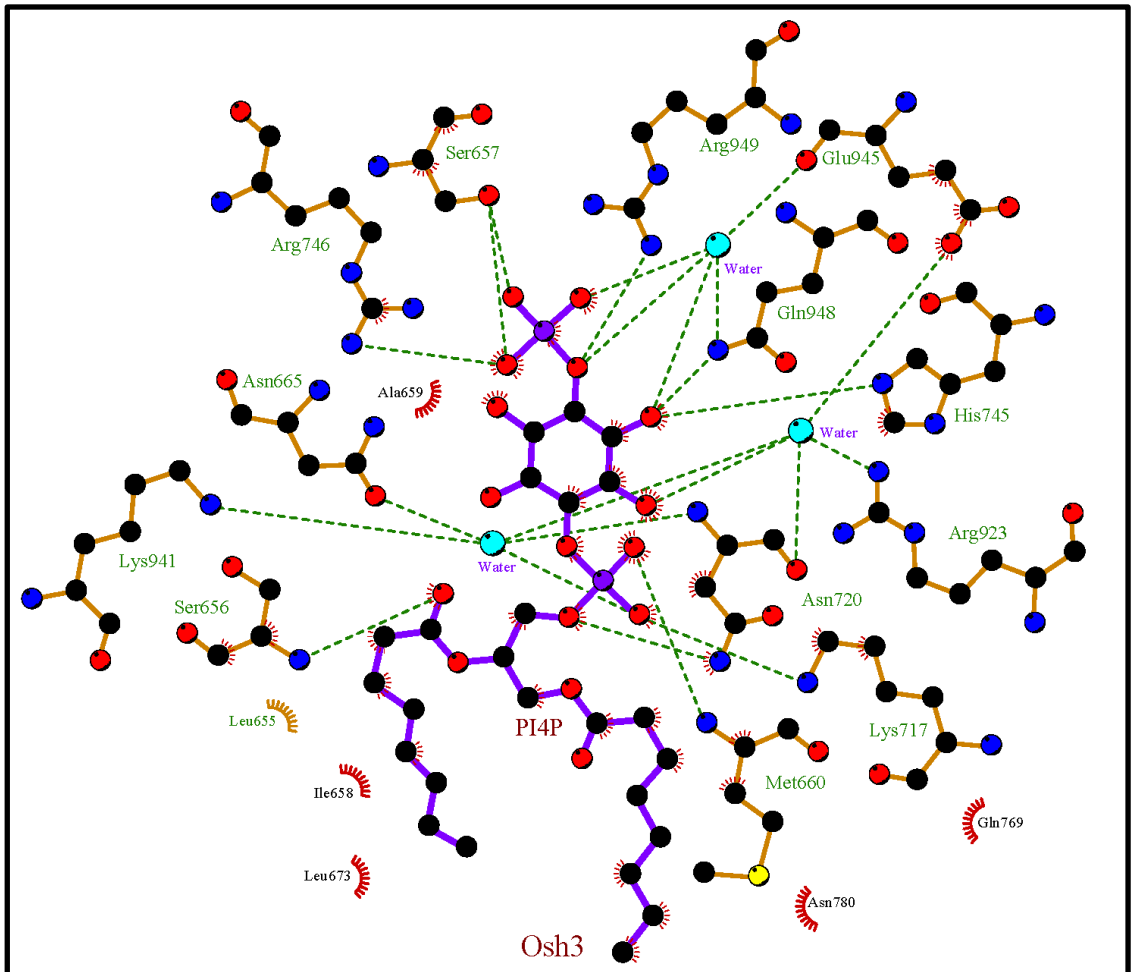

Figure 5: Diagram of PI4P Bound Osh3 LBD

Molecular interaction diagram of PI4P bound to the Osh3 ligand binding pocket (PDB: 4INQ).[39] The residues that interact with polar groups on PI4P are conserved in the yeast and human OSBP/ORPs. The interaction diagram was generated with LigPlot+.

cluster, at the bottom of the tunnel, is not conserved.[21,35,37,39] In Osh 4 the polar cluster is N96 forms a direct hydrogen bond with the 3-hydroxyl group, the remainder of the cluster is composed of W46, Y97, N165 and Q154 forming water mediate interactions with 3-hydroxyl and two water molecules.[37] Unlike Osh4, the 3-hydroxyl forms two hydrogen bonds with two residues, D881 and K1007, in Osh1.[35] The bottom Osh1 polar cluster is completed with Y912 that forms a water-mediated hydrogen bond with the 3-hydroxyl.[35]

Even, though Osh3 is unable to bind sterols, it still possesses a polar cluster Y763, T677, N780, and Q799.[39]

Phosphatidylserine (PS) binding to Osh6 requires the highly conserved K126 to form a water-mediated hydrogen bond and N129 to form a direct hydrogen bond to the carboxylate anion of the PS head group.[38] The acyl chains of PS dock in the steroidal binding pocket, where L64. I67, L69, I73, V124 form hydrophobic interactions.[38] H157 and H158 (fingerprint residues), K182 and K351 are not involved in PS binding but are needed for PI4P binding.[38]

1.3 Known OSBP/ORP Small Molecule Ligands, Oxysterols, and ORPphilin Compounds

1.3.1 Overview

The OSBP/ORPs are known to be lipid sensing and lipid transporting proteins.[2] Cells depend on proper lipid regulation and metabolism to function properly.[43] Lipids provide structural support and can serve as effective relays in signaling pathways.[43,44] As a result, multiple proteins have evolved to build, metabolize, sense, and bind lipids. A significant lipid of interest is cholesterol, which can alter the physical properties of cellular membranes, is involved in signaling pathways, and whose metabolites are also important an organism's development.[45,46] This subsection will discuss major lipid classes that are critical in imparting cellular structure, have roles in signaling pathways and are essential in metabolic pathways (**Figure 6**). This subsection will also cover lipid

binding proteins that regulate cholesterol development or are regulated by cholesterol metabolites.

1.3.2 Cellular Lipid Classes

Fatty acids (FA) are simple lipids that are found in cells and whose basic structure is a 12 to 22 carbon acyl chain connected to a carboxylic acid.[47] The FA is an 18 carbon stearic acid, which is a component in phosphatidylinositide-4-phosphate (**Figure 6**).

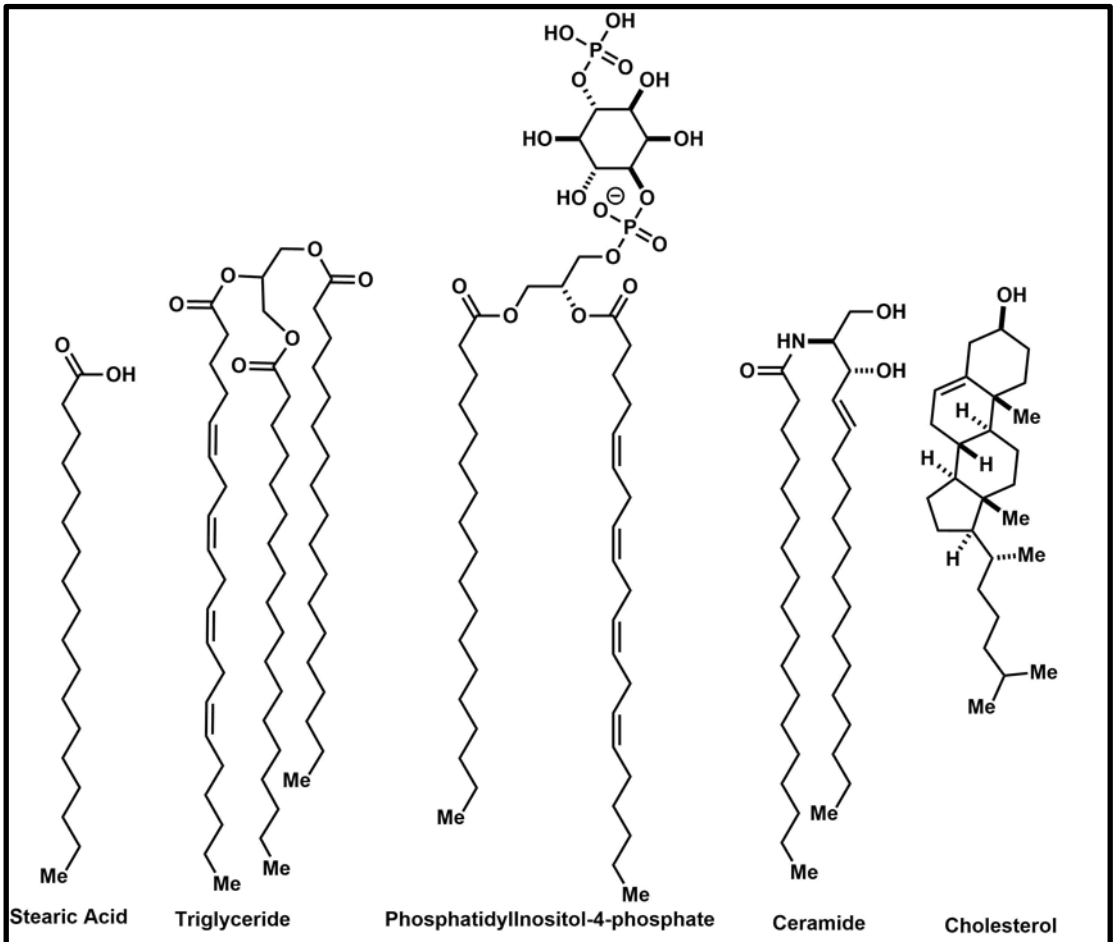

Figure 6: Representatives of Each Lipid Group that binds or is regulated by the OSBP/ORPs

Structures of lipids that are representative of the lipids that the OSBP/ORP family bind (phospholipids, cholesterol/oxysterols) or regulate.

FA molecules are synthesized with acetyl-CoA and NADPH by the enzyme fatty acid

synthase (FAS).[48] Fatty acids can be fully saturated or can have unsaturated, possessing cis and trans stereochemistry. TG is a major energy-storing molecule and is composed of three FA molecules (**Figure 6**).[49] The representative TG in the figure is composed of two stearic acids that are saturated with hydrogen, and an arachidonic acid that has unsaturated bonds. TG molecules are kept in neutral lipid droplets, which are unique organelles that contain a neutral lipid core and phospholipid monolayer surrounding it.[49,50]

Phospholipids are a diverse lipid class and are the major component of cellular membranes. The basic phospholipid structure is composed of two fatty acids bound to a glycerol molecule at C-1, and C-2 position, with the C-3, is bound to a phosphate group.[51] The phosphate is referred to as a head group and can be further modified with other polar molecules. The molecules include choline, ethanolamine, serine, glycerol, and inositol.[51] Each of these lipids possesses unique biochemical properties. For signaling, they are organized at subcellular positions, including different organelles or the plasma membrane (PM).[43] The composition of the fatty acyl chains can vary significantly between phospholipids and phospholipid classes. Phosphatidylinositol is unique in that it has a fixed acyl chain composition consisting of stearic acid at C-1 and an arachidonic acid at C-2.[52]

All eukaryotic cells contain sphingolipids, and these lipids are essential for proper neuronal cell function.[53] Sphingolipids are lipids that are like phospholipids in structure, but instead of having a glycerol base, they possess a sphingosine base. Sphingosine is an amino alcohol with a long hydrocarbon tail and is one of the intermediate products in sphingolipid metabolism.[54] De novo synthesis of sphingolipids occurs in the ER and requires serine palmitoyl transferase to combine palmitic acid and serine, to create

dihydrosphingosine.[54] Dihydrosphingosine is then converted into dihydroceramide and then reduced to ceramide. Ceramide is also synthesized in the ER and transported to the Golgi through ceramide transfer protein, where they are used to make sphingomyelin, cerebrosides, and gangliosides. Ceramide has been shown to have pro-apoptotic effects, inducing ER stress and generating autophagy/mitophagy.[55,56] Cancer cells can counter the effects of ceramide by using ceramidase and sphingosine kinase to generate sphingosine-1-phosphate, which stimulates cell division.

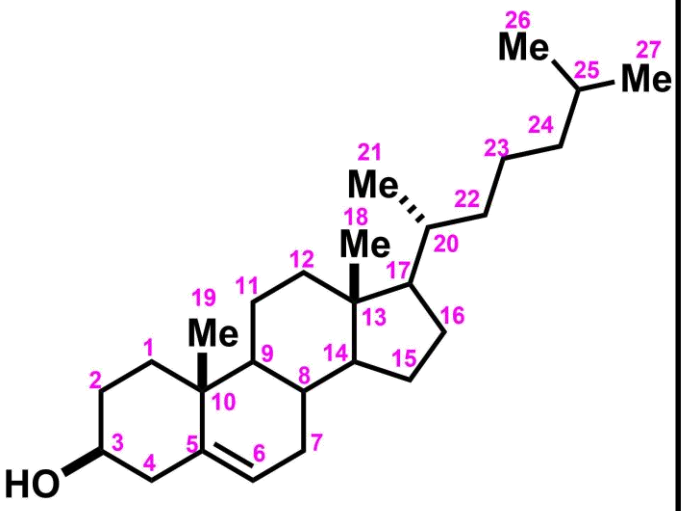

Figure 7: Numbering System for Cholesterol

Cholesterol is an important lipid with many biological roles and is required in the synthesis of several biomolecules. Compared to the other lipid classes, it has a unique fused multi-ring structure. The steroidal core has four rings (A, B, C and D ring). Cholesterol also has a hydroxyl on carbon 3 of the A ring, and an octyl side chain bound to the D ring and has a unique numbering scheme (**Figure 7**).[46] The unique structure of cholesterol makes it useful in maintaining plasma membrane fluidity. Cholesterol synthesis is very complex and is regulated by many systems, with the enzyme HMG-CoA reductase being the rate limiting step.[57,58] Overproduction of cholesterol is linked with a heightened risk of developing cardiovascular diseases, and atherosclerosis.[59] Cholesterol is transferred

across the body as cholesterol esters (CE), in lipoprotein balls and is stored in neutral lipid droplets. Cholesterol is needed for synthesizing vitamin D. Cholesterol is needed to synthesize five major classes of steroid hormones: progestogens, glucocorticoids, mineralocorticoids, androgens, and estrogens. Cholesterol is needed to make bile acids. Lastly, oxidized derivatives of cholesterol, known as oxysterols, are created through enzymatic modification, and direct reactions with reactive oxygen species.[60] Oxysterols are generated in both the synthesis of cholesterol and its metabolism.

1.3.3 Oxysterols

Oxysterols are oxidized derivatives of steroidal compounds, primarily of cholesterol.[60,61] They can be produced enzymatically, as intermediates, in the process making cholesterol or its metabolism, and non-enzymatically they are also generated through oxidation with reactive oxygen species.[60,61] Oxysterols are involved in signaling responses, and their dysregulation can have major impacts on immune response, potentiate cancers, and facilitate the production of neurological disorders and cardiovascular diseases.[60,62] The oxysterols that are discussed in this section are hydroxycholesterols (OHC) and ketocholesterols (KC), and have been used in experiments for this dissertation: 25-OHC, 25(*R*),27-OHC, 25(*S*),27-OHC, 24(*R*)-OHC, 24(*S*)-OHC, 22(*R*)-OHC, 22(*S*)-OHC, 7α,25-diOHC, 7β-OHC, 19-OHC, 7-KC and 5α-OH,6-KC.

25-Hydroxycholesterol (25-OHC), is a derivative of cholesterol with a hydroxyl at C-25, is commonly used in studies about cholesterol homeostasis.[63] 25-OHC can be generated from several metabolic enzymes, CYP27, CYP46, CYP3A4, and 25-hydroxylase.[64] It has also been shown to be produced through the autooxidation of cholesterol but does not

appear to be of great biological importance.[64] 25-OHC and 24S-OHC act as viral inhibitors. 7α,25-dihydroxycholesterol (7α,25-diOHC) is a known agonist for the Epstein-bar virus.[62] 20α-OHC, also known as 20(*S*)-OHC, is a ligand agonist for smoothened in the Hedgehog pathway and is suspected to localize at the Golgi.[65,66] 20α-OHC has osteogenic properties through its interactions with the Hedgehog pathway.[67] 22(*R*)-OHC is an intermediate, from cholesterol, that is generated in the process of making pregnenolone that is further metabolized into hormones.[68] 22(*S*)-OHC, on the other hand, is not a naturally occurring oxysterol, but synthetically derived and useful in biological studies.[69] 24(*S*)-OHC, also known as cerebrosterol, is found in high concentrations in the brain.[70,71] 24(*R*)-OHC, epicerebrosterol, is not as common as its isomer and is only known to be formed as an intermediate in the formation of 24,25-epoxycholesterol.[72,73] The nomenclature for oxysterols at C-26 and C-27 is convoluted with multiple synonyms for these two compounds found in the literature. For the sake of simplicity, hydroxylating at C-26 on cholesterol yields 25(*S*),27-OHC and yields 25(*R*),27-OHC, and will be used for this dissertation. 25(*R*),27-OHC is a naturally occurring oxysterol that is made by CYP27A1 and is the most abundant sterol found in atherosclerotic plaques.[74,75] 7-KC plays a major role in the formation of atherosclerotic plaques and is formed through oxidation.[75] 19-OHC has biological activity but is not a biologically occurring metabolite.[76] 5α-OH,6-KC is a major metabolite from 5,6β-epoxide oxidation in the lungs.[77]

1.3.4 ORPphilins

ORPphilins a class of structurally diverse compounds that come from a diverse array of sources, and target members of the oxysterol-binding protein (OSBP)/OSBP

related protein (ORP) family (**Figure 8**). The natural product versions of these compounds were initially noted for their antiproliferative abilities.[19]

OSW-1 is a steroidal saponin extracted from the bulb of *Ornithogalum saundersiae*, a flower used in Chinese folk medicine for its medicinal properties.[78] The OSW-1 structure contains a steroidal core, with disaccharide moiety composed of xylose

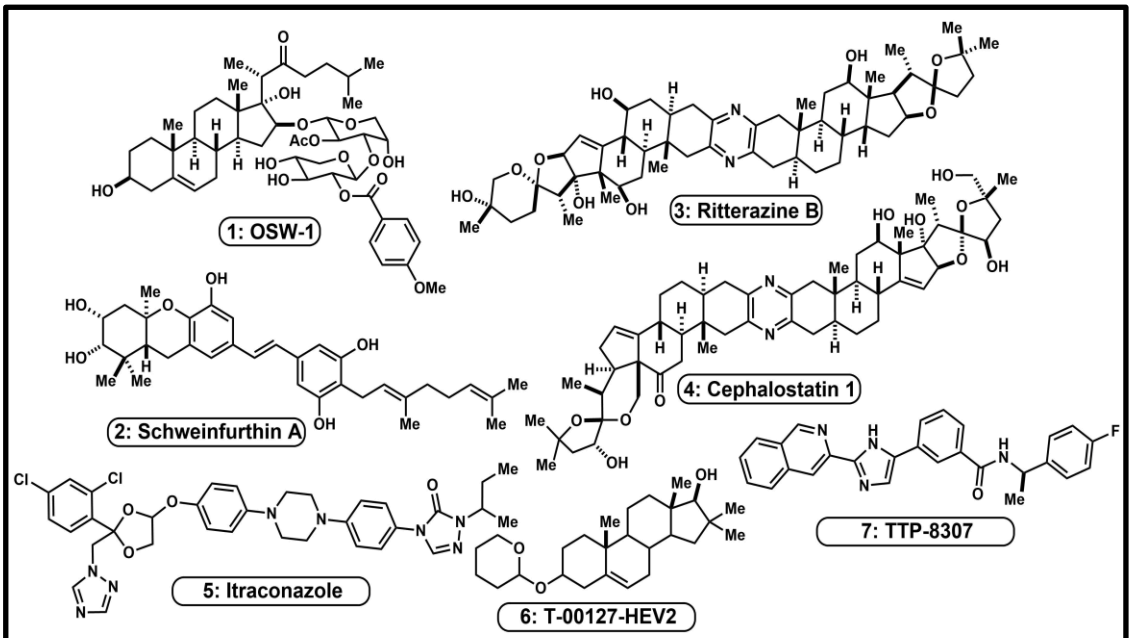

Figure 8: The ORPphilins
Chemical structures of the antiproliferative and antiviral compounds called the ORPphilins, this class of compounds includes natural products (1-4) and synthetic compounds (5-7).

and arabinose capped with a paramethoxybenzoate.[79] Initially, OSW-1 was identified as an acylated cholestane glycoside that could inhibit cyclic AMP phosphodiesterase.[78] When compared to cardiac glycosides, it was found that OSW-1 did not inhibit arterial smooth muscle and epithelial cells in rats.[80] However, it was shown that OSW-1 does slightly raise FSH levels in rats.[81]

OSW-1 was more potent as an antiproliferative compound, and its cytotoxicity pattern indicated that it might share a similar mechanism to cephalostatin 1.[82] OSW-1

induces caspase eight mediated Bcl-2-cleavage in CHO cells.[83] OSW-1 downregulates genes in Wnt, MAPK and VEGF signaling pathways, inducing necroptotic death in hepatocellular carcinoma cell line Hep3B.[84] In leukemia cells, OSW-1 causes an elevation in cytosolic Ca2+ levels which triggers the activation of caspase-3, loss of mitochondrial membrane potential, mitochondrial damage, the release of cytochrome C and the cleavage of survival factor GRP78.[85,86] Through pull-down experiments and protein mass spectrometry, the target of OSW-1 was identified as OSBP and ORP4L, and the inhibition occurred at nanomolar levels.[19] OSW-1 inhibits OSBP from exchanging PI4P with sterols, 25-OHC does not inhibit this interaction.[87]

Cephalostatins are bis-steroidal natural product compounds that were originally isolated from a marine worm *Cephalodiscus gilchristi*.[88,89] Cephalostatin 1 was identified because of its activity in the murine P388 lymphocytic leukemia system.[88] In leukemia T Jurkat cells, cephalostatin 1 induces apoptosis through release of Smac/DIABLO, inducing the disruption of the mitochondria's membrane potential.[90] However, this did not result in the release of cytochrome C or other pro-apoptotic factors, and the overexpression of Bcl-xL blocks the apoptotic effects of cephalostatin 1.[90] It was also observed that cephalostatin 1, induces apoptosis by activating caspase 4 and caspase 9 in the process causing ER stress.[91] Like OSW-1, cephalostatin was identified to target both OSBP and ORP4L with binding interactions at the low nanomolar levels.[19]

Ritterazines are bisteroidal natural products that were isolated from the marine tunicate *Ritterella tokioka*.[92] Just like cephalostatin 1, ritterazine B showed activity for the P388 system.[92] Through the COMPARE pattern recognition analysis indicated that ritterazine B acts through a similar mechanism of action as cephalostatin 1.[93] Ritterazine

B is cytotoxic in PC14 NSCLC cells and HL-60 leukemia cells, locking them at the G2/ checkpoint.[94] Ritterazine B target OSBP selectively with low nanomolar levels, and shows weak binding toward ORP4L.[19] The selectivity of OSBP over ORP4L indicates that it is possible to target individual members of the OSBP/ORP family.

The schweinfurthins are prenylated stilbenes that were first isolated from an African plant, *Macaranga schweinfurthii*.[95] Schweinfurthin A was active in the NCI-60 cell line human tumor screen, with the brain tumor subpanel being the most sensitive.[95] Schweinfurthin A inhibited proliferation in SF-295 glioblastoma cells and KR158 astrocytoma cells but had little effect in A549 lung tumor cells and primary astrocytes.[96] In KR158 cells it was shown that Schweinfurthin A alters the actin cytoskeleton and inhibits Rho signaling which results in cell death.[96] The cytotoxicity profile of schweinfurthin A indicated that it had a similar mechanism as cephalostatin 1, OSW-1 and ritterazine B; and like ritterazine B, schweinfurthin A shows a selectivity for OSBP over ORP4L.[19] Schweinfurthin G, which is extracted from the fruits of *Macaranga alnifolia*, has been shown to be bioactive as well and can also interact with OSBP and ORP1L.[97,98]

Itraconazole is a synthetic triazole compound that was developed as an orally active antifungal.[99] Through screening, itraconazole demonstrated antitumor properties that worked by inhibiting the protein smoothened in the hedgehog pathway.[100] Most recently, itraconazole was identified as broad-spectrum enterovirus replication inhibitor that works through by inhibiting OSBP.[101] Other synthetic antiviral compounds that have been identified to work through OSBP are the enviroxime-like compounds, T-00127-HEV2 and TTP-8307.[102–104]

1.4 Other Oxysterol Binding Protein Families

1.4.1 Overview

Lipids are the major component of membranes and are also important in critical signaling pathways. The regulation of lipid levels is crucial for the proper development, function, and growth of organisms. The discovery of regulatory proteins and pathways has historically been a major focus in biological research. In this section will briefly review major proteins and pathways that bind oxysterols and regulate metabolic pathways.

1.4.2 Hedgehog Signaling Pathways

The hedgehog (HH) signaling pathway is a major developmental pathway in eukaryote embryonic development and inhibition of this pathway during development results in severe deformations. The gene was isolated in fruit fly larvae, in which HH mutation produced larvae with a spiky appearance.[105] In mammals, there are three forms of hedgehog: sonic hedgehog (SHH), sonic hedgehog (SHH), Indian hedgehog (IHH) and desert hedgehog (DHH).[106] SHH has been shown to be localized to the ER where it is cleaved.[107] Before N-SHH can be secreted, the C-terminal covalently linked to cholesterol and the N-terminal half is linked to palmitate.[108,109] Secreted HH binds the plasma membrane receptor patched (Ptc), resulting in the activation of smoothened (Smo).[110] When HH is absent, Ptc prevents signal transduction by binding to Smo, which is part of the G-protein-coupled receptor superfamily.[111,112]

Certain cancers have been shown to use hedgehog signaling to stay viable, possessing an inactive Pts and an overactive Smo.[111,113] Cyclopamine was the first observed inhibitor of the HH pathway, doing so by inhibiting Smo.[112,114] Smo has two

regions where ligands can bind the first being a cytosolic cysteine-rich domain (CRD) and the second area is the seven-transmembrane domain when it adopts a heptahelical bundle fold.[115] Cyclopamine, SANT1, and Vismodegib bind the heptahelical bundle.[65] Oxysterols, especially, 20α-OHC has been shown to function as an agonist for Smo, and 22-azacholesterol was determined to function as an antagonist that can compete for the same binding pocket in the CRD.[65] Itraconazole is also HH inhibitor, but it is unknown which binding pocket it inhibits.[100]

1.4.3 SREBP Pathway

Sterol Regulatory Element-Binding Protein (SREBP) is a transcription factor that regulates the production of fatty acids, phospholipids, triglycerides, and cholesterol.[116,117] SREBP is a basic-helix-loop-helix-leucine zipper family and is synthesized in an inactive form that is bound to the ER, through its transmembrane domain.[118,119] SREBP forms a complex with SREBP cleavage-activating protein (SCAP), which is required for activation of SREBP which is accomplished through proteolytic processing.[120] SCAP can sense cholesterol levels when levels are low SCAP escorts SREBP toward the Golgi apparatus. SREBP is then cleaved Site-1 protease (S1P) and Site-2 protease (S2P), where it translocates to the nucleus and upregulates genes involved in cholesterol/lipid uptake and synthesis.[121,122] Insulin-induced gene 1 protein (INSIG) negatively regulates the SCAP-SREBP complex. When ER cholesterol levels are too high, SCAP will bind cholesterol which causes it to go a conformational shift and binds to INSIG.[123] Another level of regulation is found through 25-OHC binding to INSIG making at bind to SCAP-SREBP complex.[123] Both modes of inhibition have the same effect, of trapping SCAP in the ER and preventing SREBP from being activated. SREBP is upregulated by

transcription factors known as orphan nuclear receptors.[124] In macrophages, overproduction of cholesterol causes it to be shuttled into the mitochondria leading to damage and the overexpression of interleukin 1β causing inflammation.[125] 25-OHC levels can negatively regulate SREBP2 to abrogate this effect.[125]

1.4.4 Liver X Receptors

Liver X receptors (LXR) are major transcription factors that regulate lipid, lipoprotein, and carbohydrate metabolism.[126] Initially, LXR was categorized as an orphan nuclear receptor, until oxysterols, especially 24(*R*)-hydroxycholesterol, were shown to be their ligands.[127,128] Upon binding oxysterols, LXR forms an obligate heterodimer with retinoid X receptor (RXR). This complex then translocates to nuclease and upregulates genes required for the synthesis of cholesterol and fatty acids.[129] LXR has two isoforms LXRα and LXRβ, and share 80% amino acid identity in their DNA-binding and ligand-binding domains.[126] LXRα controls cholesterol metabolism and lipoprotein regulation in metabolically active tissues like the liver, small intestine, kidney, macrophages, and adipose tissue.[126] LXRβ has been shown to be important in immune system regulation and maintaining cholesterol homeostasis in the central nervous system.[130]

1.5 The OSBP/ORPs in Human Disease

1.5.1 Overview

As previously discussed, each OSBP/ORP has a unique role to ensure healthy cellular function. Currently, some OSBP/ORPs, (OSBP, ORP4L, ORP5) appear to be very promising targets for drug development and inhibiting other OSBP/ORP members may lead to unintended side effects.[19,101,102,131–133] The OSBP/ORPs have highly conserved sequences, bind many of the same ligands, but each member has a unique

biological role. In this section, we review the relationship between aberrant OSBP/ORP levels or loss of function mutations resulting in the manifestation of diseases and genetic disorders.

1.5.2 Subfamily-I: OSBP and ORP4

In 2011, it was shown that Oxysterol Binding Protein (OSBP) was the target of anti-proliferative natural products.[19] OSBP inhibition also has been shown to weaken some viral infections. Primarily, enteroviruses and hepatitis C virus (HCV) require OSBP to replicate virus particles.[101,134] When these viruses infect a host, they have been shown to build new compartments from their host's organelles. These new compartments are called membranous webs or replication organelles (RO).[101,134] OSBP, which normally localizes to the MCS between the ER and Golgi, is recruited to the RO and ER MCS instead.[101] HCV uses an ER-anchored non-structural protein to guide both VAP and OSBP into its desired position.[135] HCV requires also requires that OSBP and CERT be unphosphorylated, and so knocks down the expression of protein kinase D (PKD) to ensure this is the case.[136] OSBP is believed to enrich the new RO with cholesterol in PI4P dependent manner. [101,135]

The VAPB-P56S mutant causes a familial form of Amyotrophic Lateral Sclerosis (ALS). This mutant protein is prone to aggregation and disrupts the traffic between the ER and other organelles.[137,138] In Drosophila, it was shown that OSBP was unable to bind the ALS mutant form of VAP-B, leading to aberrant ER morphology.[137]

ORP4 promotes survival for a subset of rapidly dividing cells. For example, RNAi silencing of all ORP4 isoforms induces growth arrest, but not cell death in HEK293 and HELA cells.[139] Silencing ORP4 in IEC-18 cells rapidly induces apoptosis.[139] ORP4L

mRNA was found to be upregulated in the blood samples of cholangiocarcinoma patients.[140] ORP4L is expressed chronic myeloid leukemia and is also expressed in many metastatic cancers.[141,142] ORP4L is most notably T-cell acute lymphoblastic leukemia.[133,141–143] In leukemia cells, ORP4L acts as a metabolic switch that controls whether a cell stays in the citric acid cycle or use lactic acid fermentation.[133] ORP4L accomplishes this by acting as a scaffold for T-cell receptors, G protein ($G\alpha_{q/11}$) which then recruit phospholipase C β3.[133] This, in turn, leads to the production of inositol trisphosphate (IP3) and Ca^{2+}, which lead to the activation of pyruvate dehydrogenase.[133] Expression of ORP4S and ORP4L has been linked with a decrease in HCV infection.[144]

1.5.3 Subfamily-II: ORP1 and ORP2

Macrophages overexpressing ORP1L led to the development of atherosclerotic lesions in LDL receptor-deficient mice.[145] How ORP1L does this is unknown, but it is believed that this mechanism might be through ABCG1, ABCG5 apoE, and PLTP.[145] ORP1L downregulation through microRNA-499a results in decreased levels of serum HDL.[146] Moreover, expression of a nonfunctional truncation mutant OSBPL1A p.C39X led to the low HDL and cholesterol efflux.[147] ORP1L is a potential antibacterial target for a zoonotic pathogen that causes Query Fever, Q Fever.[148] ORP1L is also recruited to the parasitophorous vacuoles of *Coxiella burnetii*.[149] *C. burnetii* is a gram-negative intracellular bacterium that uses the large lysosome like vacuoles it forms to replicate.[148,149]

ORP2 mutations have been associated with deafness. Whole-exome sequencing, with cosegregation analysis, identified a heterozygous frameshift mutation, that prematurely truncates ORP2, and the missense ORP2L195M mutation are both

respectively present in deaf individuals examined.[150] Tissue staining shows that outer and inner hair cells have clusters of enriched ORP2.[151] The mechanism by which ORP2 causes hearing loss is not fully understood. It appears that the mutations in ORP2 could cause misregulation of DIAPH1 and lead to morphological problems in hair cell cilia.[151,152] It is also possible that the reduction ORP2 may decrease HDL levels, as was shown with ORP1, but this hypothesis needs to be experimentally validated.[153]

1.5.4 Subfamily-III: ORP3, ORP6, and ORP7

ORP3 was observed to upregulated as a result of aberrant SUMOylation of liver receptor homolog 1 (LRH-1).[154] In mice this caused increased activity of SREBP and the manifestation of nonalcoholic fatty liver disease.[154] ORP3 overexpression has been observed in various cancers.[155] ORP3 can disrupt the formation of VAPB-P56S aggregates, in the process ameliorating its negative effects organelles and the stress that leads to ALS.[138] Expression of ORP3 and FMO4 correlated with greater overall survival of glioblastoma patients, who were being treated with lomustine and bevacizumab.[156] Mutations in ORP3 are associated with metastatic breast cancer.[157] Conversely, ORP3 is upregulated in pancreatic ductal carcinoma.[158]

ORP6 has been associated with dyslipidemia and is located on chromosome 2, which has been linked to premature coronary artery disease.[159,160] Atherosclerotic plaques have been shown to contain a decrease in ORP6 expression.[161] Knocking down of ORP6 results in misregulation of endosomes, reduces the esterification of cholesterol and an increase of free cholesterol.[161] ORP6 is positively correlated with HDL and apoAI

levels.[161] Large-scale genome-wide association has identified SNPs in ORP6 can increase the risk of Alzheimer's disease.[162]

ORP7 mRNA as upregulated in both tumors induced by *Opisthorchis viverrini* (liver fluke) and was also detected in the blood cells of patients with cholangiocarcinoma.[140] Genome-wide association studies have linked SNPs in ORP7 to increased LDL and total cholesterol levels.[163,164]

1.5.5 Subfamily-IV: ORP5 and ORP8

ORP5 is overexpressed in pancreatic cancers and linked to its invasiveness and poor prognosis.[131] Preliminary evidence has linked ORP5's role in pancreatic cancer to altered cholesterol metabolism and induced SREBP2 expression.[132] Furthermore, it was also shown that HDAC5, which also has a sterol response element is involved in the ORP5 mechanism.[132] These results were determined with the use of statins and HDAC inhibitors that showed cell growth reduction in ORP5-positive pancreatic cancer cell lines.[132] Furthermore, ORP5 was also upregulated in metastatic lung cancers.[165] Knockdown in ORP5 leads to decreased cell proliferation and migration.[166] SNPs of ORP5 has even been linked to alcohol dependence, along with a cluster of other genes on chromosome 11.[167] ORP5 expression was shown to correlate to LDL production in the leukocytes of healthy human subjects.[168]

ORP8, as well as ORP5, has been shown to be involved in lipid regulation and metabolism.[31,169] In the macrophages of atherosclerotic lesions, both ORP8 mRNA and protein are overexpressed compared to healthy cells which lead to suppression of ABCA1.[27] LDL receptor knock out mice are a common model to study atherosclerotic lesion development. Mice injected with bone marrow-derived cells resulted in in

increased levels of VLDL and triglycerides and decreased lesion size.[170] It was also shown that the knockdown of mouse ORP8 yield higher levels of HDL and apoAI.[171] In gastric and hepatocellular cancers ORP8 expression is knockdown. ORP8 overexpression has been shown to induce ER stress in gastric cancers.[172] In hepatocellular carcinoma cells, ORP8 overexpression induces Fas-mediated apoptosis.[173] Moreover, in hepatic cancer cells ORP8 is required to maintain the cytotoxic effects of 25-OHC.[174] However, ORP8 mRNA is overexpressed in the late stages of liver fluke induced cholangiocarcinoma progression.[140,175] Whether ORP8 induction, in this case, is a defensive result of the cell, or physiological requirement of the parasite is not known.

1.5.6 Subfamily-V: ORP9

ORP9 mRNA is down-regulated in the poor survival group of subjects with early to mid-stage colorectal cancer.[176] ORP9 SNPs were correlated to higher incidence of atherosclerosis, in cerebral infarction patients, using polymerase chain reaction-restriction fragment length polymorphism (PCR–RFLP).[177]

1.5.7 Subfamily-VI: ORP10 and ORP11

ORP10 overexpression has been observed in individuals infected with the dengue virus.[178] Moreover, shRNA knockdown of ORP10 gene expression resulted in significant reduction in DENV2 replication. RXRA was also upregulated during dengue infection, suggesting the virus' mechanism of pathogenicity requires ORP10 and the LXR pathway.[178] ORP10 is connected to dyslipidemia through multiple genetic studies. ORP10 silencing was shown to result in increased lipogenesis and apoB-100 secretion in hepatic cells.[2,179,180] SNPs in ORP10 have been linked to hypercholesterolemia, high triglyceride levels, hypertension, and peripheral arterial disease.[179,181–183] Regarding

cancer diagnostics, ORP10 SNPs have been found in prostate cancers and B-cell lymphoma and are potential biomarkers for these diseases.[184,185]

The body of research that connects ORP11 with diseases is sparse. There are links between SNPs in ORP11 and risk factors for diabetes and cardiovascular disease in obese individuals.[186] Mutations in ORP11, in combination with mutations in POLR1A, were observed in two brothers with a neurological disorder that causes ataxia, psychomotor retardation, cerebellar and cerebral atrophy, and leukodystrophy.[187]

1.6 Cellular Biology of the OSBP/ORPs

1.6.1 Overview

As previously stated, humans have 12 OSBP/ORP genes and with alternative splicing can express different isoforms of OSBP/ORP proteins.[4] Since their discovery, the OSBP/ORPs have remained understudied when it comes to their functions inside cells. Advances have been made to understand certain members, e.g., OSBP, ORP1, and ORP5, but other members have not yet been studied to the same level of detail.[2] Each OSBP/ORP member has a unique cellular/tissue expression pattern and is known that each ORP has a role in either metabolic sensing or cellular signaling.[2] In yeast, ORP proteins have been shown to have a functional redundancy in which the total knockdown of all ORPs resulted in cell death.[188] It appears that this functional redundancy does not hold for the human OSBP/ORPs. This section reviews what is known about OSBP/ORP cellular functions.

1.6.2 Subfamily-I: OSBP and ORP4

OSBP is ubiquitously expressed in tissues. Upon ligand binding, OSBP localizes in between the ER and the trans-Golgi.[189] The FFAT motif on OSBP recognizes both

VAP-A and VAP-B.[190] The PH domain weakly recognizes PI4P, but it requires GTPase arf1 to localize to Golgi.[191] It has been shown that a significant cellular role for OSBP is the regulation of cholesterol transport to the Golgi and PI4P to the ER.[87,192] This effect has been shown to be a four-step cycle in which OSBP, first, localizes in between the ER and Golgi, second cholesterol is shuttled to the Golgi, after which PI4P is shuttled to the ER, and finally, the PI4P is hydrolyzed by phosphatase Sac1, which alters the chemical gradient in the ER that allows for cholesterol transport to occur.[193]

OSBP is also instrumental in the biogenesis of sphingolipids. When translocated at the MCS, OSBP binds to CERT. CERT also has a pleckstrin homology domain, that is similar to OSBP that recognizes pools of PI4P on the Golgi.[194] When localized to the Golgi, CERT transfers ceramide to the Golgi, increasing the synthesis of sphingomyelin. Increased levels of cholesterol combined with sphingomyelin production, creates an enriched microdomain of cholesterol and sphingomyelin that are necessary for the protein and lipid sorting, and the secretory pathway.[189]

Moreover, OSBP has been observed to function as a scaffold in signaling pathways. OSBP has been shown to be involved in ERK signaling; low cholesterol levels cause OSBP to coordinates two phosphatases (PTPPBS and PP2A) to dephosphorylate pERK.[195] It was demonstrated that removing the PH domain, also reduced the complexing and dephosphorylation. OSBP has been shown to be phosphorylated by JAK2, recruit STAT3 to be phosphorylated resulting in STAT3 translocating to the nucleus.[196]

ORP4L is necessary for cellular proliferation and maintaining proper Golgi morphology.[22] Mice testis lacking ORP4 expression resulted in low sperm numbers and of those produced they had low motility and abnormal morphology.[197] ORP4 has multiple

isoforms, ORP4L has been shown to be necessary for cell proliferation and survival.[139] ORP4L is recruited to localize both at the ER-Golgi MCS and the PM.[22] Changing the amino acid residues HHK to AAA in the fingerprint motif in the LBD weakens the ability of ORP4L to bind to VAP-A on the ER.[198] The ER-Golgi association is controllable through 25-OHC and is also dependent on the presence of OSBP.[22] The association between ORP4L and the PM is ligand-independent, interacts in areas that contain vimentin and rich in PI4P.[22,199] The PH domain appears to regulate the degree at which ORP4 interacts with vimentin.[139] ORP4M, has an inactive truncated PH domain and acts more similarly to ORP4S decreasing its selectivity for PI4P and vimentin localization.[139]

ORP4L has selective tissue expression in the brain, heart, and testis.[18,197] ORP4L may be implicated in regulating the energetics of cells, considering that it affects energetics in cancer cells that overexpress ORP4L.[133] Moreover, low constitutive expression of ORP4 in hepatocytes has been shown to control the formation of lipid droplets.[144]

1.6.3 Subfamily-II: ORP1 and ORP2

ORP1 and its transcription variants appear to have roles as a cholesterol sensor and endosomal trafficking.[200] ORP1L directly interacts Rab7 on LE and alters the morphology of this organelle.[29] ORP1L functions as a cholesterol sensor for LE and uses its FFAT to bind VAP proteins on the ER. ORP1L can transfer the LE cholesterol to the ER.[201] This transfer requires Niemann-Pick C1 (NPC1) to load cholesterol into the LE membrane.[201] PI4P is also needed for this cholesterol transfer, ORP1L can bind PI4P, but it is not known if this cholesterol is exchanged in a countertransport manner.[201] The FFAT on ORP1L prevents VAP from removing dynein–dynactin subunit, $p150^{Glued}$, from the

LE.[202] ORP1S Upon ligand binding ORP1S translocates to the nucleus and help LXR bind regulatory elements and increase transcription.[203] Both isoforms have different tissue distribution patterns, ORP1L is most abundant in the brain and lungs, and ORP1S has higher expression in skeletal muscle and heart.[28] ORP1L and ORP1S have increased expression in monocytes, with ORP1L expression being higher.[28]

ORP2 is ubiquitously expressed in tissues.[23] ORP2 binds neutral density organelles and may have cholesterol a cholesterol-mediated role in triglyceride metabolism.[204] The hydrolysis of triglycerides is dependent on the ability of ORP2 to bind VAP proteins on the ER.[198] Like ORP4L, changing residues HHK to AAA will weaken the association between ORP2 and VAP-A.[198] ORP2 can translocate to the nucleus and help LXR bind regulatory elements and increase transcription of genes that regulate glucocorticoid synthesis.[205] Moreover, overexpression of ORP2, in stably transfected CHO cells, resulted in enhanced cholesterol efflux and decreased levels of esterified cholesterol.[23] ORP2 is also shown to regulate cytoskeletal actin in hepatocytes.[206] This ability is most likely due to interactions with diaphanous homologue1 (DIAPH1), a protein that binds to actin to affect cell shape and motility.[152]

1.6.4 Subfamily-III: ORP3, ORP6, and ORP7

ORP3 binds actin in the plasma membrane. ORP3 decrease leads to increases in PI4P.[138] ORP3 is expressed in monocytes, epithelial and neuronal cells.[28] ORP3 does not have a well-established subcellular localization pattern.[2] However, ORP3 can recognize sites on the ER and also the plasma membranes.[207] Overexpressing ORP3 and VAP cause alterations in the morphology of the ER.[207] ORP3 has been shown to interact with R-Ras altering actin organization and affecting cellular adhesion.[155] The effect of ORP3 on R-

Ras activity depends on ORP3's phosphorylation state. In order to have proper ORP3-R-Ras interaction, hyperphosphorylated ORP3 must bind VAP-A and associate to the PM.[25] Overexpression of ORP3 was also positively correlated with Akt phosphorylation.[25]

ORP6 is involved in regulating cholesterol efflux and homeostasis by affecting the early lysosomal network.[2] ORP6 has a two-fold upregulation, in macrophages that are loaded with acylated-LDL.[5] More recently, ORP6 was shown to be a transcriptional target of LXR in macrophages and hepatocytes.[161] Conversely, ORP6 is negatively regulated by microRNAs, miR-33, and miR-27b.[161] ORP6 co-localization was shown to occur between the endolysosomal network and the ER, as well as the ER and the PM.[161,208]

ORP7 is involved in the autophagosome pathway.[209] Treating 293A cells with 25-OHC causes ORP7 interacts with GATE-16, inducing the degradation of SNARE protein GS28.[209] ORP7 does not have a well-established subcellular localization pattern.[2] Bimolecular complementation fluorescence (BiFC) has shown the FFAT on ORP7 does associate with VAP proteins, upon binding 25-OHC.[198]

1.6.5 Subfamily-IV: ORP5 and ORP8

ORP5 is anchored to the ER via its TM domain, ORP5 has no isoforms, and have multiple diverse cellular functions. ORP5 can interact with the PM and shuttle in PI4P, from the PM, with PS, from ER, in a countertransport.[169] ORP5-LBD was shown to bind the outer mitochondrial membrane protein PTPIP51.[210] This interaction localizes ORP5 at an ER-mitochondria MCS and induces the delivery of PS to the mitochondria.[210] Silencing ORP5 also causes aberrant mitochondrial morphology and function.[210] ORP5 is also known to interact with LEs and extract cholesterol, loaded by NPC1.[26] ORP5L is also important in oocyte development, as mutations in ORP5 have been associated with

triploidy.[211] ORP5 levels are associated with cell proliferation and migration, and in order to have this a fully functional LBD is needed.[166] ORP5 can localize mTOR to lysosomes.[166]

ORP8 is most closely related to ORP5 and has been shown to have overlapping functions with that protein. ORP8 is bound to the endoplasmic reticulum and localize to the mitochondria by binding the outer mitochondrial membrane protein PTPIP51.[210] Also like ORP5, ORP8 can interact with the PM and drive same PI4P-PS countertransport.[169] It was shown in vitro, that the PS PIP countertransport is possible with multiple PIPs, and transport is most efficient with PI3P and PI(4,5)P.[31] Increased expression of ORP8 negatively regulates ABCA1 and cholesterol efflux from macrophages.[27] In BiFC experiments, ORP8 was shown to interact with Nucleoporin Nup62 and in the process suppress the function of SREBP.[212] In mouse macrophages it was shown that ORP8-Nu62 interaction resulted in decreased migration.[213] It is hypothesized the ORP8 may sequester Nu62, dismantling the nuclear pore complex, and inhibiting transport to the nucleus.[213] Another interacting partner of ORP8 is sperm associated antigen 5 (SPAG5), a protein that binds the mitotic spin and regulates its position, indicating that ORP8 may have a role in mitosis.[214]

1.6.6 Subfamily-V: ORP9

Like OSBP, ORP9 can localize between the Golgi and the ER. OSBP demonstrated the ability to bind both [^{3}H]25-OHC and [^{3}H]cholesterol, and ORP9 did not demonstrate this ability.[215] ORP9S has been shown to mimic the function of the yeast ORP Kes1p.[216] ORP9S is a substrate for PDK2 and overexpression of ORP9L results in a reduction of Akt phosphorylation.[217] ORP9L mutants that are unable to bind to ER have

been shown to localize to large vesicular structures.[218] ORP9 is expressed in both long and short forms. ORP9 binds 25-OHC. ORP9 is phosphorylated at S287 by PDK2.

1.6.7 Subfamily-VI: ORP10 and ORP11

ORP10 seems to have roles that are involved in lipid metabolism and regulation. ORP10 as it associates with microtubules and the Golgi to regulate the secretion of apolipoprotein B-100.[180] ORP10 has been shown to interact with DIAPH1 as a binding partner. DIAPH1 coordinates cellular dynamics by affecting microtubule function.[152] ORP10 has also been shown to dimerizes with ORP9L.[180]

ORP11 has been shown to localize with the Golgi and LE. It has also been shown to dimerize with the ORP9, which contains an FFAT motif.[219] Indicating an intersection of signaling where the ER, Golgi, and LE are affected by two ORPs.

1.7 Ligand Binding to OSBP/ORPs

1.7.1 Overview

OSBP was discovered for its ability to bind 25-hydroxycholesterol, and since then it has also been shown to bind cholesterol, phospholipids and a wide range of small molecule inhibitors.[8,19,101,102,192] As previously described, the OSBP/ORP LBD is a large domain that can accommodate complex binding to a diverse array of lipids and natural products. The [^{3}H]25-hydroxycholesterol ([^{3}H]25-OHC) binding assay that we are using is based on a binding assay described by Taylor and Kandutsch.[12] This technique measure the ability of compounds to bind competitively against tritiated 25-OHC, which uses a charcoal-dextran suspension that removes unbound ligand and the remaining protein-ligand complex is measured through scintillation counting.[12] A modification to this assay uses TALON resins, to pull down the protein-ligand complex.[215,220] Other techniques that

have been used to study OSBP/ORP binding include microscale thermophoresis, ELISA, and surface plasmon resonance experiments.[98,101]

1.7.2 Cholesterol and Oxysterols

It was observed that cholesterol levels were affected by OSBP levels, but it was not initially not believed to be one of its ligands.[14,221] Eventually, it was determined through His-tagged OSBP, and pull-down experiments that cholesterol is a ligand with a K_D of 173 nM.[195,222] 25-OHC is a common ligand for oxysterol binding studies and have been studied extensively with OSBP, possessing the highest affinity of all the oxysterols with a K_D ranging from 8 to 32nM.[13,19,221,223]

Initially, ORP4L was not observed to bind to 7-KC, 25-OHC or cholesterol specifically.[17] ORP4L has been shown to bind 25-OHC with a K_D ranging from 10nM to 54nM, and with a K_D of 68nM for cholesterol.[19,139,199] The short isoform ORP4S was observed to have similar binding constants.[139]

ORP1L has been shown to bind both 25-OHC and 22(*R*)-hydroxycholesterol (22(*R*)-OHC).[145] ORP1L was shown to bind 25-OHC with a K_D of 97 nM; for ORP1S the K_D ranges from 84 to 167 nM.[224] It was shown that ORP1S could bind cholesterol with a K_D of 393 nM.[203] ORP1S has a high-affinity for 22(*R*)-OHC with a K_D of 96 nM.[203] ORP2 does not have a high-affinity for 25-OHC with a K_D of 3.9 μM.[224] However, it does show high-affinity for 22(*R*)-OHC with a K_D of 14 nM.[204] ORP2 also binds 7-KC with a K_D of 160 nM, but there was no specific binding detected with 27-OHC.[204]

The ORP5 LBD has been shown to be able to extract dehydroergosterol in lipid exchange assays, indicating an ability to bind sterols.[26] No binding assay to determine binding constants have been reported for ORP5. The ORP8 LBD was shown to have

specific binding to 25-OHC, weak binding to 24(*S*)-OHC and there was no specific binding for 7-KC.[27]

Binding constants of ORP9 and its ligands have not been determined. However, ORP9L can bind and extract cholesterol from liposomes.[215] ORP9S is also able to extract fluorescent sterols, cholestatrienol and dehydroergosterol.[225]

ORP10 can extract cholesterol from membranes but has not been shown to bind oxysterols in vitro.[180] There is currently no data on what ligands ORP11 can bind. It was shown it was possible to photo-crosslink 25-OHC to ORP3, ORP5, ORP6, and ORP7 revealing the possibility of using this binding assay with more family members.[224] However, for this type of experiment it is possible that the compound is crosslinking non-specifically in aliphatic portions of proteins.

1.7.3 Phospholipids

The ability to bind phospholipids, especially PIPs, has been observed for many OSBP/ORP members. There has only been one reported binding assay that focused on phospholipids and OSBP/ORPs. ORP5 and ORP8 LBD PIP ligand binding were studied using isothermal titration calorimetry (ITC), and acyl chain truncated water-soluble forms of the lipids.[31] ORP5 and ORP8 were observed to bind PI3P, PI4P, PI5P, PI(3,4)P, PI(3,5)P, PI(4,5)P and PI(3,4,5)P at micromolar levels.[31] The remaining studies involve lipid exchange assays that give can confirm binding exist but it is difficult to report binding constants. OSBP, ORP1, ORP4 has been shown to exchange cholesterol for PI4P between two membranes.[87,139,201] ORP10S interacts most visibly with PI3P in lipid

overlay assays.[216] ORP10S, which has no PH domain, has also been observed to extract PS in liposomal lipid exchange experiments.[38]

1.7.4 ORPphilins and Other Inhibitors

The ORPphilins are structurally diverse inhibitors that have moderate to high-affinity for at least two members of the OSBP/ORP proteins (**section 1.3.4**).[19,98] Their interactions with the OSBP/ORP proteins have been studied in many ways, one being through competitive inhibition of [^{3}H]25-OHC in a charcoal-dextran binding assay with results being reported as inhibition constants (K_i). Few have been studied through direct binding assays. While some reported constants but have been validated as targeting an OSBP/ORP through a series of cellular studies.

The potent inhibitor OSW-1 binds both OSBP with a K_i of 26 nM and ORP4L with a K_i of 54 nM.[19] Cephalostatin 1 is a large steroidal compound that binds OSBP with a K_i of 39 nM and binds ORP4L with a K_i of 78 nM.[19] Certain compounds showed marked selectivity for OSBP over ORP4L. Ritterazine B binds OSBP with a K_i of 28 nM, but with ORP4L it was not possible to establish way complete inhibition constant.[19] Schweinfurthin A is specific for OSBP binding with a K_i of 68nM, ORP4L bound with a K_D of 2,600 nM[19] It was shown that Schweinfurthin G is also cytotoxic and interact with OSBP.[98] Immobilized Schweinfurthin G analogs were shown to bind ORP1L and ORPS with sub-micromolar affinity via SPR.[98] Itraconazole is a purely synthetic triazole antifungal has been reported to bind OSBP with a K_D of 430 nM using microscale thermophoresis.[101] Synthetic antiviral compounds T-00127-HEV2 and TTP-8307 also target OSBP, but their OSBP binding constants have not been reported.[102,103]

Chapter 2: Profiling Ligand Binding to OSBP and ORP4L with Oxysterols and Oxysterol Analogs

Juan Nuñez*, Anh Le*, Cori Malinky*, Sophia Sakers*, Gianni Manginelli*, Hailee Rau*, Naga Rama Kothapalli *, and Anthony Burgett*

*Department of Chemistry and Biochemistry, University of Oklahoma, 101 Stephenson Pkwy, Norman, Oklahoma, 73019, United States

Juan Nuñez was responsible for writing this chapter. He was responsible for all experiments and data analysis for this chapter, unless otherwise specified. Dr. Naga Rama Kothapalli mentored and assisted in cloning and tissue culture work. Juan synthesized the compounds SA-7 and SA-8 with the assistance of Dr. Anh Le. Dr. Anh Le, Cori Malinky, Sophia Sakers, Gianni Manginelli and Hailee Rau made compounds SA-9 to SA-17.

Chapter 2: Profiling Ligand Binding to OSBP and ORP4L with Oxysterols and Oxysterol Analogs

2.1 Abstract

Human OSBP and ORP4L are closely related members of the OSBP/ORPs, a highly conserved lipid-binding protein family found in eukaryotes. Both OSBP and ORP4L were found to be targets of a structurally diverse anti-proliferative family as the class of natural product compounds known as the ORPphilins. Recent research has indicated that selective inhibition of OSBP can be used to treat certain viral infections and that inhibiting ORP4L is a potential new route to personalized cancer treatments for certain cancers driven by ORP4L expression. Currently, the structure-activity relations (SAR) that determine ligand binding affinity and selectivity to the OSBP/ORP family are poorly understood. Our research details the profiling of ligand binding to OSBP or ORP4L using a diverse library of small molecule ligands, which includes oxysterols and oxysterol analogs. The major results of this study show that the position and stereochemistry of the hydroxyl on the oxysterol side chain are important to high-affinity inhibition binding to both OSBP or ORP4L. We also generated a library of 20-hydroxycholesterol analogs with various side chains, and the inhibition binding of these analogs demonstrates the iso-hexyl side chain found in oxysterols cannot be significantly changed without reducing binding affinity. Additionally, saturation of the C5-C6 alkene in 25-hydroxycholesterol does not alter OSBP and ORP4L binding affinity.

2.2 Introduction

2.2.1 The Cellular Role of OSBP and ORP4L

Oxysterol-binding protein (OSBP) and OSBP-related proteins (ORP) subfamily-I is the most studied and most understood subfamily, which offers the most promising drug targets for potential cancer and viral drug development. Subfamily-I is composed of oxysterol-binding protein (OSBP), and OSBP-related protein 4L (ORP4L), which shares 54% sequence similarity to OSBP.[5] OSBP and ORP4L also have similar domain organizations with N-terminal pleckstrin homology (PH) domains and FFAT motifs that direct their subcellular localization upon ligand binding (**see chapter 1 section 1.2.4**).[139,198,226] Despite their sequence similarities, OSBP and ORP4L, have different cellular functions. OSBP exhibits a ubiquitous expression in the tissues. Ligand binding to OSBP alters its cellular localization translocating the protein between the trans-Golgi, and ER.[227] OSBP can exchange cholesterol and phosphatidylinositol-4-phosphate between organelles, and this function is exploited by viruses to assist in their replication.[101] Many viruses, including the *Enteroviruses* genus of viruses, recruit OSBP to their viral replication organelle in order to enrich this organelle with cholesterol.[101,102,144]

In contrast, ORP4L has a distinct and limited tissue expression pattern in normal tissues. ORP4L is not known to affect lipid membrane levels, nor is its localization known be changed upon ligand binding. ORP4L is, however, highly expressed in cancer cell lines and T-cell acute lymphoblastic leukemia (T-ALL) cells collected from patients.[133,139,142] ORP4L regulates T-ALL bioenergetics by acting as a scaffold for $G\alpha_{q/11}$, CD3ε, and PLCβ3, on the plasma membrane resulting in the hydrolysis of

phosphatidylinositol-4,5-diphosphate into inositol 1,4,5-trisphosphate (IP3).[133] The increase in IP3 leads to the release of ER Ca^{2+} leading to the activation of pyruvate dehydrogenase and the downstream initiation of oxidative phosphorylation which becomes a major source of energy production in T-ALL.[133]

2.2.2 The Therapeutic Potential of Inhibiting OSBP and ORP4L

The ORPphilins are a class of structurally-diverse anti-proliferative compounds that target OSBP and ORP4L (**see chapter 1 section 1.3.3**).[19,228] The ORPphilin compounds competitively inhibit binding between tritiated 25-OHC and OSBP or ORP4L at nanomolar concentrations.[19] Compounds like ritterazine B and schweinfurthin A show a significant selectivity for binding OSBP over ORP4L, which indicates that selective OSBP and ORP4L binding is possible.[19] Itraconazole (ITZ) is a synthetic compound that was discovered to exert its antiviral activity by inhibiting OSBP.[101] OSW-1 is a steroidal saponin natural product that competitively inhibits 25-OHC binding to OSBP and ORP4L, at nanomolar levels.[19] OSW-1 is known to have potent antiproliferative and antiviral properties.[2] We hypothesize that it might be possible to synthesize novel OSW-1 analog compounds that selectively target OSBP or ORP4L, which can then be developed as anti-viral or anti-cancer drugs.

2.2.3 Current Knowledge on the Ligand Binding Capabilities of OSBP and ORP4L

In order to create inhibitors that selectively target OSBP or ORP4L, it is necessary to have a thorough understanding of their ligand binding capabilities. The majority of OSBP/ORP binding studies have been performed using variations of a [^{3}H]-25-hydroxycholesterol/charcoal-dextran binding assay.[2] Previous binding values reported

for OSBP are actually from mouse, hamster and rabbit OSBP, which are conserved with human OSBP.[13,195,223] Various oxysterols were shown to be competitive ligands in radiolabeled 25-OHC binding assays using non-human mammalian OSBP, including in the non-purified OSBP enriched fractions. [13,199,223] There are fewer reported binding studies for ORP4L.[199] There has not been a comprehensive study that screened a library of oxysterols for comparison binding to OSBP and ORP4L, which details how modifications to an oxysterol affect binding to each subfamily-I member.

Here we report the first detailed values of human OSBP direct binding values of human OSBP to [^{3}H]-25-OHC, using the standard charcoal-dextran binding assay. Using this binding assay, we report the first competitive inhibition values of human OSBP to OSW-1 and ITZ. Further, we report detailed competitive binding profiles for a diverse array of oxysterols and steroidal compounds against OSBP and ORP4L. These results show that side chain hydroxyl position and stereochemistry affect competitive binding to OSBP and ORP4L. Lastly, we probe the importance of the oxysterol iso-hexyl side chain with a series of 20-hydroxycholesterol (20-OHC) analogs.

2.3 Results and Discussion

2.3.1 Human OSBP and ORP4L Binds 25-Hydroxycholesterol at Nanomolar Levels

Human OSBP cDNA was cloned into the mammalian expression plasmid. The tagless human OSBP (**Appendix Figure 23**) binds [^{3}H]-25-OHC with a K_D of 22 ± 5 nM (**Figure 9 and Appendix 24)**, which is consistent with the binding values of prior OSBP orthologs that were determined using similar techniques.[221,223,229] Competitive binding experiments of non-radioactive 25-OHC with the radioactive [^{3}H]-25-OHC

compound indicate that the K_i, 25 ± 6 nM, which is similar to the [^{3}H]-25-OHC OSBP K_D (**Figure 9 and Appendix 25**). We observed the same relationship when we studied ORP4L, the K_i of 55 ± 8 nM (**Figure 9 and Appendix Figure 25**)is consistent with the K_D of 54 ± 23 nM, which was previously determined.[19]

2.3.2 ORPphilins: OSW1 and Itraconazole Do Not Bind to OSBP or ORP4L in a Similar Manner

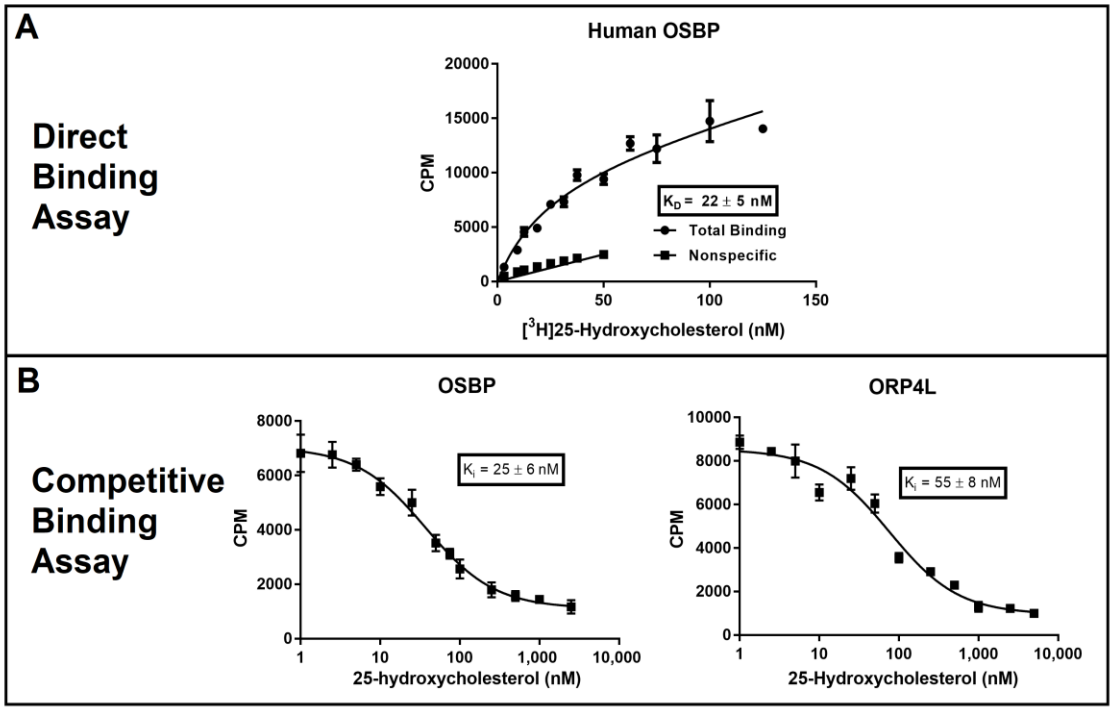

Figure 9: OSBP and ORP4L Members Bind 25-Hydroxycholesterol at Low Nanomolar Levels

Representative binding curves showing (A) a direct [^{3}H]-25-hydroxycholesterol binding assay of Human OSBP (K_D of 22 ± 5 nM) showing that 25-hydroxycholesterol is a high-affinity ligand, and (B) competitive binding assays of 25-hydroxycholesterol against [^{3}H]-25-hydroxycholesterol with OSBP or ORP4L generated K_i values, which matched their reported K_D values. (A and B) K_D and K_i values are mean ± s.d. from at least three independent experiments.

Previously, OSW-1 was shown to compete for 25-OHC binding to rabbit OSBP and human ORP4L.[19] Rabbit and human OSBP have 98% amino acid sequence similarity,

and they appear to bind compounds with nearly similar affinities.[19,221,222] OSW-1 binds human OSBP with a K_i of 9 ± 7 nM, which is slightly lower than the K_i against rabbit OSBP of 26 ± 9 nM.[19] For ORP4L, OSW-1 has K_i value of 40 ± 10 nM, which holds with the previously determined value of 54 ± 20 nM.[19] Overall, these results show that OSBP and ORP4L are responding to the binding assay as expected (**Figure 10 and Appendix Figure 26**).

Previous research shows that ITZ binds directly to OSBP (K_D = ~430 nM); however, this experiment did not determine if ITZ binds competitively with 25-OHC.[101] Also, ITZ is suspected to be a ligand for ORP4L, but there are no reported binding experiments.[101] ITZ does not show strong competitive binding with 25-OHC binding in OSBP. At best, the binding experiments indicate that ITZ is a low-affinity compound for OSBP with a K_i that is greater than 90 μM. Also, ITZ shows no competitive inhibition for ORP4L, (**Figure 10 and Appendix Figure 27**). It was not possible to fully establish the bottom of the competition binding curve due to poor solubility of ITZ. Increasing concentrations of ITZ beyond 100 μM led to an increased error in the binding curves. Our binding experiments show a much weaker OSBP K_i than what the previously reported OSBP K_D.[101] While this result seems contradictory; a possible explanation is that ITZ and 25-OHC do not bind on the same positions on OSBP. Likewise, while it appears that ITZ does not bind ORP4L, the assay only shows that the compound does not inhibit 25-OHC-

ORP4L binding and it is still possible that ITZ binds ORP4L.

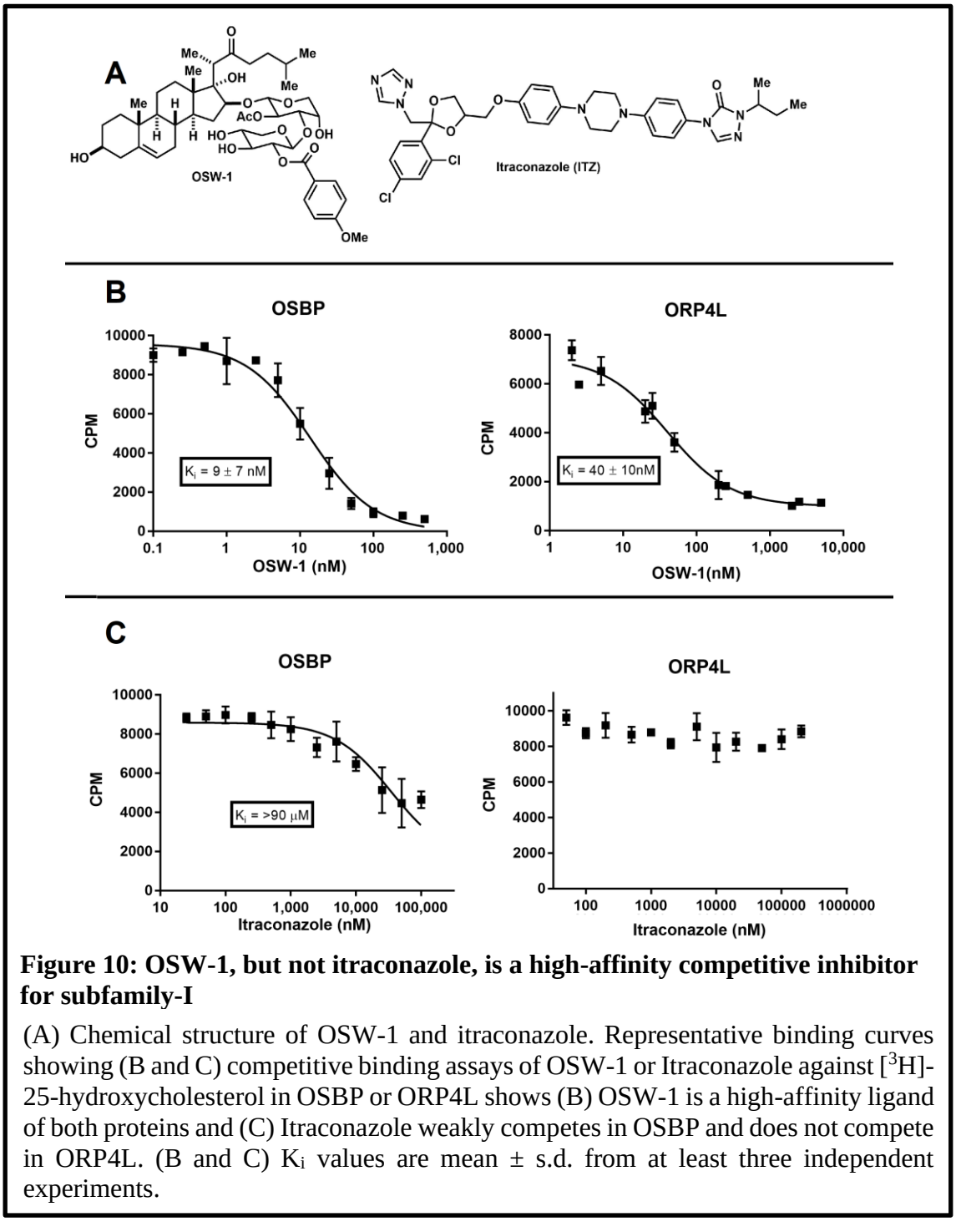

Figure 10: OSW-1, but not itraconazole, is a high-affinity competitive inhibitor for subfamily-I

(A) Chemical structure of OSW-1 and itraconazole. Representative binding curves showing (B and C) competitive binding assays of OSW-1 or Itraconazole against [^{3}H]-25-hydroxycholesterol in OSBP or ORP4L shows (B) OSW-1 is a high-affinity ligand of both proteins and (C) Itraconazole weakly competes in OSBP and does not compete in ORP4L. (B and C) K_i values are mean ± s.d. from at least three independent experiments.

2.3.3 Oxysterols Reveal hydroxylation and Stereochemistry Affect Competitive Binding to OSBP or ORP4L

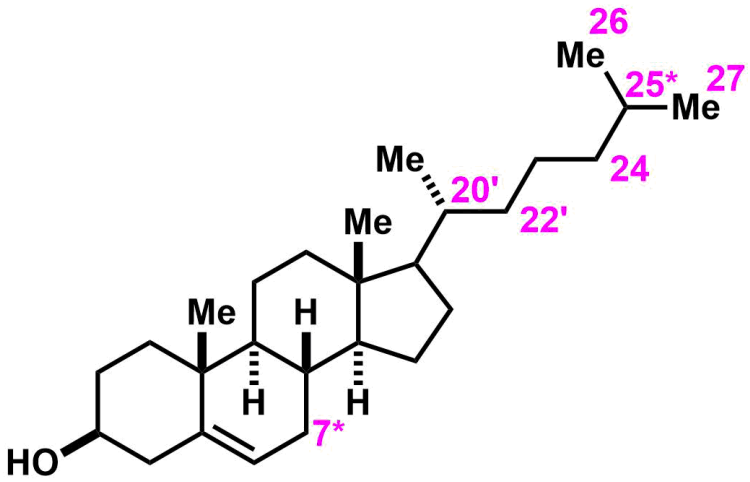

Figure 11: Oxysterol Hydroxylation Substitution Positions

Each primary oxysterol that was tested had a hydroxyl on one of the numbered carbons. The secondary oxysterols had two hydroxyls and are noted with an asterisk or an apostrophe.

The side chain hydroxylation of oxysterols has been indicated as being important in the oxysterol binding to OSBP and ORP4L, but side chain hydroxylation has not been systematically profiled to determine the structure-activity relation (SAR) of bind to OSBP and ORP4L.[199,223] To determine the importance of the side chain hydroxyl in interacting with OSBP or ORP4L, several oxysterols were tested in the [^{3}H]-25-OHC inhibition binding assay which produced inhibition binding constants (K_i values) for each compound. The initial oxysterols tested are 20-hydroxycholesterol (20-OHC), 22-hydroxycholesterol (22-OHC), 24-hydroxycholesterol (24-OHC), and 27-hydroxycholesterol (27-OHC) (**Figure 11**). These compounds vary from 25-OHC through the position of the hydroxyl group on the side chain; in the case of 24-OHC and 27-OHC, the hydroxylation position is one carbon removed from the position in 25-OHC. When possible, the commercially available stereoisomers of these oxysterols were tested.

The oxysterols were run in triplicate independent experiments to produce averaged K_i values (**Table 1**).

Table 1: Observed Ligand Binding Data in OSBP and ORP4L Measured by Displacement of [^{3}H]-25-Hydroxycholesterol

Oxysterol Ligands	OSBP K_i (nM)	ORP4L K_i (nM)
20(*S*)-Hydroxycholesterol	140 ± 30	320 ± 90
22(*R*)-Hydroxycholesterol	>27000	>53000
22(S)-Hydroxycholesterol	>28000	>3000
24(*R*)-Hydroxycholesterol	120 ± 60	>1000*
24(*S*)-Hydroxycholesterol	320 ± 80	340 ± 140
25(*R*),27-Hydroxycholesterol	70 ± 20	>680*
25(*S*),27-Hydroxycholesterol	160 ± 70	>870
7a,25-Dihydroxycholesterol	80 ± 40	90 ± 60
20(*R*),22(*R*)-Dihydroxycholestol	>12000	>16000

* indicates majority of curves were non-sigmoidal

The results of inhibition binding experiments to OSBP and ORP4L revealed that the positioning and stereochemistry of hydroxylation are important in protein interactions. Moreover, minor alterations to side chain hydroxylation dramatically impacted each protein. 24(*R*)-OHC binds OSBP with a K_i of 120 ± 60 nM, which is approximately a 4-fold reduction in inhibition binding compared to 25-OHC (see **Appendix Figure 28**). The epimer of 24(*R*)-OHC, 24(*S*)-OHC interacts with OSBP with a ~2.5-fold higher K_i of 320 ± 80 nM. For ORP4L, the 24(*R*)-OHC inhibition binding curves did not produce interpretable inhibition binding results. The 24(*R*)-OHC inhibition binding results failed to produce a sigmoidal response indicative of single-site inhibition. Instead, the curve flattens out in the middle and fails to drop to the minimal level expected at high concentrations. However, the 24(*S*)-OHC inhibition binding curves displayed normal sigmoidal inhibition curves with, ORP4L, producing a K_i value of 340 ± 140 nM (**Table 1 and Appendix Figure 29**), which suggest that the abnormal inhibition binding

of 24(*R*)-OHC to ORP4L is indicative of a more complicated interaction of 24(*R*)-OHC with ORP4L protein.

In OSBP, the K_i for 25(R),27-OHC is 70 ± 20 nM. However, we report a lower interaction for 25(*S*),27-OHC in OSBP (K_i = 160 ± 70 nM). In ORP4L, 25(*S*),27-OHC appears to be a weak micromolar competitive inhibitor and a K_i value could not be determined. Similarly, 25(*R*),27-OHC did not produce a sigmoidal inhibition curve for inhibition binding with ORP4L. Binding curves for 25(*R*),27-OHC and 25(*S*),27-OHC to OSBP or ORP4L are found in the Appendix (**Figure 30 and Figure 31**).

[^{3}H]-22(*R*)-OHC is a high-affinity ligand for ORP1 and ORP2 (subfamily-II) and has been shown to bind OSBP weakly.[145,203,204] In the [^{3}H]-25-OHC competitive binding assay, 22(*R*)-OHC displays low-affinity interactions with an apparent K_i value of >36 μM for OSBP. There was no indication of interaction between 22(*R*)-OHC and ORP4L. Similarly, 22(*S*)-OHC produced K_i values of >38 μM for OSBP but did show a higher affinity interaction with ORP4L of ~3.4 μM. 22(*R*)-OHC. These results show that unlike the other side hydroxyl positions at C20, C24, C25, and C27, hydroxylation at the C22 is not well tolerated for OSBP and ORP4L competitive binding. Binding curves for 22(*R*)-OHC and 22(*S*)-OHC to OSBP or ORP4L are found in the Appendix (**Figure 32 and Figure 33)**

Unlike 22-OHC, 20(*S*)-OHC interacts with OSBP with a K_i of 140 ± 30 nM and ORP4L with a K_i of 320 ± 90 nM in the binding assay.[67] These results indicate that the subfamily-I ligand binding domain (LBD) has an additional hydroxyl binding pocket capable of high-affinity interactions with the 20-hydroxyl position, which is consistent with crystallographic data from yeast ORP LBD.[37] Moreover, 20(*S*)-OHC has been

shown to bind OSBP from other species, but these are the first reported for interactions of 20(*S*)-OHC with human OSBP and ORP4L.[17,19,139,199] Binding curves 20(*S*)-OHC to OSBP or ORP4L are found in the Appendix (**Figure 34**).

Oxysterols with additional oxidation at positions other than the side chain, such as the C7 position of the B-ring, have not been extensively tested for binding to the OSBP/ORPs. Previously published reports indicate that cholesterol and oxysterols that have hydroxyls or carbonyl groups at C7 can interact with some OSBP/ORPs.[37,196,223] 7α,25-OHC is an oxidized form of 25-OHC that has a hydroxyl at the C-7 position in the (*S*)-configuration. 7α,25-dihydroxycholesterol (7α,25-OHC) interacts with OSBP with a K_i of 80 ± 40 nM, and ORP4L bound 7α,25-diOHC with a K_i of 90 ± 60 nM. These inhibition binding results are consistent to previously reported results of 7-keto-25-hydroxycholesterol interacting with mouse OSBP.[223] These results indicate that substitutions to the C7 position of the B-ring of the oxysterols are accommodated in OSBP and ORP4L binding. Binding curves 7α,25-OHC to OSBP or ORP4L are found in the Appendix (**Figure 35**).

Oxysterols with multiple hydroxyls on the side chain were also tested for interactions with OSBP or ORP4L. Testing 20(*R*),22(*R*)-dihydroxycholesterol, also named Oxy-16, shows that hydroxylation at the C22 detrimentally overrides the positive effects of C20 hydroxylation on OSBP or ORP4L interactions. Oxy-16 is a commercially available compound that was initially believed to be a Hedgehog antagonist. 20(*R*),22(*R*)-dihydroxycholesterol shows weak binding with K_i values of 26 μM for OSBP and 3.6 μM for ORP4L. The binding curves for 20(*R*),22(*R*)-dihydroxycholesterol to OSBP or ORP4L are found in the Appendix (**Figure 36**). 5α-hydroxy-6-ketocholesterol

(5αOH6KC) is a metabolite formed when cholesterol is exposed to ozone.[77] This compound is generally found in lung epithelial cells.[77] It was determined that 5αOH6KC has very weak to no competitive binding against OSBP (**Appendix Fig 37)**. Hydroxylation at the C5 and C6 positions does not provide high-affinity OSBP interaction; unlike the at other positions that enhance OSBP binding, such as the C25 position. 19-Hydroxycholesterol is an oxysterol with the hydroxyl on the steroidal core, not the side chain. In the [^{3}H]-25-OHC competitive binding assay 19-OHC interferes with the binding assay, appearing to be an allosteric enhancer of OSBP. However, the increasing radioactivity also appears in experiments with LacZ, which suggest that 19-OHC is forming micelles that prevent the [^{3}H]-25-OHC from adsorbing to the charcoal/dextran (**Appendix Figure 38**). We cannot determine if 19-OHC is a competitive ligand for OSBP.

2.3.4 20(S)-Hydroxycholesterol and 7α,25-Dihydroxycholesterol Induce OSBP Cellular Localization Similar to 25-Hydroxycholesterol

Upon cellular treatments with established ligands like 25-hydroxycholesterol, OSBP has been observed to change cellular localization patterns.[19,101,198] Binding a ligand alters OSBP localization from a diffuse ER and cytoplasm pattern to strong localization near the Golgi.[19,101,198] The changes in OSBP localization upon cellular treatment is an important confirmation that interactions measured in the *in vitro* assay also exist in cells. Cells were treated with multiple oxysterols, which interact with OSBP in the [^{3}H]-25OHC competitive ligand binding assay, to detect any changes in OSBP localization (**Figure 12**). For OSBP cellular experiments, 25-OHC is typically dosed at 10 μM even though the K_D for OSBP is ~ 20 nM, which is required due to the compound not being specific

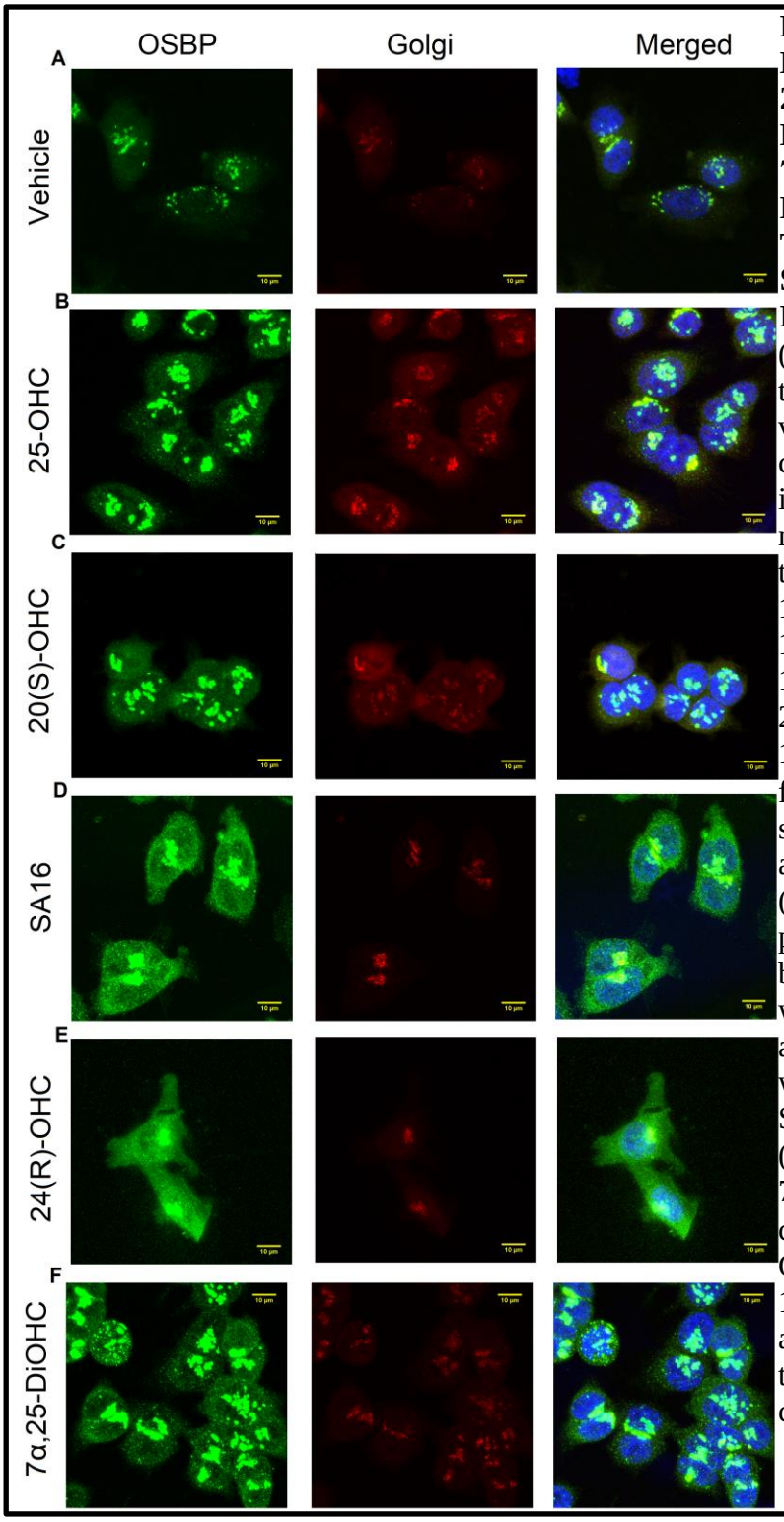

Figure 12: 25-Hydroxycholestolerol, 20(S)-Hydroxycholesterol, and 7α,25-Dihydroxycholesterol Treatments Induce Similar Cellular OSBP Localization Patterns (A-F) OSBP (green) and trans-Golgi (red) were visualized in HCT-116 cells using immunofluorescence microscopy. Cells were treated with vehicle (A), 10µM 25-OHC (B), 10µM 20(*S*)-OHC (C), 10µM SA-16 (D), 10µM 24(*R*)-OHC (E), and 10µM 7α,25-DiOHC (F) for 4 hours and then stained using primary antibodies for OSBP (green) and trans-Golgi protein TGN46, followed by secondary staining with fluorescent antibodies. Nuclei (blue) were stained with DAPI. Scale bars are 10 µm. (C&F) 20(*S*)-OHC and 7α,25-DiOHC show clustering and an increase OSBP signal. (D&E) SA-16 and 24(*R*)-OHC show an increased OSBP signal that is more dispersed compared to the controls.

for OSBP and to overcome limited cellular uptake from media.[19] Moreover, HCT116

adenocarcinoma cells treated with 10 μM of either 20(*S*)-Hydroxycholesterol (OSBP K_i = 140 ± 30 nM), sterol analog 16 (SA-16) (OSBP K_i = 890 nM) (see **Section 2.3.5**, **Fig 14**), 24(*R*)-Hydroxycholesterol (OSBP K_i = 120 ± 60 nM), 7α,25-dihydroxycholesterol (OSBP K_i = 80 ± 40 nM), or 25-Hydroxycholesterol (OSBP K_i = 25 ± 6 nM). Compared to the ethanol vehicle control, the oxysterol treatments increased the intensity of the OSBP fluorescent signal. This effect may be due to ligand binding enhancing the primary OSBP-antibody binding to the protein. Previous OSBP imaging reports used different antibodies that are not commercially available. The immunofluorescent results indicate that 20(*S*)-OHC, and 7α,25-dihydroxycholesterol cause OSBP to cluster more at the Golgi and produces a stronger fluorescence signal, which closely resembles the pattern of 25-OHC. In contrast, 24(*R*)-OHC did not cause a similar localization pattern, despite having a similar Ki to 20(*S*)-OHC. SA-16, which is a compound with the lowest inhibition binding to OSBP, did not a strong localization pattern. Repeat micrographs of 20(*S*)-OHC, 7α,25-diOHC, 25-OHC are also shown (**Appendix Figure 39**).

2.3.5 Structure-Activity Relationship of 20-Hydroxycholesterol Analogs to OSBP or ORP4L using the [^{3}H]-25-Hydroxycholesterol Binding Assay

Determining the structure-activity relationship (SAR) of oxysterol binding to OSBP or ORP4L requires compounds with specific structural features designed to probe the compound-protein interaction. A small library of compounds based on the 20-OHC scaffold was synthesized and tested for interaction to OSBP or ORP4L with the [^{3}H]-25-OHC competition binding assay. We chose 20-OHC as the parent compound because it performs well in the [^{3}H]-25-OHC binding assay with OSBP (K_i of 140 ± 30 nM) and ORP4L (K_i = 320 ± 90 nM) making it a reference point for our analogs. Unlike the other

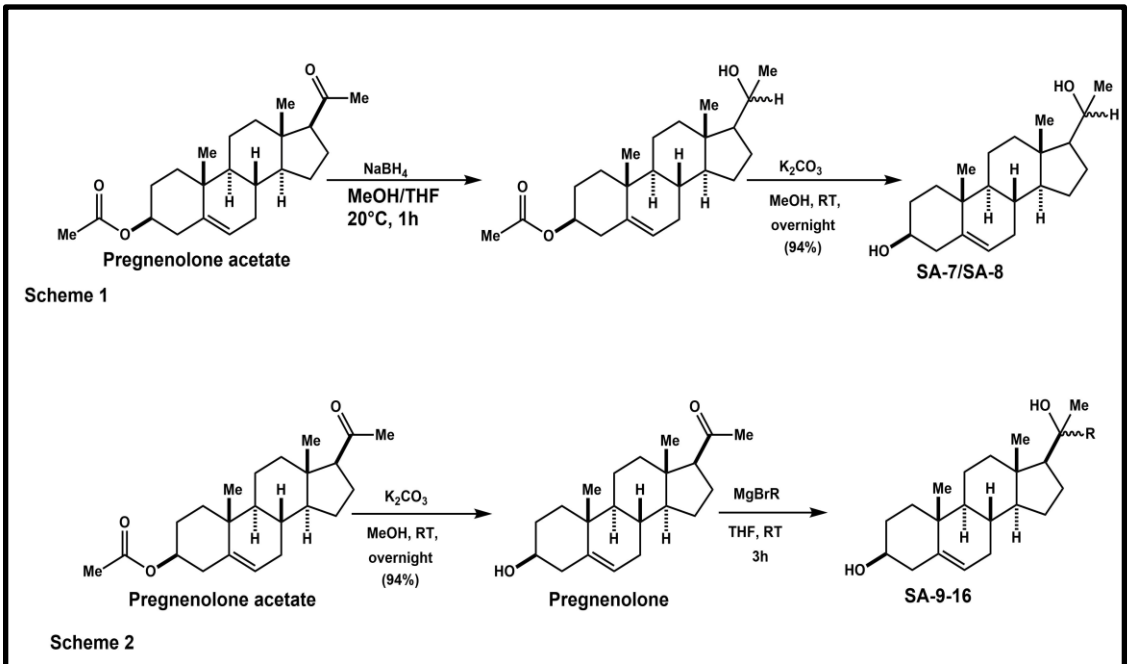

Figure 13: Synthetic Schemes for 20-Hydroxycholesterol Analogs

Scheme 1: Reduction of pregnenolone acetate with NaBH4 followed by removal of the acetate with K_2CO_3, which produces analogs SA7 (R-epimer) and SA8 (S-epimer).
Scheme 2: The acetate is removed, followed by the addition of the alkyl group via the Grignard reaction, which produced analogs SA-9 to SA-16

high-affinity oxysterols, 20-OHC has its hydroxyl (C20) in the between the steroidal core and the isohexyl side chain (**Figure 11**), which allows us to create 20-OHC analogs that have truncated or modified side chains. The 20-OHC analogs made have side chains of different length and branching chains (**Table 2**). The shortest analogs were synthesized by reducing and deprotecting pregnenolone acetate (**Scheme 1, Figure 13**). The remaining analogs are accessed with Grignard reactions on the C20-ketone of pregnenolone, which allows us to use alkyl magnesium bromide reagents to produce compounds that have different hydrocarbon side chains (**Scheme 2, Figure 13**).

The sterol analog (SA) compounds were tested for their ability to displace [^{3}H]-25-hydroxycholesterol (**Table 2**). SA-7, (*R)*-pregenolol, and SA-8, (*S)*-pregenolol, have

a hydrogen atom instead of an isohexyl sidechain and show no competitive binding to either OSBP or ORP4L at any concentration below 100 μM. The remaining analogs, which have alkyl side chains of different lengths, show differing degrees of competitive binding to OSBP and ORP4L. Binding curves for SA-7 and SA-8 to OSBP or ORP4L can be found in the Appendix (**Figure 40 and Figure 41)**. SA-9 has an ethyl side chain with a C20-(*S*)-configuration. SA-9 only showed partial competitive binding with 25-OHC at the highest concentration of 100μM; binding curves are found in the Appendix (**Figure 42**). SA-10, (*R*) epimer with an ethyl side chain, was not produced at high enough levels to test in the binding assay. SA-11 ((*S*)-epimer) and SA-12, ((*R*)-epimer) have isobutyl side chains. These compounds show some inhibition binding in the micromolar range for OSBP and ORP4L, but the competitive binding was not strong enough to fully determine binding constants because the curves failed to bottom out at 100 μM. Binding curves for SA-11 and SA-12 to OSBP or ORP4L are found in the Appendix (**Figure 43 and Figure 44)**.

SA-16 possess an isopentyl sidechain, instead of an isohexyl, that is in the (*S*)-configuration. Out of all the analogs, SA-16 was the analog with the highest competitive affinity to both OSBP and ORP4L. Compared to the K_i values for the parent compound 20(*S*)-OHC [OSBP K_i = 140 ± 30 nM; ORP4L K_i = 320 ± 90 nM], SA-16 is a weaker competitive inhibitor. However, SA-16 does tend to compete for 25-OHC better in OSBP (K_i = 900 nM) than with ORP4L (K_i = 2.0 ± 0.5 μM), the binding curves are found in the Appendix (**Figure 45**). The yield of SA-17, (*R*) epimer, was not at high enough levels to test in the binding assay. Nonetheless, these experiments show that the presence of the

isohexyl sidechain is necessary to have optimal competitive binding to OSBP and ORP4L.

SA-13 ((*S*)-epimer) and SA-14 ((*R*)-epimer) have octyl side chains, which make them the largest analogs we generated. SA13 and SA14 show partial inhibition binding of [^{3}H]-25-OHC at high micromolar concentrations; the lack of complete inhibition binding curve over the concentrations tested prevents the generation of Ki values. SA-13, the (*S*)-analog, was indicated to have stronger interactions than SA-14, the (*R*) analog. Binding curves for SA-13 and SA-14 to OSBP or ORP4L can be found in the **Appendix** (**Figure 46** and **Figure 47)**. These results show that a full isohexyl side chain is necessary for optimal oxysterol binding and that a long, straight-chain alkyl group disrupts the interaction.

Table 2: Observed Ligand Binding Data of 20-Hydroxycholesterol Analogs (SA-7 to SA-16) in OSBP or ORP4L. Measured by Displacement of [^{3}H]-25-Hydroxycholesterol

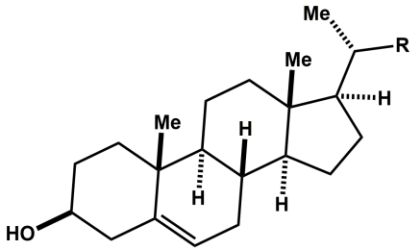

SA compound

Analog	R Group	OSBP (K_i)	ORP4L (K_i)
SA7	R= H (R)	N.B.	N.B.
SA8	R= H (S)	N.B.	N.B.
SA9	R= Me (R)	>28000 nM	>28000 nM
SA10	R= Me (S)	No data	No data
SA11	R= Me (R) Me	>22000 nM	>29000 nM
SA12	R= Me (S) Me	>57000 nM	>41000 nM
SA13	R= (R) Me	>12000 nM	>19000 nM
SA14	R= (S) Me	>95000 nM	>89000 nM
SA15	R= Me (R) Me	No data	No data
SA16	R= Me (S) Me	~910 nM	~2000 nM

2.3.6 Screening Non-oxysterol compounds for OSBP or ORP4L via competitive inhibition of 25-Hydroxycholesterol Binding

To identify novel OSBP or ORP4L ligands, we screened eight structurally diverse steroidal compounds for inhibition binding in the [^{3}H]-25-OHC competitive binding assay (**Figure 14**). Compound SA-2 is 25-hydroxycholesterol with the C5-C6 alkene reduced and a trans relative stereochemistry between the A and B rings. SA-2 has a K_i of approximately 28 nM against OSBP, and a K_i of 35 ± 4 nM against ORP4L (**Figure 14**). SA-2 binding curves can be found in the Appendix (**Figure 48**). This discovery means

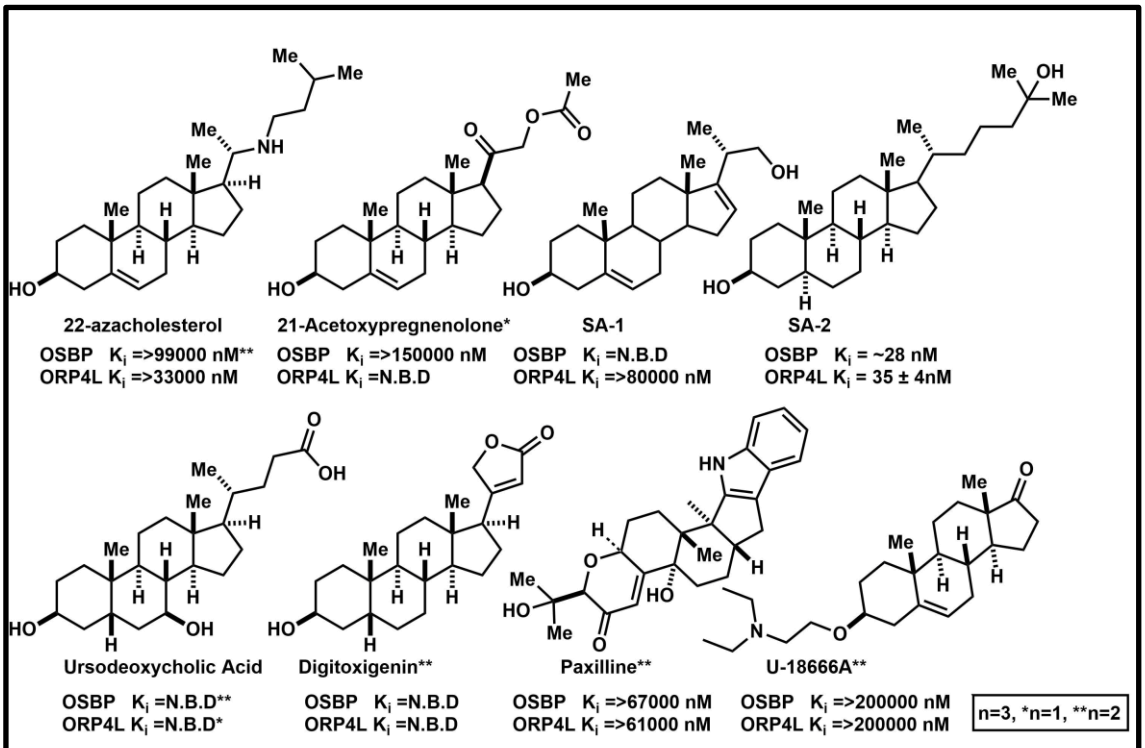

Figure 14: Non-oxysterol Steroidal Compounds Tested in the Competitive Binding Assay

Structurally diverse set of steroidal compounds that were screened against OSBP or ORP4L in the competitive [^{3}H]-25-hydroxycholesterol binding assay. SA-2 demonstrated high-affinity competitive binding. Compounds that were not tested in triplicate are noted with an * or **. K_i values are mean ± s.d. from at least three independent experiments.

that future steroidal compounds that target subfamily-I can use the more stable and simplified saturated compounds.

SA-1 is a steroidal compound with a truncated side chain, a C22-hydroxyl, and a C16-C17 alkene in the steroidal D-ring. The SA-1 compound has the potential to be the parent compound for novel ORPphilins. SA-1 did not interact with OSBP at any concentration tested. For ORP4L, SA-1 began to displace 25-OHC past 10 μM, but only partial inhibition was present at 100 μM; binding curves can be found in the Appendix (**Figure 49**). SA-1 has features that we have determined to result in weak competitive binding to subfamily-I, primarily it has no oxysterol side chain in OSBP and ORP4L binding. 21-acetoxypregnenolone was tested but did not show high-affinity binding with either protein (**Appendix Figure 50**). SA-1 and SA-2 are the only compounds that were synthesized in lab, the remaining compounds in this screen were purchased from commercial sources.

22-Azacholesterol (22-NHC) is reported to be a strong competitor for 20(*S*)-OHC binding in Smoothened in the Hedgehog pathway and screened this compound because 20(S)-OHC is high-affinity OSBP/ORP ligand.[65] 22-NHC shows micromolar competitive inhibition of >100 μM for OSBP and an apparent K_i of 53 μM for ORP4L. Binding curves for 22-NHC to OSBP or ORP4L can be found in the Appendix (**Figure 51**). The performance of 22-NHC in the binding is one of the few instances where a ligand potentially shows specificity for ORP4L over OSBP. Cholesterol is reported to be an OSBP and ORP4L ligand, but cholesterol did not show any inhibition binding for [^{3}H]-25-OHC in our assay, likely due to poor solubility or availability in the binding lysate.[195] The ability of 22-azacholesterol to participate in the [^{3}H]-25-OHC competition binding

assays suggests that the incorporation of the presence of the nitrogen at the 22-position gives the compound enough polarity to make it soluble in the lysate. The estimated logP of 22-NHC is 5.54, and the logP of cholesterol is 7.39. The interaction of 22-NHC with ORP4L, although weak, suggests that compounds incorporating nitrogen into oxysterol side chain could be used for OSBP/ORP binding.

U-18666A is a synthetic steroidal compound that induces a cellular phenotype similar to Niemen-Pick Type C disease, (**Figure 14**).[230] Multiple OSBP/ORP members have been shown to coordinate with the NPC1 protein or are involved in cholesterol transport that results in the NPC phenotype.[26,161,201,215] For this reason, U-18666A was tested to see if could bind OSBP and ORP4L. The compound shows an extremely weak to non-existent interaction in experiments with OSBP or ORP4L in the competitive binding assay; displacing 25-OHC at 200 μM. Binding curves for U-18666A to OSBP or ORP4L can be found in the Appendix (**Figure 52**). The possibility that U-18666A binds other OSBP/ORPs other than OSBP and ORP4L remains, mainly because other OSBP/ORPs have been shown to interact with NPC1.[26,161,201,215] Moreover, U-18666A has some structural similarities to the ORPphilin THEV2, and it is possible to modify U-18666A to become a more effective ligand.

Paxilline is a complex steroidal compound with biological effects that are unrelated to OSBP/ORP functions. However, paxilline shares some structural similarities to the ORPphilin compounds cephalostatin 1 and ritterazine B (**Figure 8, Chapter 1.3.4**).[231] The similarly between paxilline and the ORPphilins did not extend to ligand binding in OSBP or ORP4L. Paxilline competed with 25-OHC binding to OSBP with an approximate K_i of >100 μM and ORP4L with an approximate K_i of ~47 μM; the binding

assays were done in duplicate because of their low affinity (**Appendix Figure 53**). Like with 22-NHC, this compound seems to be more selective towards ORP4L, but both have high K_i micromolar values.

Ursodeoxycholic acid (UA) is a bile acid produced in nutria, beavers, and bears; its structure is an oxidized sterol with a C7 hydroxyl, a propionic acid side chain, and a saturated cis A-B ring fusion (**Figure 14)**.[232] The results show no competitive binding to either OSBP or ORP4L. The absence of binding is best explained by the structure of the steroidal core, which is bent due to the cis A-B ring fusion. Like UA, digitoxigenin has a cis stereochemistry at the ring fusion. Digitoxigenin also does not show competitive 25-OHC binding for OSBP in an initial experiment, and it was not tested for interactions with ORP4. Binding curves for UA and digitoxigenin can be found in the Appendix (**Figure 54 and Figure 55**).

Existing structural data on the yeast ORP ligand binding domain reveal that their binding pockets that can only accommodate linear compounds like cholesterol and ergosterol.[21] Assuming that this steroidal binding pocket is similar in the human OSBP/ORPs, it would explain why the bent cis-A-B ring fused steroidal compound would not be able to bind OSBP or ORP4L.[21,35]

2.3 Conclusion

This study focused on determining the structural activity relations required to interact with OSBP and ORP4L in our 25-hydroxycholesterol competitive binding experiments. We studied a variety of oxysterol compounds, including a small library of synthetic oxysterols made in the lab. Oxysterols with hydroxyls at C20, C24, C26, and C27 show strong interactions with OSBP producing binding curves with low nanomolar

K_i values. Oxysterols with hydroxylation at C22 is detrimental to competitive binding in both proteins. Oxy-16, the oxysterol which is hydroxylated at C20 and C22, has weak micromolar binding, which indicates that adverse effects of C22-hydroxylation override the positive effects of C20 hydroxylation. The stereochemistry of the sidechain hydroxyls also influenced competitive binding. The most noticeable effect on stereochemistry was the failure of the 24(*R*)-hydroxycholesterol and 25(*R*),27-hydroxycholesterol epimers to show binding to ORP4L, whereas 24(*S*)-hydroxycholesterol and 25(*S*),27-hydroxycholesterol does not produce competitive curves. However, even with OSBP, the K_i values were different between isomers. The synthetic 20-OHC analogs (i.e., SA7-SA16 compounds) revealed that the entire isohexyl sidechain needs to remain intact to have optimal competitive binding.

The compounds we tested indicate that the structure of the sterol core can affect whether a steroidal ligand can bind OSBP or ORP4L. Adding a hydroxyl at C7 is tolerable for competitive as was observed with 7α,25-dihydroxycholesterol. Moreover, an oxysterol that is reduced at the C5-C6 can still bind if A-B ring core is in the trans-configuration. The cis-configuration of the fused A-B ring core of a molecule produces a bent molecular shape that cannot be accommodated for competitive binding. These studies offer valuable information that will guide the design and development of selective OSBP/ORP targeting compounds. These results will be especially useful for on-going efforts to make new analogs of the OSW-1-compounds that selectively interact with OSBP or ORP4L.

2.4 Experimental Procedures:

2.5.1 Materials and Reagents

[^{3}H]-25-Hydroxycholesterol (25-OHC) was purchased from Perkin-Elmer. All the oxysterol compounds were purchased from Cayman Chemical and Sigma-Aldrich. Paxilline, U-18666A, and digitoxigenin were purchased from Cayman Chemical. 22-azacholesterol, 21-acetoxypregnenolone, pregnenolone acetate, and itraconazole were purchased from Sigma Aldrich. Norit SA2 charcoal was obtained from Cabot Corporation. Pregnenolone acetate and the alkyl halides used to generate the 20-hydroxycholesterol analogs were purchased from Sigma Aldrich. The OSW-1 compound used was obtained through total synthesis in the Burgett lab or from isolation from the natural source.

2.5.2 Plasmids and Cloning

Human OSBP was obtained in a pOTB7 vector from the Mammalian Gene Collection (Thermo Fisher). OSBP was PCR amplified to contain 5' NheI and 3' HindIII cut sites. The cDNA construct was cloned into the pcDNA 3.1/myc-His (-) C mammalian expression vector (Sigma-Aldrich). OSBP was cloned in a manner where OSBP expresses without the myc-His tag. The ORP4L construct containing 5' NheI and 3'HindIII cut sites was PCR amplified from HCT116 cDNA. The LacZ construct containing 5' NotI and 3' BamHI cut sites was PCR amplified from K-12 *E. coli* genomic DNA. The completed plasmids were propagated in DH5α *E. coli* and isolated through miniprep and maxiprep kits (Thermo Scientific). Gene sequences were verified through the Oklahoma Medical Research Foundation (OMRF).

2.5.3 Tissue Culture

HEK293T cells were grown in complete Dulbecco's Modified Eagle's Medium (DMEM) at 37°C. HCT116 cells were grown in complete McCoy's 5A Medium at 37°C. Cells were passaged using TrypLE™ Express Enzyme (ThermoFisher Scientific) for 10 minutes at 37°C.

Microscopy

50,000 HCT116 cells were seeded on glass coverslips in 12 well plates and incubated for 16 hours at 37°C. The cells were treated with vehicle or 10 μM of a compound and incubated for 4 hours at 37°C. The cells were fixed with 4% paraformaldehyde in PBS for 10 min. The cells then were washed with ice-cold 1% BSA in PBS 0.1% tween 20 (BSA/PBST) and permeabilized for 5 min with 0.5% Triton X-100 in PBS. The cells were then washed with PBS three times. Then blocked for 30 min at room temperature with BSA/PBST. The coverslips were then incubated overnight at 4 °C with a primary antibody solution (1:100 Novus Mouse α OSBP1 (1F2) NBP2-00935 and 1:500 for Novus Rabbit α TGN46 NBP1-49643) in BSA/PBST. The primary antibody solution was removed, and the coverslips were washed three times with 1X PBS. The secondary antibody (1:500 Abcam Goat α Mouse 488 and 1:500 Abcam Donkey α Rabbit 594) in BSA/PBST was added to the coverslips and incubated at room temperature, for 1 hour, in the absences of light. The secondary antibody solution is removed, and the coverslips are washed three times with BSA/PBST. The coverslips were additionally washed three times with 1X PBS before being soaked in a 300 nM DAPI solution for 10 minutes. The coverslips were mounted with Vecta-shield hard mounting media. The slides were incubated in the dark, at room temperature, for roughly 24 hours. The slides were stored

at -20°C. The images were generated with a Leica SP8 Scanning Confocal Microscope using an x63 glycerol/oil immersion objective lens. Imaging was done at the University of Oklahoma Samuel Roberts Noble Microscopy Laboratory.

Transfections and Protein Preparation

HEK293T cells were seeded at $4x10^6$ in 10 cm^2 plates and incubated at 37°C, for 24 hours. The day of the transfection, a 3 mL solution 24 µg of plasmid, opti-MEM (ThermoFisher Scientific), and Lipofectamine 2000 is prepared according to the manufacturer's instructions. The DMEM is removed and gently replaced with the transfection solution. The plate is incubated for 4 hours at 37°C. Then 12 mL of antibiotic-free DMEM is carefully added to the plate and is incubated for 42 hours. The transfection media is removed, and the cells are washed with cold PBS. The cells are lysed with 2 mL of solution at room temperature for 5 minutes shaking at 250 RPM. The lysis solution is composed of M-PER Mammalian Protein Extraction Reagent (ThermoFisher Scientific), 1x HALT protease inhibitor with EDTA (ThermoFisher Scientific), and 5mM DTT. The lysate is then centrifuged for 1 hour at 100,000 g at 4 ºC in a TLA-100.3 rotor (Beckman Coulter) in an Optima TLX ultracentrifuge. The protein concentration of the supernatant (S100 lysate) was determined using a Bradford assay. The S100 lysate was diluted to 0.2 mg/mL with binding buffer (50 mM HEPES pH 7.4, 50 mM KCl, 5 mM DTT, 1x HALT Protease Inhibitor with EDTA). Due to the high level of expression of OSBP in HEK293T, the 0.2 mg/mL OSBP tagless S100 protein lysate was then further diluted 1:4 with non-transfected HEK293T 0.2 mg/mL S100 lysate. The lysates were aliquoted, snap-frozen in liquid N2 and stored at –80 °C until use in the binding assay. When they are used, the lysates were quickly thawed on ice, with brief periods of hand warming.

2.5.4 [^{3}H]-25-Hydroxycholesterol Charcoal/Dextran Binding Assay

Preparation of the Charcoal/Dextran (C/D) Suspension

Successful use of this assay requires careful preparation of the charcoal-dextran to remove fine particles. The procedure to prepare the suspension is based on a protocol from Taylor and Kandutsch.[12] Between washes the charcoal is sedimented by centrifugation at 1000 g for 20 min. 1 g Norit SA2 charcoal (Cabott) is added test tube 15mL falcon tube and washed with 10ml of 1M HCl and followed with a wash of 10ml diH20. The charcoal is then washed with 10ml of 5% $NaHCO_3$ and followed with a wash of 10ml diH2O. The charcoal is then washed five times with 10ml of 5% Dextran 500,000 (Spectrum) in 10 mM Tris-HCl buffer, pH 8. The charcoal is then washed twice with 10ml of 10mM Tris-HCl and 3mM sodium azide buffer, pH 8, and stored at 4°C in 20 ml of 10mM Tris-HCl, 3mM sodium azide pH 8 buffer. The night before its use 1g of Dextran 500,000 was added to the charcoal and allowed to dissolve overnight.

Direct Binding Assay

One direct binding experiment, done with three technical replicates, requires binding lysate (~5.5 mL) that is prepared so that in a "V"-shaped 96-well plate, each well contains 60µL of 0.2 mg/mL S100 lysate, 7.5 µL 20% polyvinyl alcohol (PVA), 5.6 µL 2M KCl, 0.4 µL binding buffer, the total volume in the well is 73.5 µL. Then 1.5 µL serial dilutions in 100% ethanol, starting at 125nM, [^{3}H]-25-Hydroxycholesterol was added to the wells using a multichannel pipettor. For non-specific binding interactions, 1.5 µL serial dilution [^{3}H]-25-hydroxycholesterol combined 40x 25-hydroxycholesterol is added to an additional set of wells on the same plate. The saturation curve required 12 concentration points for specific binding and 8 concentration points for non-specific binding. Wells for

non-specific binding was not used for LacZ, the negative control. The assay was developed in the same way as the competitive assay and is described further down.

Competitive Binding Assay

One competitive binding experiment, done with three technical replicates, requires binding lysate (~2.8 mL) that is prepared so that in a "V"-shaped 96-well plate, each well contains ach well should contain 60µL of 0.2 mg/mL S100 lysate, 7.5 µL 20% PVA, 5.6 µL 2M aq. KCl, 20nM [^{3}H]-25-hydrocholesterol and binding buffer. The volume of the [^{3}H]-25-hydroxycholesterol ligand will vary depending on the stock concentration, the total volume in the well should be 73.5 µL. Eleven serial dilutions of the competitive, inhibitors that are dissolved in 100% ethanol (Oxysterols) or DMSO (ORPphilins), are added to wells using a multichannel pipettor. 25-hydroxycholesterol, the established high-affinity ligand, was used as a positive control.

For both competitive and direct, the assay is incubated for 16 hours at 4°C. Afterward, 60 µL of the binding lysate mixture was transferred to a new 96-well v-shaped plate containing 30 µL of room temperature Charcoal/Dextran. The plate was lightly agitated and incubated on a shaker at 250rpm at room temperature for 30 minutes. The plate was then spun at 1900xg for 15 minutes at 4°C. Then 30 µL of supernatant was transferred to OptiPlates (Perkin Elmer) containing 170 µL of Microscint-20 (Perkin Elmer). The plates were sealed with TopSealA-Films (Perkin Elmer). The plate was vortexed at max speed for one minute to ensure thorough mixing.

The data were analyzed with GraphPad Prism 7 using non-linear regression to analyze binding curves. Binding curves with R^2 values of 0.85 were the cutoff to report values. K_D and K_i values ± standard deviation were calculated from at least 3 biological

replicates. To determine the sampling size, we used a one sample t-test from our results ($P \leq 0.1$).

2.5.5 Western Blot

Overexpressed protein lysate concentration is determined through Bradford assay. 10µg of S100 lysate is loaded onto 7.5% or 10% SDS-PAGE gels and electrophoresed at 180 V for 50 min. Samples were transferred to nitrocellulose (Bio-Rad 1620112) using a Trans-Blot® Turbo™ unit at 1.3 A, 25 V for 15 min. The membrane was blocked with 5% milk protein 1X Tris-buffered saline with 0.2% Tween-20 (TBST) solution for 30 minutes. The membrane was washed 4 times, 5 min each, with 1X TBST. The membrane was incubated overnight at 4°C with a 1:2,000 dilution of mouse anti-OSBP (A-5) antibody (Santa Cruz Biotechnology) or a 1:25,000 dilution of a goat anti-myc (NB600-335) antibody (Novus), each in a 1% milk protein 1X TBST solution. The membrane was washed 4 times with 1X TBST. The membrane was incubated with 1:3000 dilution of a goat anti-mouse or a 1:5000 dilution of a donkey anti-goat antibody, each in a 1% milk protein 1X TBST solution for 30 minutes at room temperature. The blot is then washed 4 times with 1X TBST and 1 time with 1X Tris-buffered saline (TBS), 5 min each. The blots were incubated in Clarity™ ECL (Bio-Rad 1705061) and imaged on the Bio-Rad ChemiDoc™ Imaging System using the chemiluminescence setting. Ladder images True Blue™ Protein Ladder (Gold Biotechnology) were taken using the colorimetric setting. Examples of developed blots with merged ladders for ORP4L-myc-His, LacZ-myc-His and OSBP tagless are shown in the Appendix **(Fig 23)**.

2.5.6 General Method for the Synthesis of 20-Hydroxycholesterol Analogs

Pregnenolone Acetate Reduction and Deprotection

Pregnenolone acetate was reduced with 2 equivalents of $NaBH_4$ and 1 equivalent of $CeCl_3$ in MeOH/THF.[233,234] The acetate protecting group was removed with $K_2(CO)_3$, yielding SA-7 and SA-8. The compounds were purified using a Luna 5µm C8(2) 100Å Phenomenex semi-prep column, with different MeCN/0.1% formic acid in H_2O gradient in an LCMS-2020 system (Shimadzu). The structure of pregnenolone acetate and the purified products were determined through NMR and are shown in the Appendix (**Fig 56**, **Appendix Fig 57**, and **Appendix Fig 58**).

Grignard Reaction

The remaining analogs were synthesized with the Grignard reaction. Alkyl halides were reacted with magnesium metal to create Grignard reagents, which were then used to attack pregnenolone acetate. The acetate protecting group was removed with $K_2(CO)_3$, yielding the remaining analogs. The compounds were purified and isolated with an LCMS-2020 system (Shimadzu). The compounds were purified using a Luna 5µm C8(2) 100Å Phenomenex semi-prep column, with different MeCN/0.1% formic acid in H_2O gradient in an LCMS-2020 system (Shimadzu). The purified products were verified through NMR.

Chapter 3: Developing A Systematic Biochemical Approach to Study Ligand Binding to OSBP

Juan Nuñez*, Anh Le*, Paul Sims*, Naga Rama Kothapalli *, and Anthony Burgett*

*Department of Chemistry and Biochemistry, University of Oklahoma, 101 Stephenson Pkwy, Norman, Oklahoma, 73019, United States

Juan Nuñez was responsible for writing this chapter. He was responsible for all experiments and data analysis for this chapter, unless otherwise specified. Juan mentored undergraduates, Ms. Bliss Baird (OU F.Y.R.E), Ms. Courtney Martin (OU F.Y.R.E), and Mr. Matthew Finneran (OU Structural Biology R.E.U), in molecular biology to clone ORP genes into the mammalian expression vectors. Dr. Naga Rama Kothapalli mentored and assisted in protein purification. Dr. Paul Sims donated the Sephadex column and carried out the Ammonium Sulfate precipitation.

Chapter 3: Developing A Systematic Biochemical Approach to Study Ligand Binding to OSBP

3.1 Abstract

Oxysterol-binding protein (OSBP) is a lipid binding protein with a conserved ~50 kDa C-terminal ligand binding domain (LBD). The LBD can bind to an array of structurally-diverse lipid ligands including oxysterols and phospholipids. In cells, OSBP is reported to counter transport cholesterol and phosphatidylinositol-4-phosphate (PI4P) between the ER and Golgi membranes. Recently, OSBP was determined to be essential for the replication of a range of human pathogenic viruses. The ORPphilin compound OSW-1 is a complex steroidal compound fused with a disaccharide moiety that has anti-viral and anti-proliferative abilities. The anti-viral properties of OSW-1 are caused by inhibiting OSBP. OSW-1 binds to OSBP with a high-affinity (OSW-1 K_i = 9 ± 7 nM), which is measured through competitive inhibition binding assays with a tritiated 25-hydroxycholesterol (25-OHC), a known high-affinity OSBP ligand. The protein structure of human OSBP or OSBP-related proteins (ORPs) have not been determined, and therefore, there is limited information on how the OSW-1-compound interacts with OSBP on the molecular level. An understanding of the structure-activity relations (SAR) of OSBP and the OSW-1-compound interaction would allow for the design of improved OSW-1 analog compounds for potential anti-viral drug development. To better understand this interaction, a model of the OSW-1 compound binding to OSBP was generated to a diagram which key residues that are essential in OSW-1-OSBP interactions. We hypothesize that the structure of OSW-1 mimics both the steroidal and

PI4P binding to OSBP simultaneously. A series of OSBP residues important for interacting with the OSW-1, but not binding 25-OHC, were identified and mutated. The selected residues are thought to be important in mediating the contact between ORP proteins and PIPs. One OSBP mutant, OSBP H522A, was successfully tested in ligand binding assays, and the H522A mutant showed substantially reduced interactions with the OSW-1 compound supporting our model. Additionally, the SAR of OSW-1 and OSBP was further explored through the testing for binding interaction of a series of OSW-1-derived compounds to OSBP. Further, progress in the purification of overexpressed OSBP is detailed.

3.2 Introduction

3.2.1 The OSBP/ORP Ligand Binding Domain

The molecular level interactions of oxysterol binding protein (OSBP), and the OSBP-related proteins (ORPs), with ORPphilins, are not understood, but it is likely that they bind at the ligand binding domain (LBD). The OSBP/ORP LBD is the most common domain of this protein family.[21] The LBD is a large domain that can bind different type oxysterols and some phospholipids.[21] Unfortunately, there is no structural data for the human OSBP/ORPs. However, there is structural data for a few yeast OSBP/ORPs, including structures with bound ligands that are established ligands for the human OSBP/ORPs.[2,21] The structural data that is most relevant to OSBP is of yeast ORPs bound to 25-OHC or phosphoinositide-4-phosphate (PI4P).[21] In mammalian cells, OSBP counter transports cholesterol and PI4P between the ER and Golgi membranes; this lipid transport function between organelle is believed to be hijacked during viral replication to control lipid levels in viral replication organelles.[87,101,192] In experiments with OSBP,

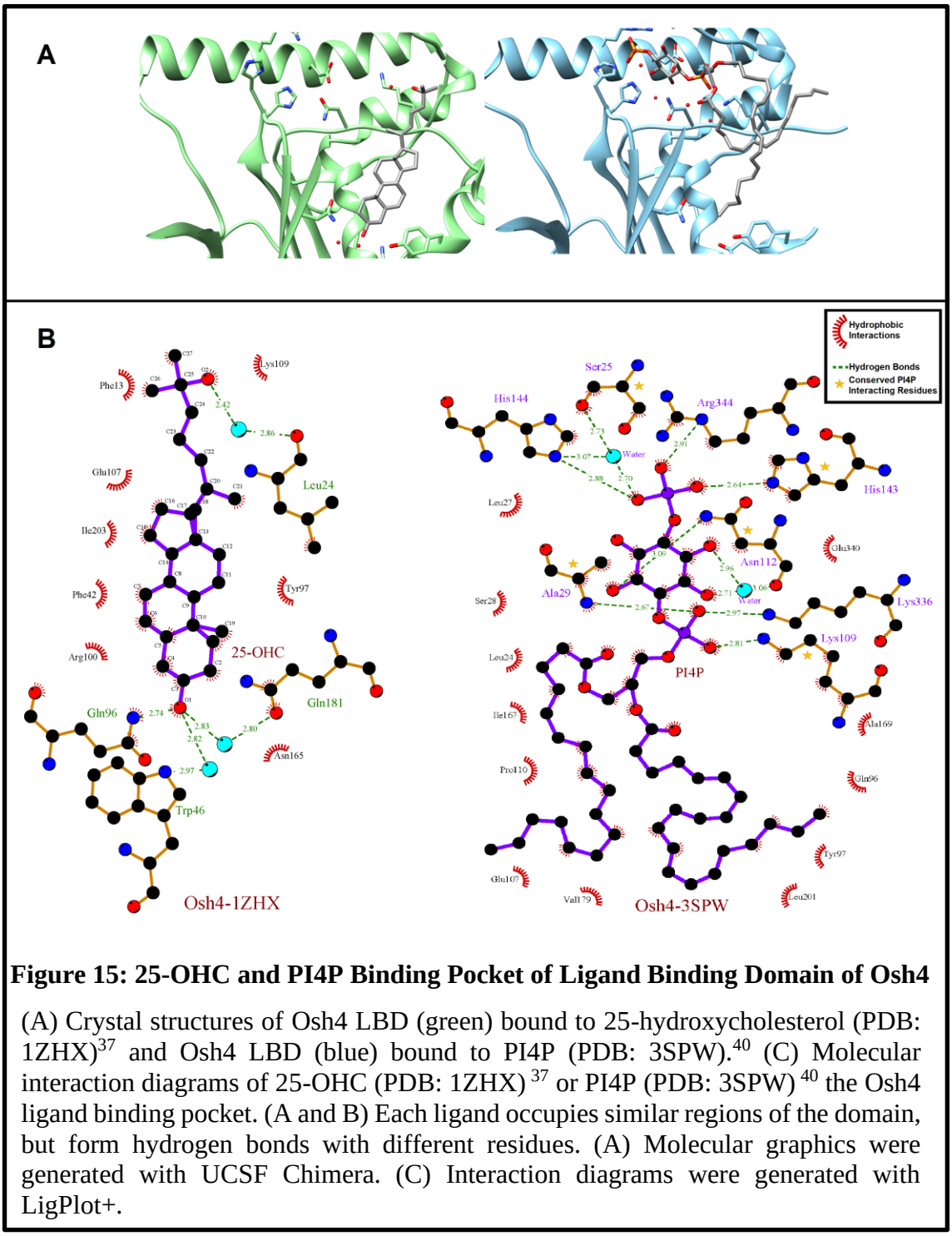

Figure 15: 25-OHC and PI4P Binding Pocket of Ligand Binding Domain of Osh4

(A) Crystal structures of Osh4 LBD (green) bound to 25-hydroxycholesterol (PDB: 1ZHX)[37] and Osh4 LBD (blue) bound to PI4P (PDB: 3SPW).[40] (C) Molecular interaction diagrams of 25-OHC (PDB: 1ZHX) [37] or PI4P (PDB: 3SPW) [40] the Osh4 ligand binding pocket. (A and B) Each ligand occupies similar regions of the domain, but form hydrogen bonds with different residues. (A) Molecular graphics were generated with UCSF Chimera. (C) Interaction diagrams were generated with LigPlot+.

OSW-1 competitively inhibits the 25-hydroxycholesterol in binding assays and inhibits the exchange of sterols and PI4P between membranes in lipid exchange experiments.[19,87]

These experiments suggest that OSW-1 inhibits both the binding interactions of sterols and PIPs.

Currently, there are only four yeast ORP LBD structures that have been solved: Osh1, Osh3, Osh4 and Osh6.[21] The Osh3 LBD is closest to OSBP in amino acid sequence similarity, but it can only bind phospholipids making it challenging to model the steroidal OSW-1.[39] However, Osh4 can bind both PI4P and various sterols, and it can exchange cholesterol for PI4P in liposomal lipid exchange experiments.[37,40,42] In particular, Osh4 has been crystallized with 25-OHC (PDB: 1ZHX) and Osh4 with PI4P (PDB: 3SPW) (**Figure 15**). [37,40] In Osh4, 25-OHC, and PI4P occupy the same hydrophobic regions of the ligand binding domain, but these molecules use different residues to form hydrogen bonds (**Figure 15**). Moreover, the residues that form stabilizing interactions with PI4P are conserved in both yeast and human LBDs.[21] Studies have shown that it is possible to generate OSBP mutants that have some of these highly conserved basic residues (H522, H523, and K524) replaced with alanine residues, which remove the ability of the mutant OSBP to extract PI4P from membranes but preserves their ability to extract sterols, in lipid exchange assays.[87,192] However, these OSBP mutants have not been tested for direct OSW-1 or 25-OHC binding.[139,235]

3.2.2 Structure of OSW-1

OSW-1 is a steroidal saponin natural product with potent antiproliferative and antiviral properties, which exhibits its cytotoxic effects by inhibiting OSBP function.[19,86] OSW-1 has an aglycone consisting of an oxidized sterol connected through the C16-hydroxyl to a para-methoxybenzoate-containing disaccharide moiety.[79] Since

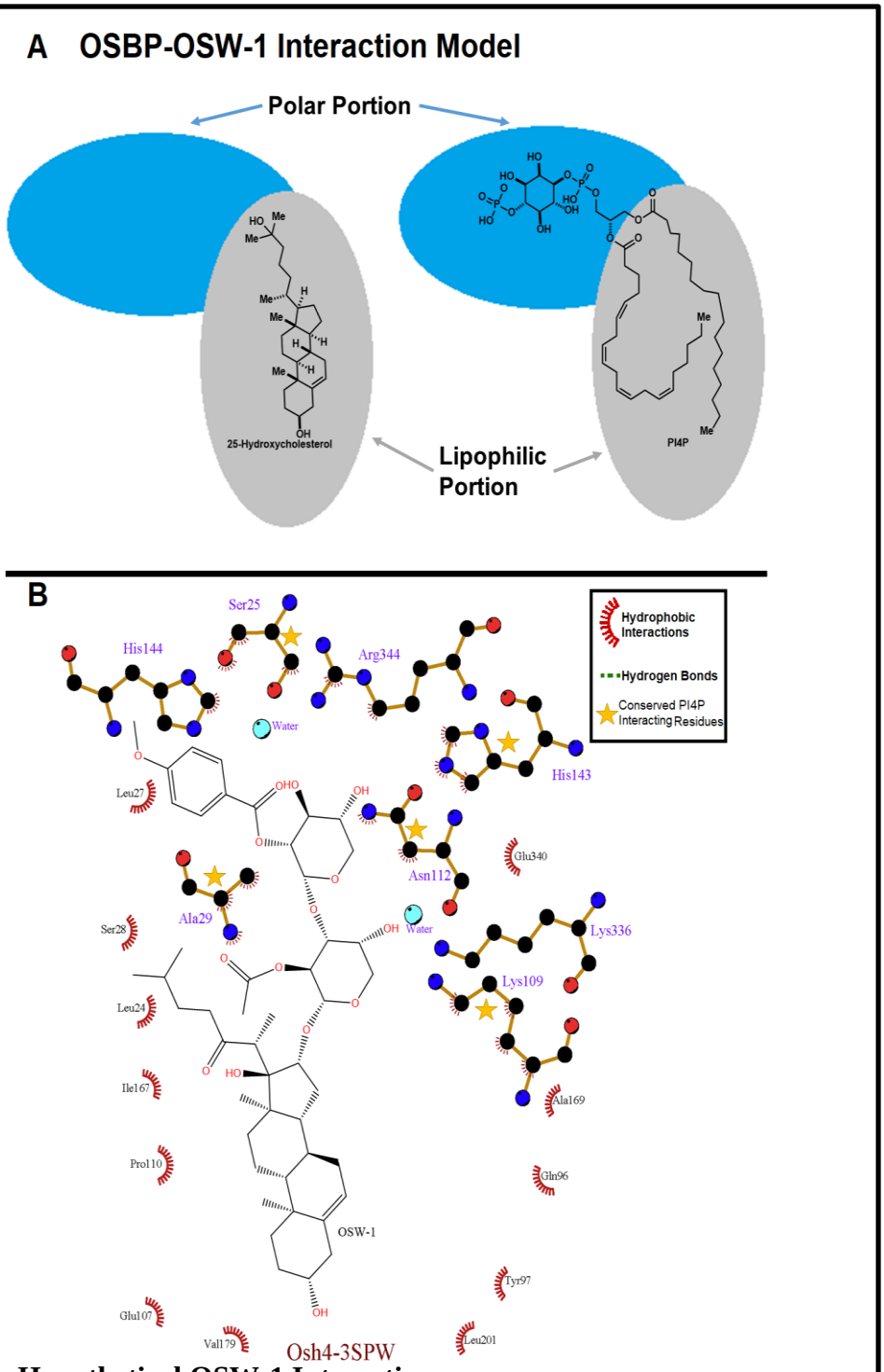

Figure 16: Hypothetical OSW-1 Interaction
(A) Simplified diagram of an OSBP/ORP LBD bound to an oxysterol or PI4P (B) 2D molecular interaction the Osh4 binding pocket (PDB: 3SPW)[40] with OSW-1 replacing PI4P, showing potential residues that can interact with OSW-1. The interaction diagram was generated with LigPlot+, using (PDB: 3SPW) [40] and the PI4P was replaced with a 2D structure of OSW-1 (ChemDraw).

OSW-1 has a steroidal core it is expected that part of the molecule occupies the lipophilic portion of the LBD that is normally occupied by 25-OHC or the acyl chains of PI4P (**Figure 16**). However, it is uncertain where the disaccharide moiety and the para-methoxybenzoate are placed during binding.

It is possible that the isohexyl side chain and the arabinose-xylose moiety have torsional freedom that could allow OSW-1 to adopt conformations that could allow it to occupy regions of the binding pocket that PI4P would typically occupy. More specifically OSW-1 could interact with both the oxysterol binding pocket and with the residues conserved for PI4P binding (**Figure 16**). It is possible to use mutations to determine important amino acid residues that affect OSW-1 binding that will not affect binding to 25-hydroxycholesterol (25-OHC). Through these experiments, we can develop detailed diagrams that establish which residues are essential in the OSW-1-OSBP interaction (**Figure 16**). Also, OSW-1 has two hydroxyls on the xylose part of the disaccharide moiety that is not required for high-affinity binding, which can be useful to produce fluorescent compounds.[19] However, these functional groups also beg the question of how OSW-1 is interacting with OSBP. OSW-1 is a complex, flexible molecule that can adopt many conformations to bind the pocket, and these mutations will allow us to begin to understand this type of interaction OSW-1 and OSBP have.

3.3 Results and Discussion

3.3.1 Site-Directed Mutagenesis of OSB

The five residues targeted for OSBP mutation are methionine 436, lysine 493, asparagine 496, histidine 522, and lysine 736. These residues are conserved in all OSBP/ORP proteins and are likely to form interactions with OSW-1 (**Figure 16**). In the

yeast structures, the residues that correspond to methionine 436 are not involved in direct ligand binding interactions.[37,38,40] However, the amide in the backbone of these residues form hydrogen bonds with the polar head group of PI4P, and by changing this residue to proline, the backbone hydrogen bond donor should be removed.[37,38,40] OSBP residues K493 and N493 are conserved to the yeast residues that form part of the end of the central alpha-helix, and these residues hydrogen bond to the 1-phosphate of PI4P.[38–40] OSBP H522A is in the "fingerprint" of the ligand binding domain and is the most conserved histidine among the other ORPs.[63] The yeast histidines in the fingerprint region are used to form direct hydrogen bonds with the 4-phosphate in PI4P.[39,40]In Osh3 and Osh4, this histidine is involved in forming direct hydrogen bonds with the inositol sugar (Osh3) or

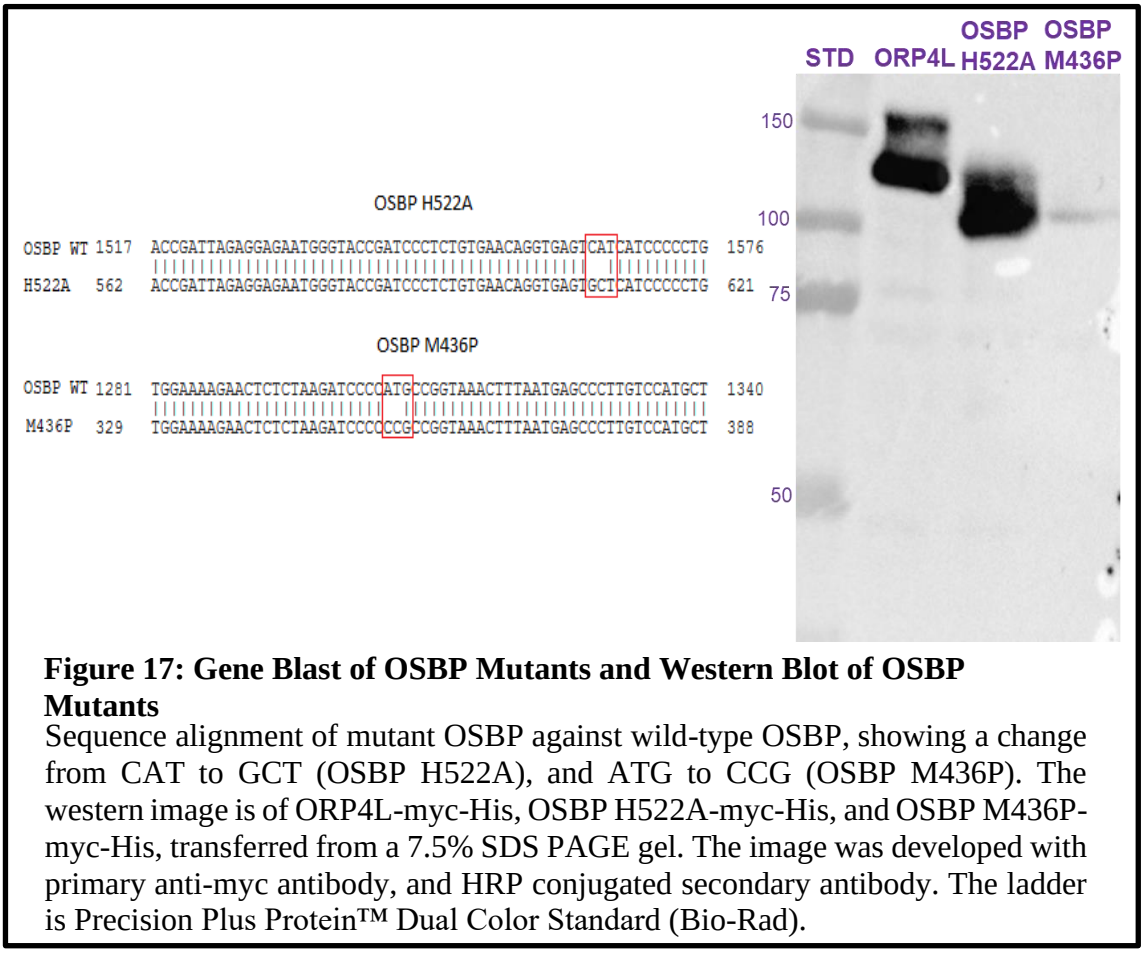

Figure 17: Gene Blast of OSBP Mutants and Western Blot of OSBP Mutants

Sequence alignment of mutant OSBP against wild-type OSBP, showing a change from CAT to GCT (OSBP H522A), and ATG to CCG (OSBP M436P). The western image is of ORP4L-myc-His, OSBP H522A-myc-His, and OSBP M436P-myc-His, transferred from a 7.5% SDS PAGE gel. The image was developed with primary anti-myc antibody, and HRP conjugated secondary antibody. The ladder is Precision Plus Protein™ Dual Color Standard (Bio-Rad).

the 4-phosphate group (Osh4).[39,40] In yeast, residues conserved with OSBP K736 are used to form hydrogen bonds directly with the phosphoinositol head group.[39]

To create the OSBP binding mutants we used human OSBP as a template for site-directed mutagenesis. The primers were designed using the specifications from the QuikChange II Site-Directed Mutagenesis kit (Agilent). OSBP is a relatively large (2.4 Kb) GC-rich gene, which makes it challenging to work with when it comes to molecular biology. Out of the initial planned site-directed mutagenesis reactions, two successful mutants were generated, OSBP M436P and OSBP H522A (**Figure 17**). Fortunately, OSBP H522A expresses at a high enough level to be used in the binding assay.

3.3.2 Binding Profile of OSBP H522A

OSBP H522A can bind [^{3}H]-25-OHC with a K_D value of 12 nM. Using cold 25-OHC as a direct competitor for [3H]-25-OHC, OSBP H522A produced a K_i of 53 nM. These results indicate the H522A is unchanged from the wild-type OSBP binding 25-OHC in the *in vitro* assay, which supports our proposed model. With the condition of low nanomolar binding to 25-OHC being met, it is possible to test the mutant for inhibition binding to the OSW-1 compound. Binding 25-OHC is an essential requirement to continue this experiment and is consistent with the structural data in Osh4.

OSW-1 produced a K_i value of 18 nM against wild-type OSBP-myc-His, which is consistent with previously established values for our OSBP experiments and with literature values (**Figure 18**).[19] However, OSBP H522A displayed a substantially weaker competitive binding affinity with an apparent K_i = 400 nM. The OSW-1 inhibition binding graph will require additional high concentration points to produce a bottom

typical of these binding curves. These initial results suggest the H522A mutation is substantially reducing OSW-1 binding while not affecting 25-OHC (**Figure 18**).

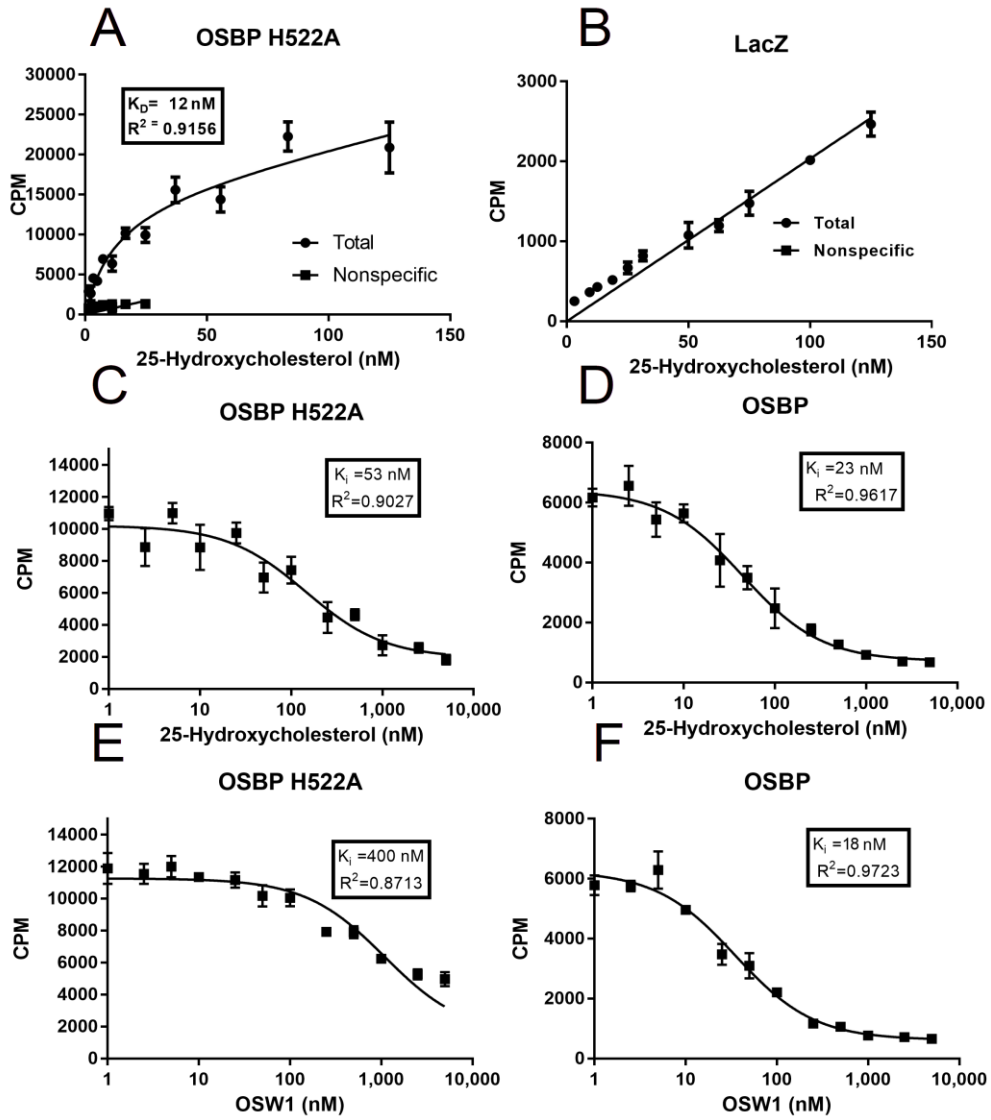

Figure 18: Binding Assays of OSBPH522A and wild-type OSBP

(A and B) Direct [^{3}H]-25-hydroxycholesterol binding assay of (A) OSBP H522A, (B) and LacZ as a negative control. (C-F) Competitive [^{3}H]- 25-hydroxycholesterol binding assays with 25-hydroxycholesterol or OSW-1. (A and C) OSBP H522A binds 25-hydroxycholesterol with a high-affinity (apparent K_D = 12nM and apparent K_i = 53nM. (D and F) Wild-type OSBP competitive ligands with high-affinity 25-hydroxycholesterol (apparent K_i = 23nM) or OSW-1 (apparent K_i =18 nM) (E) OSBP H522A binds OSW-1 with a decreased competitive affinity (apparent K_i = 400 nM).

3.3.3 Binding Assay of OSW-1 Analogs

Initially, OSW-1 analogs were used to discover that OSBP and ORP4L were the targets of the ORPphilins.[19] OSW-1 derived compounds produced by adding an aromatic amine linker to the compound were tested for interactions with OSBP and ORP4L (**Figure 18**). These analogs, especially the free amine analogs OA-2 and OA-3, can be further developed into new OSW-1 analogs, including possibly fluorescent OSW-1 analogs. OA-2, OA-3, and OA-5 were produced in the Burgett research group by Dr. Anh Le and other organic chemists. In compound OA-5, the amine is protected as part of the Alloc protecting group. OA-5 was previously reported to bind OSBP with low Ki values

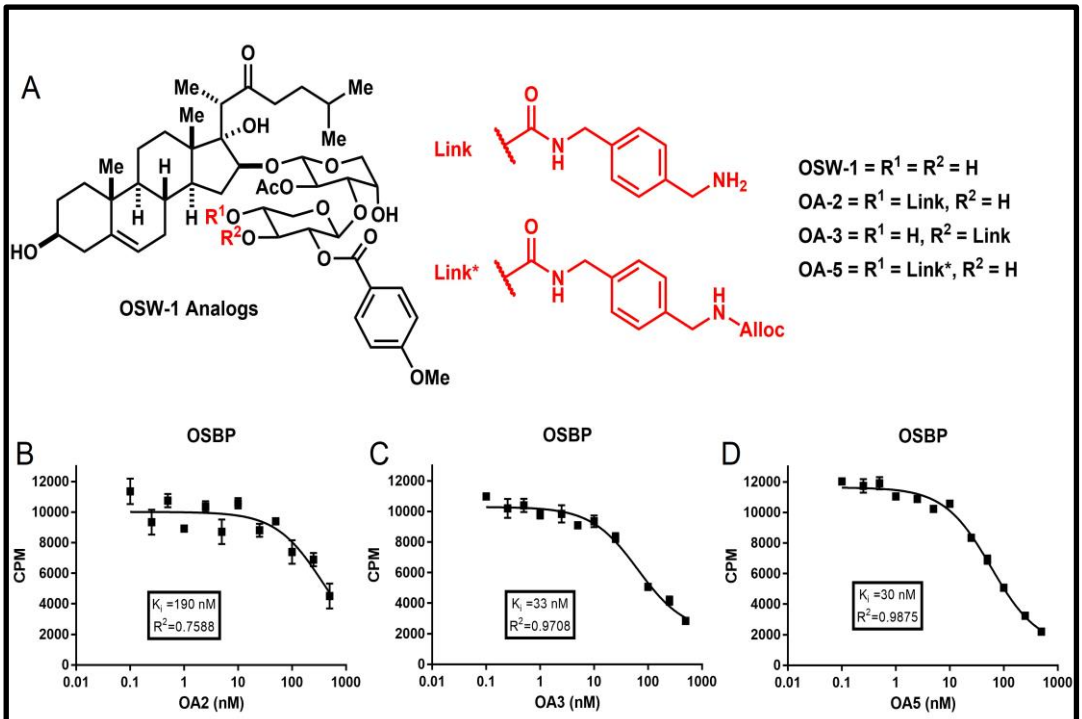

Figure 19: OSW-1 Analogs and Apparent Competitive Binding to OSBP

(A) Chemical structure of OSW-1, OA-2, OA-3 and OA-5. (B-D) Competitive [^{3}H]-25-hydroxycholesterol binding assays with (B) OA-2, (C) OA-3, and (D) OA-5. (B) OA-2 is the weakest competitive inhibitor (apparent K_i = 100) (C and D) OA-3 (apparent K_i = 33 nM) and OA-5 (apparent K_i = 30 nM) are a similar high binding affinity.

in the [^{3}H]-25-OHC competitive binding assay, but the OA-2 and OA-3 compounds have never been evaluated for OSBP interaction.[19] The free amine OSW-1 analog OA-3 retains a low apparent K_i value identical to OSW-1 for OSBP. OA-2 exhibits weaker apparent binding interactions, which is consistent with previous indications of substituents on the 4-xylose hydroxyl.[19] These results show that OSW-1-amine analogs interact with OSBP identical to the OSW-1-compound, and these compounds can be used to install a fluorophore for additional OSW-1 cellular experiments.[19]

3.3.4 Purification of Overexpressed OSBP

Currently, there are no successful methods to produce purified and fully functional overexpressed OSBP protein. Access to pure OSBP would allow for extensive biochemical and structural characterization of OSBP. We purified tagless OSBP using ammonium sulfate precipitation combined with size exclusion chromatography (SEC). The tagless OSBP protein expresses at much higher levels in HEK293T cells than the myc-His-tagged protein. After the ammonium sulfate precipitation and resuspension, the samples were split and purified by two different columns: a Sephadex column (courtesy of Dr. Paul Sims), the beads (Sigma-Aldrich) were reconstituted in 10mM Tris buffer and hand-poured into a column for gravity filtration, and an ENrich™ SEC 650 column (Bio-Rad) for HPLC purification. All fractions, including those collected before chromatography, were assayed for binding of 25 nM of [^{3}H]-25OHC (**Table 3**). The binding results show that the Sephadex Column Fractions 6 and 8, and SEC Column Fraction 1 were the most enriched for 25-OHC binding activity, which is indicative of OSBP enrichment. Additionally, the 25-OHC binding activity is also evidence of that the partially purified OSBP is functional. Interestingly, the purified fractions were stored at

4°C for several weeks before testing. This long-term stability of ammonium sulfate

Table 3: OSBP Tagless Purification Table Ammonium sulfate precipitation followed by size exclusion chromatography (Sephadex column or SEC 650 column), tested for apparent binding of [^{3}H]-25-Hydroxycholesterol

Fraction	Total Protein (mg)	Activity Counts Per Minute (CPM)	Specific Activity (CPM/mg)	Yield (%)
Crude Lysate	1200	1321	1	100
Ammonium Sulfate Supernatant	1999	66	0	167
Sephadex Column Fraction - 1	151	456	3	13
Sephadex Column Fraction - 2	99	491	5	8
Sephadex Column Fraction - 3	2403	7304	3	200
Sephadex Column Fraction - 4	1017	4521	4	85
Sephadex Column Fraction - 5	702	2686	4	59
Sephadex Column Fraction - 6	424	6041	14	35
Sephadex Column Fraction - 7	246	2088	8	20
Sephadex Column Fraction - 8	324	6307	19	27
SEC 650 Column Fraction - 1	251	5408	22	21
SEC 650 Column Fraction - 2	151	1695	11	13
SEC 650 Column Fraction - 3	172	1873	11	14

Protein concentration was deteremined through Bradford assay

Activity was determined by charcoal dextrant binding assay

enriched OSBP is much different from the stability of overexpressed OSBP in the lysate. OSBP lysate from mammalian cells must be snap frozen, stored at -80°C, and quickly thawed when used to preserve 25-OHC binding activity.

Affinity chromatography of OSBP-myc-His-tagged protein was also attempted. The OSBP-myc-His was transfected and overexpressed in HEK293T cells with the established protocols, and then overexpressed lysate was absorbed to a nickel resin. Fractions were eluted off the nickel resin using increasing concentrations of imidazole. A 10% SDS-PAGE with a colloidal Coomassie stain identified the fractions that possessed the eluted purified OSBP-myc-His protein (**Figure 20**). This method produces highly

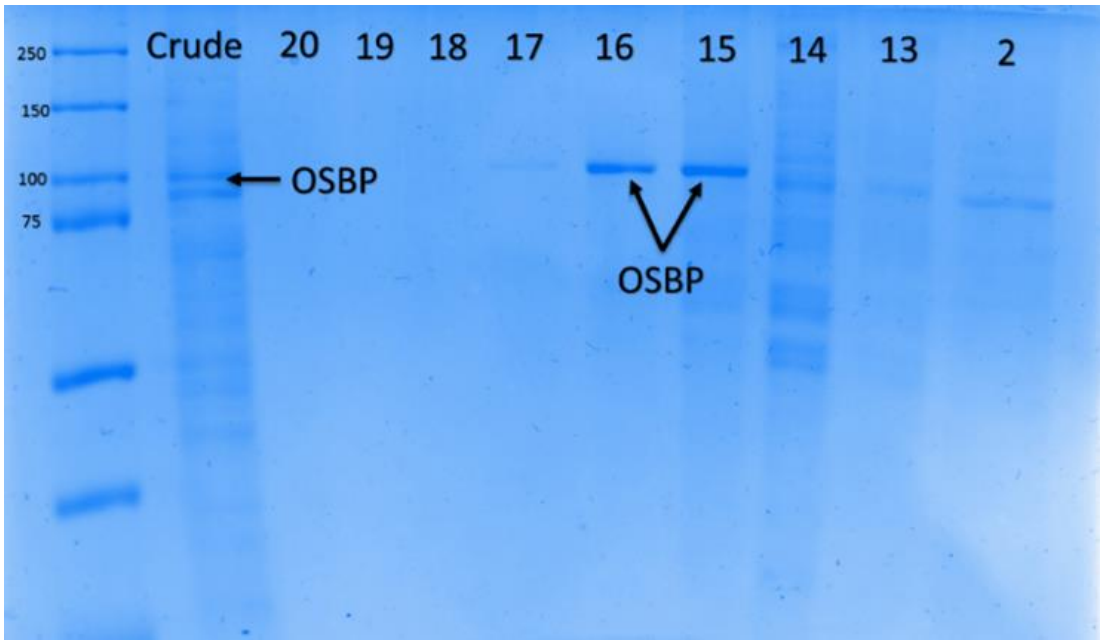

Figure 20: Colloidal Coomassie Stain of OSBP-Myc-His Fractions in a 10% SDS-PAGE Gel

Ni-NTA column purified OSBP-Myc-His fractions in a 10% SDS-PAGE gel stained overnight with colloidal Coomassie. Crude is lysate from HEK293T overexpressing OSBP-myc-His. Fractions 16 and 15 are the most purified compared and appear to be enriched with OSBP. The ladder is Precision Plus Protein™ Unstained Standard (Bio-Rad)

enriched OSBP fractions, and the method could form the basis for large-scale purification of OSBP.

3.3.5 Obtaining OSBP/ORP Plasmids

To further establish a detailed understanding of OSBP/ORP ligand binding, additional, a representative member of each OSBP/ORP subfamily was cloned in order to evaluate ligand binding. ORP cDNAs, isolated from HCT-116 cells, were PCR amplified and cloned into pcDNA™ 3.1/myc-His(-) C. The current ORPs that have been cloned from HCT-116 cDNA are ORP2, ORP3, ORP5, and ORP11. ORP1, ORP9, ORP10, ORP1A in pcDNA™4/HisMax A were given to us by Dr. Vesa Olkkonen. ORP9 was kept pcDNA™4/HisMax A because it does not have restriction sites that are compatible with pcDNA™3.1/myc-His(-)C. Future research will express and evaluate these ORP proteins for ligand binding.

3.4 Conclusion

The information, procedures, and tools developed in this chapter will allow us to design and test novel OSW-1 analogs. The initial results indicate that OSW-1 requires residues that are needed for PI4P binding in order to exert strong competitive binding. These experiments suggest that OSW-1, and possibly other ORPphilins, acts as a hybrid PI4P-cholesterol ligand for OSBP. More experimentation will need to be done to determine exact details that impart high-affinity.

Purifying expressed mammalian OSBP/ORPs is currently an unmet research need. Ammonium sulfate precipitation of tagless OSBP combined with size-exclusion chromatography produces highly enriched functional OSBP. The ammonium sulfate enriched OSBP fractions are very stable stored at 4°C. Affinity chromatography of His-

tagged OSBP produces enriched OSBP in fewer steps than ammonium precipitation. Future research in the lab will build on these purification efforts to develop methods to produce pure OSBP and other OSBP/ORPs on experimentally useful scales.

3.5 Experimental Procedures

3.5.1 Materials and Reagents

[^{3}H]-25-Hydroxycholesterol was purchased from Perkin-Elmer. 25-hydroxycholesterol was purchased from Cayman Chemical Company. Norit SA2 charcoal was obtained from Cabot Corporation. QuikChange II, Site-Directed Mutagenesis kit, was ordered from Agilent Technologies. Primers were ordered from Sigma-Aldrich. The OSW-1 and OA compounds compound used were obtained through total synthesis in the Burgett lab or from isolation (OSW-1) from the natural source.

3.5.2 Plasmids and Mutations

Human OSBP in pcDNA™ 3.1/myc-His(-) C mammalian expression vector (Sigma-Aldrich) was used as the template for site-directed mutagenesis. Primers were designed using the specifications from the QuikChange II Site-Directed Mutagenesis kit (Agilent),

Table 4: OSBP Site-Directed Mutagenesis Primers

Forward Primer Name	Primer 5' to 3'
FO_M436P	GAACTCTCTAAGATCCCCCCGCCGGTAAACTTTAATGAG
FO_K493A	GTCTTCCGCACCAGTGCGCCATTCAACCCACTG
FO_N496A	ACCAGTAAGCCATTCGCCCCACTGCTTGGGGAG
FO_H522A	CTCTGTGAACAGGTGAGTGCTCATCCCCCTGCTGCTGCG
FO_K736A	GAAGCAAATGCGGAGGCGCAGCGCCTGGAGGAA
Reverse Primer Name	Primer 5' to 3'
RO_M436P	CTCATTAAAGTTTACCGGCGGGGGGATCTTAGAGAGTTC
RO_K493A	CAGTGGGTTGAATGGCGCACTGGTGCGGAAGAC
RO_N496A	CTCCCCAAGCAGTGGGGCGAATGGCTTACTGGT
RO_H522A	CGCAGCAGCAGGGGGATGAGCACTCACCTGTTCACAGAG
RO_K736A	TTCCTCCAGGCGCTGCGCCTCCGCATTTGCTTC

Table 4. The PCR and transformation were followed as directed by the QuikChange II manual. Colonies were selected, grown in LB-Amp broth, then the plasmid was extracted, and the presence of the mutation was verified through the Oklahoma Medical Research Foundation (OMRF).

3.5.3 Tissue Culture

HEK293T cells were grown in complete Dulbecco's Modified Eagle's Medium (DMEM) at 37°C. Cells were passaged using TrypLE™ Express Enzyme (ThermoFisher Scientific) for 10 minutes at 37°C. Cells are seeded at $4X10^6$ in 10 cm^2 plates and transfected with 24 µg of plasmid after 24 hrs.

3.5.4 Charcoal/Dextran Binding Assay

The [^{3}H]-hydroxycholesterol charcoal/dextran binding assay is the same as in chapter 2.

3.5.5 Protein Purification

Size Exclusion Chromatography

OSBP pcDNA™3.1/myc-His(-) C (Tagless) was transfected into HEK293T. After 48 hours, the cells were lysed using MPER/HALT and centrifuged at 100,000 xg, for 1 hour at 4°C. The supernatant was precipitated with the gradual addition of solid ammonium sulfate until the lysate reached 50% saturation. The resulting precipitate was resuspended in a 10mM Tris HCl buffer pH 7.4. Size exclusion chromatography was done through a Sephadex column or Bio-Rad NGC™ Medium-Pressure Liquid Chromatography System with Enrich SEC650, 10/300 mm, column. All fractions were stored at 4°C and were tested for apparent binding.

Nickel Affinity Chromatography

HEK293T cells were transfected with L OSBP pcDNA™3.1/myc-His(-) C (Tagless). The cells were lysed, at 48 hours, using MPER/HALT (with no DTT) and centrifuged at 100,000xg at 4°C. The sample was purified using a Bio-Rad NGC™ Medium-Pressure Liquid Chromatography System. The loading buffer is 150 mM monopotassium phosphate, 150 mM KCl, 10 mM imidazole, pH 8. The elution buffer is150 mM monopotassium phosphate, 150 mM KCl, 500 mM imidazole, pH 8. The system was using a Nuvia IMAC Ni-charged, 5 mL, column at 4°C. The samples were collected under 1.0 mL/min flow rate in 1.0mL fraction size, with a total of 12 fractions from the elution step.

3.5.6 Western Blot

The Western blot protocol is the same as in chapter 2.

Chapter 4: Conclusion and Future Outlook

The research presented in this dissertation is designed to study the ligand binding capabilities of oxysterol-binding protein (OSBP) and OSBP-related protein (ORP) subfamily-I, namely OSBP and ORP4L. The first chapter focused primarily on the sterol-binding capabilities of human OSBP and ORP4L. We chose to use human OSBP for our binding profiles to avoid any potential species-specific effects from studying non-human OSBPs. The initial results with human OSBP reveal that this protein binds 25-hydroxycholesterol and OSW-1 with a similar affinity to the rabbit OSBP.[19] Through the oxysterol binding profiles, we identified structure-activity relations (SAR) for the interaction of oxysterols with OSBP or ORP4L.

The position of the hydroxyl on the steroidal side chain is essential for strong interactions with OSBP and ORP4L, as determined using the [^{3}H]-25-hydroxycholesterol competitive binding assay. Specifically, high-affinity interaction with OSBP or ORP4L were observed with hydroxylation at C20, C24, and C27, but not C22. The 22-OHC oxysterols show weak interactions with OSBP or ORP4L. Hydroxylation at C22 negatively interacts with both OSBP and ORP4L, based on the weak binding of the 20(*R*),22(*R*)-dihydroxycholesterol compound. The weak interaction of 22-OHC with OSBP and ORP4L is especially interesting since the OSW-1 structure has a C22 carbonyl. It is possible a C22 carbonyl does not negatively interact with OSBP the same way a hydroxyl does, or OSW-1 might not perfectly overlap in the same binding pocket as 22-OHC. Previous pharmacological studies with OSW-1 have questioned the importance of the presence of this carbonyl.[79]

The results also indicate that stereochemistry of side chain hydroxylation influences competitive binding to the OSBP and ORP4L. The (*R*)-configuration of 24-hydroxycholesterol and 27-hydroxycholesterol did not show strong competitive binding compared to the (*S*)-configuration in ORP4L. For OSBP, the (*R*) epimers of these oxysterols did bind with nanomolar competitive affinities. OSBP also tends to bind (*S*) epimers of 24-hydroxycholesterol and 27-hydroxycholesterol with slightly weaker binding affinities than the (*R*). It is evident that the configuration of the molecule influences how it binds to these proteins. OWS-1 is a steroidal compound, the information we have developed can allow us to generate OSW-1 analogs with modified steroidal features of that can potentially target a single member of the OSBP/ORP family.

To better probe the role of the oxysterol side chain on the SAR of OSBP and ORP4L binding, we made a library of 20-hydroxycholesterol analogs with various side chains. 20(*S*)-hydroxycholesterol can be used as to establish as a baseline for our experiments. The 20-OHC analogs we generated never reached the same degree of competitive binding affinity as the parent compound. Our results show that the compounds that are binding in the steroidal ligand binding domain require either a side chain or something identical to the isohexyl side chain found on cholesterol. These results also carry implications for future analogs of OSW-1, which possess the isohexyl side chain, although the C22 of the side chain is oxidized to the ketone. Future OSW-1 analogs will likely require the same or a minimally altered isohexyl side chain. Other studies have indicated that the iso-hexyl acyl chain is not necessary for the pharmacological activity of the OSW-1 compound.[79]

Chapter Three focuses on biochemical properties of human OSBP and ways to use these properties to study ligand binding. Our goal is to develop a detailed understanding of how ORPphilins are binding in the OSBP/ORP ligand binding pocket, specifically OSW-1 with OSBP (see **Chapter 3 Figure 16**). We began mutational studies that are based on the highly conserved residues that interact with phosphoinositide-4-phosphate in yeast ORP crystal structures. These studies are the first to suggest that the OSW-1 compound's high-affinity binding relies on, at least, one residue (histidine 522) that is also used to interact with PI4P. Testing more residues more will lead to detailed interaction diagrams (see **Chapter 3 Figure 16B**), which will then allow us to generate a stronger model and design more effective OSW-1 analogs.

In chapter three, we also investigate parameters that will allow us to test OSBP/ORP ligand binding further. Through our efforts to purify overexpressed OSBP with ammonium sulfate, we found that OSBP enriched fractions were more stable under refrigeration conditions than unfractionated OSBP lysate. We also produced apparent Ki values for OSW-1 analogs that have the potential to be further developed as novel probe analogs, including the fluorescent analogs. The fluorescent OSW-1 could be used to develop a direct OSW-1 binding assay for the OSBP/ORPs, which would allow for an OSW-1 K_D to OSBP or ORP4L to be determined for the first time.

This dissertation lays the groundwork to build the next generation of OSW-1 based ORPphilin compounds that can be potentially used as chemical probes for research and drug development lead compounds. The OSW-1 compound induces many interesting cellular effects through targeting OSBP and ORP4L that other OSBP/ORP ligands, such as 25-OHC, fail to cause.[19] The unique activity of OSW-1 might be explained by it

simultaneously mimicking both the sterol and PI4P when bound to OSBP. This may lock the OSBP protein in a unique state, stopping the exchange of lipids between membranes, and triggering OSBP degradation and Golgi disruption. It is possible that cell initiates the destruction of the Golgi and causes the proteasomal degradation of this "OSW-1 locked" OSBP.

The cytotoxic activity of OSW-1 likely involves targeting ORP4L instead of OSBP; this is based on the result that that RNAi silencing of OSBP does not affect cell proliferation and survival.[139] ORP4L is needed for cell survival and also affects Golgi morphology.[22,133,139] However, ritterazine B, and schweinfurthin A are cytotoxic compounds that bind ORP4L with substantially reduces affinity, as measured by K_i, than OSBP. [19] All of these results further emphasize the need to study the ligand binding capabilities of the remaining ORPs, especially with the ORPphilins.

OSBP and ORP4L, and to a greater extent all OSBP/ORPS, are enigmatic proteins especially when it comes to their ligand binding properties. For example, in OSBP all ligands induce changes in its cellular distribution; however, OSBP ligands are structurally very different and induce different biological response.[19,101,198] The ORPphilins, in particular, are interesting because their structures are the most varied and some like itraconazole appear to binding in a unique binding pocket. However, systematic, detailed binding studies will allow us to understand the rules that govern specific optimal ligand binding. These experiments will require the continued use of [^{3}H]-oxysterol binding assays, the production of novel analogs and mutational studies of the OSBP/ORP LBD. Also, the ORPphilins themselves must be developed as probes to make sure we are studying ligand binding in multiple areas. To ascertain LBD-Ligand interactions, we must

produce crystal structure of the human OSBP/ORP LBD bound to ORPphilins and endogenous ligands. Incorporating these methodologies will allow us to fully understand this protein family, which result in the production of effective novel anti-viral and anti-cancer compounds.

However, studying this protein family is limited to two disease states or even medicine. For example, oxathipiprolin (**Figure 21**), which was discovered by DuPont, has been approved by the EPA to be used as an agricultural pesticide agent to protect grapes and other crops against the infestation of *Pseudoperonospora cubensis*, which is an oomycete microorganism.[208] Oxathiapiprolin's mechanism of action was determined to be the inhibition of one of the oomycete's oxysterol-binding proteins.[208] The unexpected revelation of an OSBP/ORP as the chemical target for a microbial pest illustrates that the OSBP/ORPs are present in almost all eukaryotic organisms (**Figure 22**). Studying the ORPs of other organisms may be a way to develop more anti-fungal treatments or compounds that can help fight parasitic infections, like Plasmodium. While they may be challenging proteins to work with, they possess a vault of information, and their applications appear to be limitless.

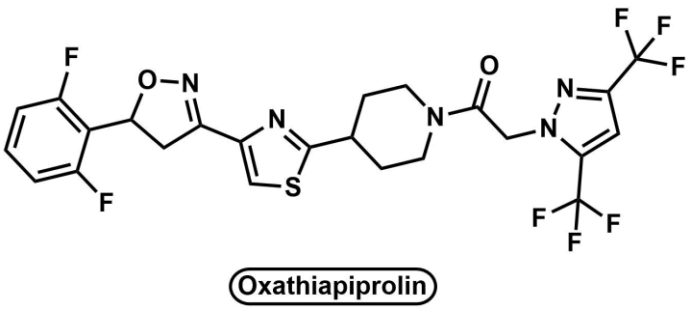

Figure 21: Oxathiapiprolin

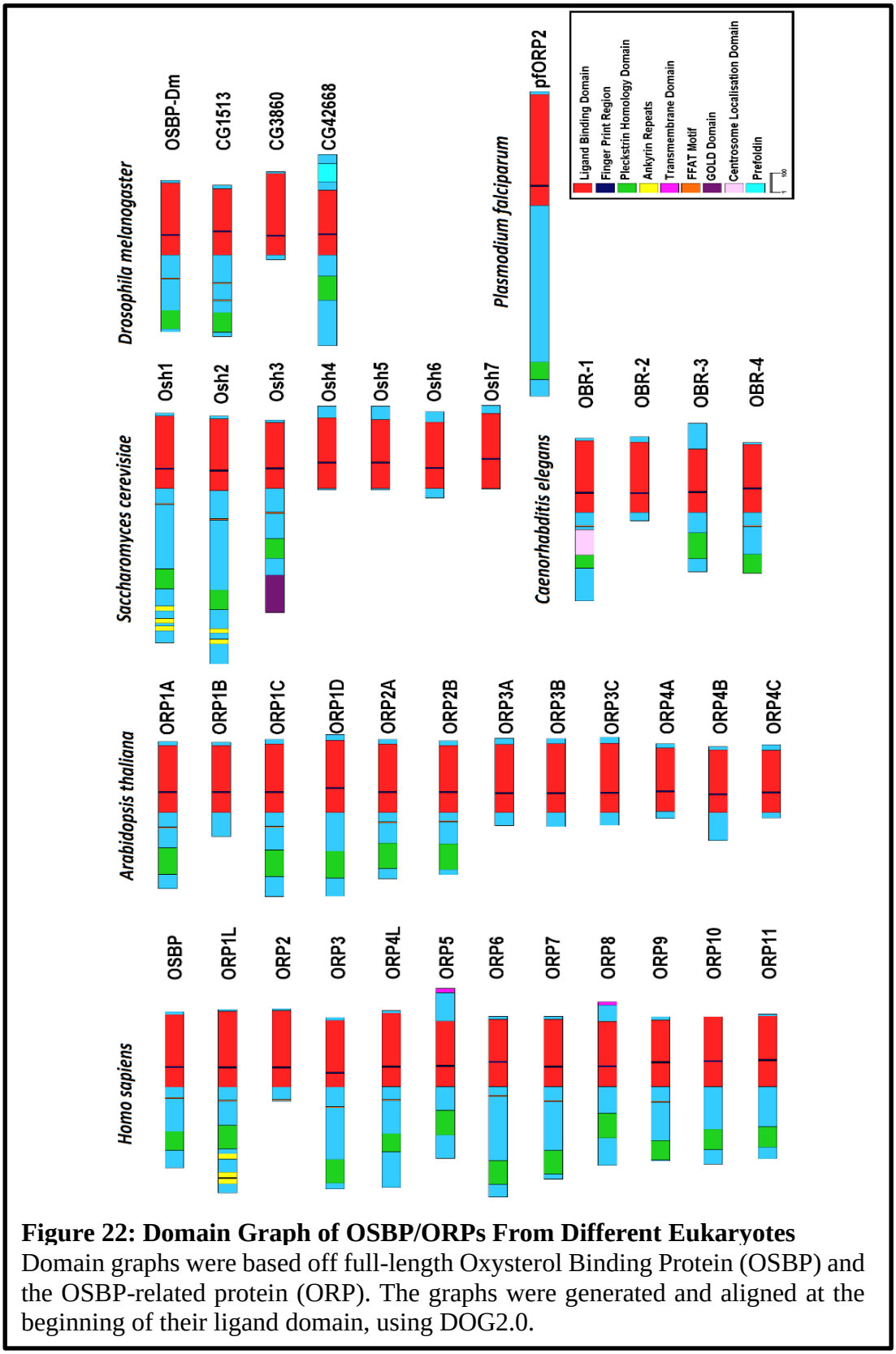

Figure 22: Domain Graph of OSBP/ORPs From Different Eukaryotes
Domain graphs were based off full-length Oxysterol Binding Protein (OSBP) and the OSBP-related protein (ORP). The graphs were generated and aligned at the beginning of their ligand domain, using DOG2.0.

References

(1) Olkkonen, V. M.; Zhou, Y.; Yan, D.; Vihervaara, T. *Eur. J. Lipid Sci. Technol.* **2012**, *114* (6), 634–643.

(2) Pietrangelo, A.; Ridgway, N. D. *Cell. Mol. Life Sci.* **2018**, No. 0123456789.

(3) Raychaudhuri, S.; Prinz, W. a. *Annu. Rev. Cell Dev. Biol.* **2010**, *26*, 157–177.

(4) Jaworski, C. J.; Moreira, E.; Li, A.; Lee, R.; Rodriguez, I. R. *Genomics* **2001**, *78* (3), 185–196.

(5) Lehto, M.; Laitinen, S.; Chinetti, G.; Johansson, M.; Ehnholm, C.; Staels, B.; Ikonen, E.; Olkkonen, V. M. *J. Lipid Res.* **2001**, *42* (8), 1203–1213.

(6) Ren, J.; Wen, L.; Gao, X.; Jin, C.; Xue, Y.; Yao, X. *Cell Res.* **2009**, *19* (2), 271–273.

(7) Waterhouse, A. M.; Procter, J. B.; Martin, D. M. A.; Clamp, M.; Barton, G. J. *Bioinformatics* **2009**, *25* (9), 1189–1191.

(8) Kandutsch, A. A.; Thompson, E. B. *J. Biol. Chem.* **1980**, *255* (22), 10813–10821.

(9) Schroepfer, G. J.; Parish, E. J.; Chen, H. W.; Kandutsch, A. A. *J. Biol. Chem.* **1977**, *252* (24), 8975–8980.

(10) Taylor, F. R.; Kandutsch, A. A. *Chem. Phys. Lipids* **1985**, *38* (1–2), 187–194.

(11) Brown, M. S.; Goldstein, J. L. *J. Lipid Res.* **2009**, *50* (Supplement), S15–S27.

(12) Taylor, F. R.; Kandutsch, A. A. *Methods Enzymol.* **1985**, *110*, 9–19.

(13) Dawson, P. a; Van der Westhuyzen, D. R.; Goldstein, J. L.; Brown, M. S. *J. Biol. Chem.* **1989**, *264* (15), 9046–9052.

(14) Ridgway, N. D.; Dawson, P. a; Ho, Y. K.; Brown, M. S.; Goldstein, J. L. *J. Cell Biol.* **1992**, *116* (2), 307–319.

(15) Jiang, B.; Brown, J. L.; Sheraton, J.; Fortin, N.; Bussey, H. *Yeast* **1994**, *10* (3), 341–353.

(16) Schmalix, W. A.; Bandlow, W. *Biochim. Biophys. Acta* **1994**, *1219* (1), 205–210.

(17) Moreira, E. F.; Jaworski, C.; Li, A.; Rodriguez, I. R. *J. Biol. Chem.* **2001**, *276* (21), 18570–18578.

(18) Laitinen, S.; Olkkonen, V. M.; Ehnholm, C.; Ikonen, E. *J. Lipid Res.* **1999**, *40*

(12), 2204–2211.

(19) Burgett, A. W. G.; Poulsen, T. B.; Wangkanont, K.; Anderson, D. R.; Kikuchi, C.; Shimada, K.; Okubo, S.; Fortner, K. C.; Mimaki, Y.; Kuroda, M.; Murphy, J. P.; Schwalb, D. J.; Petrella, E. C.; Cornella-Taracido, I.; Schirle, M.; Tallarico, J. a; Shair, M. D. *Nat. Chem. Biol.* **2011**, *7* (9), 639–647.

(20) Lemmon, M. A. *Biochem. Soc. Trans.* **2004**, *32* (Pt 5), 707–711.

(21) Tong, J.; Manik, M. K.; Yang, H.; Im, Y. J. *Biochim. Biophys. Acta - Mol. Cell Biol. Lipids* **2016**.

(22) Pietrangelo, A.; Ridgway, N. D. *J. Cell Sci.* **2018**, *131* (14), jcs215335.

(23) Laitinen, S.; Lehto, M.; Lehtonen, S.; Hyvärinen, K.; Heino, S.; Lehtonen, E.; Ehnholm, C.; Ikonen, E.; Olkkonen, V. M. *J. Lipid Res.* **2002**, *43* (2), 245–255.

(24) Loewen, C. J. R.; Roy, A.; Levine, T. P. *EMBO J.* **2003**, *22* (9), 2025–2035.

(25) Weber-Boyvat, M.; Kentala, H.; Lilja, J.; Vihervaara, T.; Hanninen, R.; Zhou, Y.; Peränen, J.; Nyman, T. a; Ivaska, J.; Olkkonen, V. M. *Exp. Cell Res.* **2015**, *331* (2), 278–291.

(26) Du, X.; Kumar, J.; Ferguson, C.; Schulz, T. a; Ong, Y. S.; Hong, W.; Prinz, W. a; Parton, R. G.; Brown, A. J.; Yang, H. *J. Cell Biol.* **2011**, *192* (1), 121–135.

(27) Yan, D.; Mäyränpää, M. I.; Wong, J.; Perttilä, J.; Lehto, M.; Jauhiainen, M.; Kovanen, P. T.; Ehnholm, C.; Brown, A. J.; Olkkonen, V. M. *J. Biol. Chem.* **2008**, *283* (1), 332–340.

(28) Johansson, M.; Bocher, V.; Lehto, M.; Chinetti, G.; Kuismanen, E.; Ehnholm, C.; Staels, B.; Olkkonen, V. M. *Mol. Biol. Cell* **2003**, *14* (3), 903–915.

(29) Johansson, M.; Lehto, M.; Tanhuanpää, K.; Cover, T. L.; Olkkonen, V. M. *Mol. Biol. Cell* **2005**, *16* (12), 5480–5492.

(30) Johansson, M.; Olkkonen, V. M. *Methods Enzymol.* **2005**, *403*, 743–758.

(31) Ghai, R.; Du, X.; Wang, H.; Dong, J.; Ferguson, C.; Brown, A. J.; Parton, R. G.; Wu, J.-W.; Yang, H. *Nat. Commun.* **2017**, *8* (1), 757.

(32) Li, H., Sato, M., Koshiba, S., Inoue, M., Kigawa, T., Yokoyama, S., (RIKEN Structural Genomics/Proteomics Initiative. Solution structure of the PH domain of Oxysterol binding protein-related protein 11 from human https://www.rcsb.org/structure/2D9X.

(33) Ferguson, K. M.; Lemmon, M. A.; Schlessinger, J.; Sigler, P. B. *Cell* **1994**, *79*

(2), 199–209.

(34) Furuita, K.; Jee, J.; Fukada, H.; Mishima, M.; Kojima, C. *J. Biol. Chem.* **2010**, *285* (17), 12961–12970.

(35) Manik, M. K.; Yang, H.; Tong, J.; Im, Y. J. *Structure* **2017**, *25* (4), 617–629.e3.

(36) Chuankhayan, P., Saoin, S., Wisitponchai, T., Intachai, K., Chupradit, K., Moonmuang, S., Kitidee, K., Nangola, S., Sanghiran, L.V., Hong, S.S., Boulanger, P., Tayapiwatana, C., Chen, C. J. Modulation of the affinity of a HIV-1 capsid-directed ankyrin towards its viral target through critical amino acid editing https://www.rcsb.org/structure/5GIK.

(37) Im, Y. J.; Raychaudhuri, S.; Prinz, W. a; Hurley, J. H. *Nature* **2005**, *437* (7055), 154–158.

(38) Maeda, K.; Anand, K.; Chiapparino, A.; Kumar, A.; Poletto, M.; Kaksonen, M.; Gavin, A.-C. *Nature* **2013**, *501* (7466), 257–261.

(39) Tong, J.; Yang, H.; Yang, H.; Eom, S. H.; Im, Y. J. *Structure* **2013**, *21* (7), 1203–1213.

(40) de Saint-Jean, M.; Delfosse, V.; Douguet, D.; Chicanne, G.; Payrastre, B.; Bourguet, W.; Antonny, B.; Drin, G. *J. Cell Biol.* **2011**, *195* (6), 965–978.

(41) Kentala, H.; Weber-Boyvat, M.; Olkkonen, V. M. *Int. Rev. Cell Mol. Biol.* **2016**, *321*, 299–340.

(42) Koag, M. C.; Cheun, Y.; Kou, Y.; Ouzon-Shubeita, H.; Min, K.; Monzingo, A. F.; Lee, S. *Steroids* **2013**, *78* (9), 938–944.

(43) van Meer, G.; Voelker, D. R.; Feigenson, G. W. *Nat. Rev. Mol. Cell Biol.* **2008**, *9* (2), 112–124.

(44) Lippincott-Schwartz, J.; Phair, R. D. *Annu. Rev. Biophys.* **2010**, *39*, 559–578.

(45) Wüstner, D.; Solanko, K. *Biochim. Biophys. Acta - Biomembr.* **2015**.

(46) Cerqueira, N. M. F. S. A.; Oliveira, E. F.; Gesto, D. S.; Santos-Martins, D.; Moreira, C.; Moorthy, H. N.; Ramos, M. J.; Fernandes, P. A. *Biochemistry* **2016**, *55* (39), 5483–5506.

(47) Stumpf, P. K. *Annu. Rev. Biochem.* **1969**, *38* (1), 159–212.

(48) McCarthy, A. D.; Hardie, D. G. *Trends Biochem. Sci.* **1984**, *9* (2), 60–63.

(49) Fujimoto, T.; Ohsaki, Y.; Cheng, J.; Suzuki, M.; Shinohara, Y. *Histochem. Cell*

Biol. **2008**, *130* (2), 263–279.

(50) Fujimoto, T.; Parton, R. G. *Cold Spring Harb. Perspect. Biol.* **2011**, *3* (3), a004838–a004838.

(51) Kelly, K.; Jacobs, R. *Phospholipid Biosynthesis*; 2011; Vol. 33.

(52) JB, M. G. D. C. S. *Biochem. J* **1984**, *2241. JB*, 933–940.

(53) Posse de Chaves, E.; Sipione, S. *FEBS Lett.* **2010**, *584* (9), 1748–1759.

(54) Hannun, Y. A.; Obeid, L. M. *Nat. Rev. Mol. Cell Biol.* **2008**, *9* (2), 139–150.

(55) Dany, M.; Ogretmen, B. *Biochim. Biophys. Acta - Mol. Cell Res.* **2015**, *1853* (10), 2834–2845.

(56) Hannun, Y. A.; Obeid, L. M. *Nat. Rev. Mol. Cell Biol.* **2017**, *19* (3), 175–191.

(57) Goldstein, J. L.; Brown, M. S. *Proc. Natl. Acad. Sci.* **1973**, *70* (10), 2804–2808.

(58) Brown, M.; Dana, S.; Goldstein, J. *J. Biol. Chem.* **1974**, *249* (3), 789–796.

(59) Nelson, R. H. *Prim. Care* **2014**, *40* (1), 195–211.

(60) Luu, W.; Sharpe, L. J.; Capell-Hattam, I.; Gelissen, I. C.; Brown, A. J. *Annu. Rev. Pharmacol. Toxicol.* **2016**, *56* (1), 447–467.

(61) Schroepfer, G. J. *Physiol. Rev.* **2000**, *80* (1), 361–554.

(62) Gatto, D.; Brink, R. *Trends Immunol.* **2013**, *34* (7), 336–341.

(63) Yan, D.; Olkkonen, V. M. In *International review of cytology*; 2008; Vol. 265, pp 253–285.

(64) Diczfalusy, U. *Biochimie* **2013**, *95* (3), 455–460.

(65) Nedelcu, D.; Liu, J.; Xu, Y.; Jao, C.; Salic, A. *Nat. Chem. Biol.* **2013**, *9* (9), 557–564.

(66) Peyrot, S. M.; Nachtergaele, S.; Luchetti, G.; Mydock-McGrane, L. K.; Fujiwara, H.; Scherrer, D.; Jallouk, A.; Schlesinger, P. H.; Ory, D. S.; Covey, D. F.; Rohatgi, R. *J. Biol. Chem.* **2014**, *289* (16), 11095–11110.

(67) Kim, W.-K.; Meliton, V.; Amantea, C. M.; Hahn, T. J.; Parhami, F. *J. Bone Miner. Res.* **2007**, *22* (11), 1711–1719.

(68) Mast, N.; Annalora, A. J.; Lodowski, D. T.; Palczewski, K.; Stout, C. D.; Pikuleva, I. A. *J. Biol. Chem.* **2011**, *286* (7), 5607–5613.

(69) Kase, E. T.; Andersen, B.; Nebb, H. I.; Rustan, A. C.; Thoresen, G. H. *Biochim. Biophys. Acta* **2006**, *1761* (12), 1515–1522.

(70) Björkhem, I.; Lütjohann, D.; Diczfalusy, U.; Ståhle, L.; Ahlborg, G.; Wahren, J. *J. Lipid Res.* **1998**, *39* (8), 1594–1600.

(71) Wang, Y.; Kumar, N.; Crumbley, C.; Griffin, P. R.; Burris, T. P. *Biochim. Biophys. Acta - Mol. Cell Biol. Lipids* **2010**, *1801* (8), 917–923.

(72) Meljon, A.; Wang, Y.; Griffiths, W. J. *Biochem. Biophys. Res. Commun.* **2014**, *446* (3), 768–774.

(73) Taylor, F. R.; Kandutsch, A. A.; Gayen, A. K.; Nelson, J. A.; Nelson, S. S.; Phirwa, S.; Spencer, T. A. *J. Biol. Chem.* **1986**, *261* (32), 15039–15044.

(74) Cali, J. J.; Russell, D. W. *J. Biol. Chem.* **1991**, *266* (12), 7774–7778.

(75) Lyons, M. A.; Brown, A. J. *Int. J. Biochem. Cell Biol.* **1999**, *31* (3–4), 369–375.

(76) Gill, S.; Stevenson, J.; Kristiana, I.; Brown, A. J. *Cell Metab.* **2011**, *13* (3), 260–273.

(77) Pulfer, M. K.; Murphy, R. C. *J. Biol. Chem.* **2004**, *279* (25), 26331–26338.

(78) Kubo, S.; Mimaki, Y.; Terao, M.; Sashida, Y. *Phytochemistry* **1992**, *31* (11), 3969–3973.

(79) Tang, Y.; Li, N.; Duan, J.; Tao, W. *Chem. Rev.* **2013**, *113* (7), 5480–5514.

(80) Honda, H.; Mimaki, Y.; Sashida, Y.; Kogo, H. *Biol. Pharm. Bull.* **1997**, *20* (4), 428–430.

(81) Tamura, K.; Honda, H.; Mimaki, Y.; Sashida, Y.; Kogo, H. *Br. J. Pharmacol.* **1997**, *121* (8), 1796–1802.

(82) Mimaki, Y.; Kuroda, M.; Kameyama, A.; Sashida, Y.; Hirano, T.; Oka, K.; Maekawa, R.; Wada, T.; Sugita, K.; Beutler, J. A. *Bioorganic Med. Chem. Lett.* **1997**, *7* (5), 633–636.

(83) Zhu, J.; Xiong, L.; Yu, B.; Wu, J. *Mol. Pharmacol.* **2005**, *68* (6), 1831–1838.

(84) Jin, J.; Jin, X.; Qian, C.; Ruan, Y.; Jiang, H. *Mol. Med. Rep.* **2013**, *7* (5), 1646–1650.

(85) Garcia-Prieto, C.; Riaz Ahmed, K. B.; Chen, Z.; Zhou, Y.; Hammoudi, N.; Kang, Y.; Lou, C.; Mei, Y.; Jin, Z.; Huang, P. *J. Biol. Chem.* **2013**, *288* (5), 3240–3250.

(86) Zhou, Y.; Garcia-Prieto, C.; Carney, D. A.; Xu, R. -h.; Pelicano, H.; Kang, Y.; Yu, W.; Lou, C.; Kondo, S.; Liu, J.; Harris, D. M.; Estrov, Z.; Keating, M. J.; Jin, Z.; Huang, P. *JNCI J. Natl. Cancer Inst.* **2005**, *97* (23), 1781–1785.

(87) Mesmin, B.; Bigay, J.; Polidori, J.; Jamecna, D.; Lacas-Gervais, S.; Antonny, B. *EMBO J.* **2017**, *36* (21), 3156–3174.

(88) Pettit, G. R.; Inoue, M.; Kamano, Y.; Herald, D. L.; Arm, C.; Dufresne, C.; Christie, N. D.; Schmidt, J. M.; Doubek, D. L.; Krupa, T. S. *J. Am. Chem. Soc.* **1988**, *110* (6), 2006–2007.

(89) Pettit, G. R.; Xu, J. P.; Williams, M. D.; Christie, N. D.; Doubek, D. L.; Schmidt, J. M.; Boyd, M. R. *J. Nat. Prod.* **1994**, *57* (271), 52–63.

(90) Dirsch, V. M.; Müller, I. M.; Eichhorst, S. T.; Pettit, G. R.; Kamano, Y.; Inoue, M.; Xu, J. P.; Ichihara, Y.; Wanner, G.; Vollmar, A. M. *Cancer Res.* **2003**, *63* (24), 8869–8876.

(91) López-Antón, N.; Rudy, A.; Barth, N.; Schmitz, L. M.; Pettit, G. R.; Schulze-Osthoff, K.; Dirsch, V. M.; Vollmar, A. M. *J. Biol. Chem.* **2006**, *281* (44), 33078–33086.

(92) Fukuzawa, S.; Matsunaga, S.; Fusetani, N. *J. Org. Chem.* **1995**, *60* (3), 608–614.

(93) LaCour, T. G.; Guo, C.; Ma, S.; Jeong, J. U.; Boyd, M. R.; Matsunaga, S.; Fusetani, N.; Fuchs, P. L. *Bioorg. Med. Chem. Lett.* **1999**, *9* (17), 2587–2592.

(94) Komiya, T.; Fusetani, N.; Matsunaga, S.; Kubo, A.; Kaye, F. J.; Kelley, M. J.; Tamura, K.; Yoshida, M.; Fukuoka, M.; Nakagawa, K. *Cancer Chemother. Pharmacol.* **2003**, *51* (3), 202–208.

(95) Beutler, J. A.; Shoemaker, R. H.; Johnson, T.; Boyd, M. R. *J. Nat. Prod.* **1998**, *61* (12), 1509–1512.

(96) Turbyville, T. J.; Gürsel, D. B.; Tuskan, R. G.; Walrath, J. C.; Lipschultz, C. a; Lockett, S. J.; Wiemer, D. F.; Beutler, J. a; Reilly, K. M. *Mol. Cancer Ther.* **2010**, *9* (5), 1234–1243.

(97) Mente, N. R.; Wiemer, A. J.; Neighbors, J. D.; Beutler, J. a.; Hohl, R. J.; Wiemer, D. F. *Bioorganic Med. Chem. Lett.* **2007**, *17* (4), 911–915.

(98) Bao, X.; Zheng, W.; Hata Sugi, N.; Agarwala, K. L.; Xu, Q.; Wang, Z.; Tendyke, K.; Lee, W.; Parent, L.; Li, W.; Cheng, H.; Shen, Y.; Taylor, N.; Dezso, Z.; Du, H.; Kotake, Y.; Zhao, N.; Wang, J.; Postema, M.; Woodall-Jappe, M.; Takase, Y.; Uenaka, T.; Kingston, D. G. I.; Nomoto, K. *Cancer Biol. Ther.* **2015**, *16* (4), 589–601.

(99) Delescluse, J.; Cauwenbergh, G.; Degreef, H. *Br. J. Dermatol.* **1986**, *114* (6), 701–703.

(100) Kim, J.; Tang, J. Y.; Gong, R.; Kim, J.; Lee, J. J.; Clemons, K. V.; Chong, C. R.; Chang, K. S.; Fereshteh, M.; Gardner, D.; Reya, T.; Liu, J. O.; Epstein, E. H.; Stevens, D. A.; Beachy, P. A. *Cancer Cell* **2010**, *17* (4), 388–399.

(101) Strating, J. R. P. M.; van der Linden, L.; Albulescu, L.; Bigay, J.; Arita, M.; Delang, L.; Leyssen, P.; van der Schaar, H. M.; Lanke, K. H. W.; Thibaut, H. J.; Ulferts, R.; Drin, G.; Schlinck, N.; Wubbolts, R. W.; Sever, N.; Head, S. A.; Liu, J. O.; Beachy, P. A.; De Matteis, M. A.; Shair, M. D.; Olkkonen, V. M.; Neyts, J.; van Kuppeveld, F. J. M. *Cell Rep.* **2015**, *10* (4), 600–615.

(102) Arita, M.; Kojima, H.; Nagano, T.; Okabe, T.; Wakita, T.; Shimizu, H. *J. Virol.* **2013**, *87* (8), 4252–4260.

(103) Albulescu, L.; Bigay, J.; Biswas, B.; Weber-Boyvat, M.; Dorobantu, C. M.; Delang, L.; van der Schaar, H. M.; Jung, Y.-S.; Neyts, J.; Olkkonen, V. M.; van Kuppeveld, F. J. M.; Strating, J. R. P. M. *Antiviral Res.* **2017**, *140*, 37–44.

(104) Albulescu, L.; Strating, J. R. P. M.; Thibaut, H. J.; van der Linden, L.; Shair, M. D.; Neyts, J.; van Kuppeveld, F. J. M. *Antiviral Res.* **2015**, *117*, 110–114.

(105) Nusslein-Volhard, C.; Wieschaus, E. *Nature* **1980**, *287* (5785), 795–801.

(106) Pathi, S.; Pagan-Westphal, S.; Baker, D. P.; Garber, E. A.; Rayhorn, P.; Bumcrot, D.; Tabin, C. J.; Blake Pepinsky, R.; Williams, K. P. *Mech. Dev.* **2001**, *106* (1–2), 107–117.

(107) Bumcrot, D. A.; Takada, R.; McMahon, A. P. *Mol. Cell. Biol.* **1995**, *15* (4), 2294–2303.

(108) Porter, J. A.; Young, K. E.; Beachy, P. A. *Science (80-.).* **1996**, *274* (5285), 255–259.

(109) Pepinsky, R. B.; Zeng, C.; Wen, D.; Rayhorn, P.; Baker, D. P.; Williams, K. P.; Bixler, S. A.; Ambrose, C. M.; Garber, E. A.; Miatkowski, K.; Taylor, F. R.; Wang, E. A.; Galdes, A. *J. Biol. Chem.* **1998**, *273* (22), 14037–14045.

(110) Rohatgi, R.; Milenkovic, L.; Corcoran, R. B.; Scott, M. P. *Proc. Natl. Acad. Sci. U. S. A.* **2009**, *106* (9), 3196–3201.

(111) Wicking, C.; McGlinn, E. *Cancer Lett.* **2001**, *173* (1), 1–7.

(112) Chen, J. K. *Genes Dev.* **2002**, *16* (21), 2743–2748.

(113) Taipale, J.; Beachy, P. A. *Nature* **2001**, *411* (6835), 349–354.

(114) Keeler, R. F.; Binns, W. *Can. J. Biochem.* **1966**, *44* (6), 819–828.

(115) Huang, P.; Zheng, S.; Wierbowski, B. M.; Kim, Y.; Nedelcu, D.; Aravena, L.; Liu, J.; Kruse, A. C.; Salic, A. *Cell* **2018**, *174* (2), 312–324.e16.

(116) Yang, T.; Espenshade, P. J.; Wright, M. E.; Yabe, D.; Gong, Y.; Aebersold, R.; Goldstein, J. L.; Brown, M. S. *Cell* **2002**, *110* (4), 489–500.

(117) Horton, J. D.; Goldstein, J. L.; Brown, M. S. *J. Clin. Invest.* **2002**, *109* (9), 1125–1131.

(118) Yokoyama, C.; Wang, X.; Briggs, M. R.; Admon, A.; Wu, J.; Hua, X.; Goldstein, J. L.; Brown, M. S. *Cell* **1993**, *75* (1), 187–197.

(119) Wang, X.; Sato, R.; Brown, M. S.; Hua, X.; Goldstein, J. L. *Cell* **1994**, *77*, 53–62.

(120) Sakai, J.; Nohturfft, A.; Cheng, D.; Ho, Y. K.; Brown, M. S.; Goldstein, J. L. *J. Biol. Chem.* **1997**, *272* (32), 20213–20221.

(121) Sakai, J.; Duncan, E. A.; Rawson, R. B.; Hua, X.; Brown, M. S.; Goldstein, J. L. *Cell* **1996**, *85* (7), 1037–1046.

(122) Duncan, E. A.; Davé, U. P.; Sakai, J.; Goldstein, J. L.; Brown, M. S. *J. Biol. Chem.* **1998**, *273* (28), 17801–17809.

(123) Radhakrishnan, A.; Ikeda, Y.; Kwon, H. J.; Brown, M. S.; Goldstein, J. L. *Proc. Natl. Acad. Sci.* **2007**, *104* (16), 6511–6518.

(124) Repa, J. J.; Liang, G.; Ou, J.; Bashmakov, Y.; Lobaccaro, J. M.; Shimomura, I.; Shan, B.; Brown, M. S.; Goldstein, J. L.; Mangelsdorf, D. J. *Genes Dev.* **2000**, *14* (22), 2819–2830.

(125) Dang, E. V.; McDonald, J. G.; Russell, D. W.; Cyster, J. G. *Oxysterol Restraint of Cholesterol Synthesis Prevents AIM2 Inflammasome Activation*; Elsevier Inc., 2017; Vol. 171.

(126) Zhao, C.; Dahlman-Wright, K. *J. Endocrinol.* **2010**, *204* (3), 233–240.

(127) Janowski, B. A.; Willy, P. J.; Devi, T. R.; Falck, J. R.; Mangelsdorf, D. J. *Nature* **1996**, *383* (6602), 728–731.

(128) Janowski, B. a; Grogan, M. J.; Jones, S. a; Wisely, G. B.; Kliewer, S. a; Corey, E. J.; Mangelsdorf, D. J. *Proc. Natl. Acad. Sci. U. S. A.* **1999**, *96* (1), 266–271.

(129) Mangelsdorf, D. J.; Evanst, R. M. *Cell* **1995**, *83* (6), 841–850.

(130) Fan, X.; Kim, H.-J.; Bouton, D.; Warner, M.; Gustafsson, J.-A. *Proc. Natl. Acad. Sci. U. S. A.* **2008**, *105* (36), 13445–13450.

(131) Koga, Y.; Ishikawa, S.; Nakamura, T.; Masuda, T.; Nagai, Y.; Takamori, H.; Hirota, M.; Kanemitsu, K.; Baba, Y.; Baba, H. *Cancer Sci.* **2008**, *99* (12), 2387–2394.

(132) Ishikawa, S.; Nagai, Y.; Masuda, T.; Koga, Y.; Nakamura, T.; Imamura, Y.; Takamori, H.; Hirota, M.; Funakosi, A.; Fukushima, M.; Baba, H. *Cancer Sci.* **2010**, *101* (4), 898–905.

(133) Zhong, W.; Yi, Q.; Xu, B.; Li, S.; Wang, T.; Liu, F.; Zhu, B.; Hoffmann, P. R.; Ji, G.; Lei, P.; Li, G.; Li, J.; Li, J.; Olkkonen, V. M.; Yan, D. *Nat. Commun.* **2016**, *7*, 12702.

(134) Wang, H.; Perry, J. W.; Lauring, A. S.; Neddermann, P.; De Francesco, R.; Tai, A. W. *Gastroenterology* **2014**, *146* (5), 1373-85.e1-11.

(135) Amako, Y.; Sarkeshik, A.; Hotta, H.; Yates, J.; Siddiqui, A. *J. Virol.* **2009**, *83* (18), 9237–9246.

(136) Amako, Y.; Syed, G. H.; Siddiqui, A. *J. Biol. Chem.* **2011**, *286* (13), 11265–11274.

(137) Moustaqim-Barrette, A.; Lin, Y. Q.; Pradhan, S.; Neely, G. G.; Bellen, H. J.; Tsuda, H. *Hum. Mol. Genet.* **2014**, *23* (8), 1975–1989.

(138) Darbyson, A.; Ngsee, J. K. *Exp. Cell Res.* **2016**, *341* (1), 18–31.

(139) Charman, M.; Colbourne, T. R.; Pietrangelo, A.; Kreplak, L.; Ridgway, N. D. *J. Biol. Chem.* **2014**, *289* (22), 15705–15717.

(140) Loilome, W.; Wechagama, P.; Namwat, N.; Jusakul, A.; Sripa, B.; Miwa, M.; Kuver, R.; Yongvanit, P. *Parasitol. Int.* **2012**, *61* (1), 136–139.

(141) Fournier, M. V; Guimarães da Costa, F.; Paschoal, M. E.; Ronco, L. V; Carvalho, M. G.; Pardee, a B.; Giumaraes, F. C. *Cancer Res.* **1999**, *59* (15), 3748–3753.

(142) Henriques Silva, N.; Vasconcellos Fournier, M.; Pimenta, G.; Pulcheri, W. A.; Spector, N.; da Costa Carvalho, M. da G. *Int. J. Mol. Med.* **2003**, *12* (4), 663–666.

(143) Li, J.; Xiao, Y.; Lai, C.; Lou, N.; Ma, H.; Zhu, B.-Y.; Zhong, W.-B.; Yan, D.-G. *Oncotarget* **2016**, *7* (40), 65849–65861.

(144) Park, I.-W.; Ndjomou, J.; Wen, Y.; Liu, Z.; Ridgway, N. D.; Kao, C. C.; He, J. J. *PLoS One* **2013**, *8* (9), e75648.

(145) Yan, D.; Jauhiainen, M.; Hildebrand, R. B.; Willems van Dijk, K.; Van Berkel, T. J. C.; Ehnholm, C.; Van Eck, M.; Olkkonen, V. M. *Arterioscler. Thromb. Vasc. Biol.* **2007**, *27* (7), 1618–1624.

(146) Chen, L.-B.; Zheng, H.-K.; Zhang, L.; An, Z.; Wang, X.-P.; Shan, R.-T.; Zhang, W.-Q. *Oncol. Rep.* **2017**, *38* (6), 3515–3521.

(147) Motazacker, M. M.; Pirhonen, J.; van Capelleveen, J. C.; Weber-Boyvat, M.; Kuivenhoven, J. A.; Shah, S.; Hovingh, G. K.; Metso, J.; Li, S.; Ikonen, E.; Jauhiainen, M.; Dallinga-Thie, G. M.; Olkkonen, V. M. *Atherosclerosis* **2016**, *249*, 140–147.

(148) Eldin, C.; Mélenotte, C.; Mediannikov, O.; Ghigo, E.; Million, M.; Edouard, S.; Mege, J. L.; Maurin, M.; Raoult, D. *Clin. Microbiol. Rev.* **2017**, *30* (1), 115–190.

(149) Justis, A. V.; Hansen, B.; Beare, P. A.; King, K. B.; Heinzen, R. A.; Gilk, S. D. *Cell. Microbiol.* **2017**, *19* (1), e12637.

(150) Xing, G.; Yao, J.; Wu, B.; Liu, T.; Wei, Q.; Liu, C.; Lu, Y.; Chen, Z.; Zheng, H.; Yang, X.; Cao, X. *Genet. Med.* **2015**, *17* (3), 210–218.

(151) Thoenes, M.; Zimmermann, U.; Ebermann, I.; Ptok, M.; Lewis, M. A.; Thiele, H.; Morlot, S.; Hess, M. M.; Gal, A.; Eisenberger, T.; Bergmann, C.; Nürnberg, G.; Nürnberg, P.; Steel, K. P.; Knipper, M.; Bolz, H. *Orphanet J. Rare Dis.* **2015**, *10* (1), 15.

(152) Li, D.; Dammer, E. B.; Lucki, N. C.; Sewer, M. B. *Mol. Biol. Cell* **2013**, *24* (6), 848–857.

(153) Raitoharju, E.; Seppälä, I.; Lyytikäinen, L.-P.; Viikari, J.; Ala-Korpela, M.; Soininen, P.; Kangas, A. J.; Waldenberger, M.; Klopp, N.; Illig, T.; Leiviskä, J.; Loo, B.-M.; Oksala, N.; Kähönen, M.; Hutri-Kähönen, N.; Laaksonen, R.; Raitakari, O.; Lehtimäki, T. *Sci. Rep.* **2016**, *6* (1), 38262.

(154) Stein, S.; Lemos, V.; Xu, P.; Demagny, H.; Wang, X.; Ryu, D.; Jimenez, V.; Bosch, F.; Lüscher, T. F.; Oosterveer, M. H.; Schoonjans, K. *J. Clin. Invest.* **2017**, *127* (2), 583–592.

(155) Lehto, M.; Mayranpaa, M. I.; Pellinen, T.; Ihalmo, P.; Lehtonen, S.; Kovanen, P. T.; Groop, P.-H.; Ivaska, J.; Olkkonen, V. M. *J. Cell Sci.* **2008**, *121* (5), 695–705.

(156) Erdem-Eraslan, L.; Van Den Bent, M. J.; Hoogstrate, Y.; Naz-Khan, H.; Stubbs, A.; Van Der Spek, P.; Bottcher, R.; Gao, Y.; De Wit, M.; Taal, W.; Oosterkamp, H. M.; Walenkamp, A.; Beerepoot, L. V.; Hanse, M. C. J.; Buter, J.; Honkoop, A. H.; Van Der Holt, B.; Vernhout, R. M.; Sillevis Smitt, P. A. E.; Kros, J. M.; French, P. J. *Cancer Res.* **2016**, *76* (3), 525–534.

(157) Lefebvre, C.; Bachelot, T.; Filleron, T.; Pedrero, M.; Campone, M.; Soria, J.-C.; Massard, C.; Lévy, C.; Arnedos, M.; Lacroix-Triki, M.; Garrabey, J.; Boursin, Y.; Deloger, M.; Fu, Y.; Commo, F.; Scott, V.; Lacroix, L.; Dieci, M. V.; Kamal, M.; Diéras, V.; Gonçalves, A.; Ferrerro, J.-M.; Romieu, G.; Vanlemmens, L.; Mouret Reynier, M.-A.; Théry, J.-C.; Le Du, F.; Guiu, S.; Dalenc, F.; Clapisson, G.; Bonnefoi, H.; Jimenez, M.; Le Tourneau, C.; André, F. *PLOS Med.* **2016**, *13* (12), e1002201.

(158) Li, H.; Wang, X.; Fang, Y.; Huo, Z.; Lu, X.; Zhan, X.; Deng, X.; Peng, C.; Shen, B. *Oncotarget* **2017**, *8* (32), 52571–52583.

(159) Nsengimana, J.; Samani, N. J.; Hall, A. S.; Balmforth, A. J.; Mangino, M.; Yuldasheva, N.; Maqbool, A.; Braund, P.; Burton, P.; Bishop, D. T.; Ball, S. G.; Barrett, J. H. *Eur. J. Hum. Genet.* **2007**, *15* (3), 313–319.

(160) North, K. E.; Martin, L. J.; Dyer, T.; Comuzzie, A. G.; Williams, J. T. *BMC Genet.* **2003**, *4* (Suppl 1), S98.

(161) Ouimet, M.; Hennessy, E. J.; van Solingen, C.; Koelwyn, G. J.; Hussein, M. A.; Ramkhelawon, B.; Rayner, K. J.; Temel, R. E.; Perisic, L.; Hedin, U.; Maegdefessel, L.; Garabedian, M. J.; Holdt, L. M.; Teupser, D.; Moore, K. J. *Arterioscler. Thromb. Vasc. Biol.* **2016**, *36* (5), 942–951.

(162) Herold, C.; Hooli, B. V.; Mullin, K.; Liu, T.; Roehr, J. T.; Mattheisen, M.; Parrado, A. R.; Bertram, L.; Lange, C.; Tanzi, R. E. *Mol. Psychiatry* **2016**, *21* (11), 1608–1612.

(163) Teslovich, T. M.; Musunuru, K.; Smith, A. V.; Edmondson, A. C.; Stylianou, I. M.; Koseki, M.; Pirruccello, J. P.; Ripatti, S.; Chasman, D. I.; Willer, C. J.; Johansen, C. T.; Fouchier, S. W.; Isaacs, A.; Peloso, G. M.; Barbalic, M.; Ricketts, S. L.; Bis, J. C.; Aulchenko, Y. S.; Thorleifsson, G.; Feitosa, M. F.; Chambers, J.; Orho-Melander, M.; Melander, O.; Johnson, T.; Li, X.; Guo, X.; Li, M.; Shin Cho, Y.; Jin Go, M.; Jin Kim, Y.; Lee, J.-Y.; Park, T.; Kim, K.; Sim, X.; Twee-Hee Ong, R.; Croteau-Chonka, D. C.; Lange, L. A.; Smith, J. D.; Song, K.; Hua Zhao, J.; Yuan, X.; Luan, J.; Lamina, C.; Ziegler, A.; Zhang, W.; Zee, R. Y. L.; Wright, A. F.; Witteman, J. C. M.; Wilson, J. F.; Willemsen, G.; Wichmann, H.-E.; Whitfield, J. B.; Waterworth, D. M.; Wareham, N. J.; Waeber, G.; Vollenweider, P.; Voight, B. F.; Vitart, V.; Uitterlinden, A. G.; Uda, M.; Tuomilehto, J.; Thompson, J. R.; Tanaka, T.; Surakka, I.; Stringham, H. M.; Spector, T. D.; Soranzo, N.; Smit, J. H.; Sinisalo, J.; Silander, K.; Sijbrands, E. J. G.; Scuteri, A.; Scott, J.; Schlessinger, D.; Sanna, S.; Salomaa, V.; Saharinen, J.; Sabatti, C.; Ruokonen, A.; Rudan, I.; Rose, L. M.; Roberts, R.; Rieder, M.; Psaty, B. M.; Pramstaller, P. P.; Pichler, I.; Perola, M.; Penninx, B. W. J. H.; Pedersen, N. L.; Pattaro, C.; Parker, A. N.; Pare, G.; Oostra, B. A.; O'Donnell, C. J.; Nieminen, M. S.; Nickerson, D. A.; Montgomery, G. W.; Meitinger, T.; McPherson, R.; McCarthy, M. I.; McArdle, W.; Masson, D.; Martin, N. G.;

Marroni, F.; Mangino, M.; Magnusson, P. K. E.; Lucas, G.; Luben, R.; Loos, R. J. F.; Lokki, M.-L.; Lettre, G.; Langenberg, C.; Launer, L. J.; Lakatta, E. G.; Laaksonen, R.; Kyvik, K. O.; Kronenberg, F.; König, I. R.; Khaw, K.-T.; Kaprio, J.; Kaplan, L. M.; Johansson, Å.; Jarvelin, M.-R.; Cecile J. W. Janssens, A.; Ingelsson, E.; Igl, W.; Kees Hovingh, G.; Hottenga, J.-J.; Hofman, A.; Hicks, A. A.; Hengstenberg, C.; Heid, I. M.; Hayward, C.; Havulinna, A. S.; Hastie, N. D.; Harris, T. B.; Haritunians, T.; Hall, A. S.; Gyllensten, U.; Guiducci, C.; Groop, L. C.; Gonzalez, E.; Gieger, C.; Freimer, N. B.; Ferrucci, L.; Erdmann, J.; Elliott, P.; Ejebe, K. G.; Döring, A.; Dominiczak, A. F.; Demissie, S.; Deloukas, P.; de Geus, E. J. C.; de Faire, U.; Crawford, G.; Collins, F. S.; Chen, Y. I.; Caulfield, M. J.; Campbell, H.; Burtt, N. P.; Bonnycastle, L. L.; Boomsma, D. I.; Boekholdt, S. M.; Bergman, R. N.; Barroso, I.; Bandinelli, S.; Ballantyne, C. M.; Assimes, T. L.; Quertermous, T.; Altshuler, D.; Seielstad, M.; Wong, T. Y.; Tai, E.-S.; Feranil, A. B.; Kuzawa, C. W.; Adair, L. S.; Taylor Jr, H. A.; Borecki, I. B.; Gabriel, S. B.; Wilson, J. G.; Holm, H.; Thorsteinsdottir, U.; Gudnason, V.; Krauss, R. M.; Mohlke, K. L.; Ordovas, J. M.; Munroe, P. B.; Kooner, J. S.; Tall, A. R.; Hegele, R. A.; Kastelein, J. J. P.; Schadt, E. E.; Rotter, J. I.; Boerwinkle, E.; Strachan, D. P.; Mooser, V.; Stefansson, K.; Reilly, M. P.; Samani, N. J.; Schunkert, H.; Cupples, L. A.; Sandhu, M. S.; Ridker, P. M.; Rader, D. J.; van Duijn, C. M.; Peltonen, L.; Abecasis, G. R.; Boehnke, M.; Kathiresan, S. *Nature* **2010**, *466* (7307), 707–713.

(164) Willer, C. J.; Schmidt, E. M.; Sengupta, S.; Peloso, G. M.; Gustafsson, S.; Kanoni, S.; Ganna, A.; Chen, J.; Buchkovich, M. L.; Mora, S.; Beckmann, J. S.; Bragg-Gresham, J. L.; Chang, H.-Y.; Demirkan, A.; Den Hertog, H. M.; Do, R.; Donnelly, L. A.; Ehret, G. B.; Esko, T.; Feitosa, M. F.; Ferreira, T.; Fischer, K.; Fontanillas, P.; Fraser, R. M.; Freitag, D. F.; Gurdasani, D.; Heikkilä, K.; Hyppönen, E.; Isaacs, A.; Jackson, A. U.; Johansson, Å.; Johnson, T.; Kaakinen, M.; Kettunen, J.; Kleber, M. E.; Li, X.; Luan, J.; Lyytikäinen, L.-P.; Magnusson, P. K. E.; Mangino, M.; Mihailov, E.; Montasser, M. E.; Müller-Nurasyid, M.; Nolte, I. M.; O'Connell, J. R.; Palmer, C. D.; Perola, M.; Petersen, A.-K.; Sanna, S.; Saxena, R.; Service, S. K.; Shah, S.; Shungin, D.; Sidore, C.; Song, C.; Strawbridge, R. J.; Surakka, I.; Tanaka, T.; Teslovich, T. M.; Thorleifsson, G.; Van den Herik, E. G.; Voight, B. F.; Volcik, K. A.; Waite, L. L.; Wong, A.; Wu, Y.; Zhang, W.; Absher, D.; Asiki, G.; Barroso, I.; Been, L. F.; Bolton, J. L.; Bonnycastle, L. L.; Brambilla, P.; Burnett, M. S.; Cesana, G.; Dimitriou, M.; Doney, A. S. F.; Döring, A.; Elliott, P.; Epstein, S. E.; Eyjolfsson, G. I.; Gigante, B.; Goodarzi, M. O.; Grallert, H.; Gravito, M. L.; Groves, C. J.; Hallmans, G.; Hartikainen, A.-L.; Hayward, C.; Hernandez, D.; Hicks, A. A.; Holm, H.; Hung, Y.-J.; Illig, T.; Jones, M. R.; Kaleebu, P.; Kastelein, J. J. P.; Khaw, K.-T.; Kim, E.; Klopp, N.; Komulainen, P.; Kumari, M.; Langenberg, C.; Lehtimäki, T.; Lin, S.-Y.; Lindström, J.; Loos, R. J. F.; Mach, F.; McArdle, W. L.; Meisinger, C.; Mitchell, B. D.; Müller, G.; Nagaraja, R.; Narisu, N.; Nieminen, T. V. M.; Nsubuga, R. N.; Olafsson, I.; Ong, K. K.; Palotie, A.; Papamarkou, T.; Pomilla, C.; Pouta, A.; Rader, D. J.; Reilly, M. P.; Ridker, P. M.; Rivadeneira, F.; Rudan,

I.; Ruokonen, A.; Samani, N.; Scharnagl, H.; Seeley, J.; Silander, K.; Stancáková, A.; Stirrups, K.; Swift, A. J.; Tiret, L.; Uitterlinden, A. G.; van Pelt, L. J.; Vedantam, S.; Wainwright, N.; Wijmenga, C.; Wild, S. H.; Willemsen, G.; Wilsgaard, T.; Wilson, J. F.; Young, E. H.; Zhao, J. H.; Adair, L. S.; Arveiler, D.; Assimes, T. L.; Bandinelli, S.; Bennett, F.; Bochud, M.; Boehm, B. O.; Boomsma, D. I.; Borecki, I. B.; Bornstein, S. R.; Bovet, P.; Burnier, M.; Campbell, H.; Chakravarti, A.; Chambers, J. C.; Chen, Y.-D. I.; Collins, F. S.; Cooper, R. S.; Danesh, J.; Dedoussis, G.; de Faire, U.; Feranil, A. B.; Ferrières, J.; Ferrucci, L.; Freimer, N. B.; Gieger, C.; Groop, L. C.; Gudnason, V.; Gyllensten, U.; Hamsten, A.; Harris, T. B.; Hingorani, A.; Hirschhorn, J. N.; Hofman, A.; Hovingh, G. K.; Hsiung, C. A.; Humphries, S. E.; Hunt, S. C.; Hveem, K.; Iribarren, C.; Järvelin, M.-R.; Jula, A.; Kähönen, M.; Kaprio, J.; Kesäniemi, A.; Kivimaki, M.; Kooner, J. S.; Koudstaal, P. J.; Krauss, R. M.; Kuh, D.; Kuusisto, J.; Kyvik, K. O.; Laakso, M.; Lakka, T. A.; Lind, L.; Lindgren, C. M.; Martin, N. G.; März, W.; McCarthy, M. I.; McKenzie, C. A.; Meneton, P.; Metspalu, A.; Moilanen, L.; Morris, A. D.; Munroe, P. B.; Njølstad, I.; Pedersen, N. L.; Power, C.; Pramstaller, P. P.; Price, J. F.; Psaty, B. M.; Quertermous, T.; Rauramaa, R.; Saleheen, D.; Salomaa, V.; Sanghera, D. K.; Saramies, J.; Schwarz, P. E. H.; Sheu, W. H. H.; Shuldiner, A. R.; Siegbahn, A.; Spector, T. D.; Stefansson, K.; Strachan, D. P.; Tayo, B. O.; Tremoli, E.; Tuomilehto, J.; Uusitupa, M.; van Duijn, C. M.; Vollenweider, P.; Wallentin, L.; Wareham, N. J.; Whitfield, J. B.; Wolffenbuttel, B. H. R.; Ordovas, J. M.; Boerwinkle, E.; Palmer, C. N. A.; Thorsteinsdottir, U.; Chasman, D. I.; Rotter, J. I.; Franks, P. W.; Ripatti, S.; Cupples, L. A.; Sandhu, M. S.; Rich, S. S.; Boehnke, M.; Deloukas, P.; Kathiresan, S.; Mohlke, K. L.; Ingelsson, E.; Abecasis, G. R. *Nat. Genet.* **2013**, *45* (11), 1274–1283.

(165) Nagano, K.; Imai, S.; Zhao, X.; Yamashita, T.; Yoshioka, Y.; Abe, Y.; Mukai, Y.; Kamada, H.; Nakagawa, S.; Tsutsumi, Y.; Tsunoda, S.-I. *Int. J. Oncol.* **2015**, *47* (1), 195–203.

(166) Du, X.; Zadoorian, A.; Lukmantara, I. E.; Qi, Y.; Brown, A. J.; Yang, H. *J. Biol. Chem.* **2018**, *293* (10), 3806–3818.

(167) Edenberg, H. J.; Koller, D. L.; Xuei, X.; Wetherill, L.; McClintick, J. N.; Almasy, L.; Bierut, L. J.; Bucholz, K. K.; Goate, A.; Aliev, F.; Dick, D.; Hesselbrock, V.; Hinrichs, A.; Kramer, J.; Kuperman, S.; Nurnberger, J. I.; Rice, J. P.; Schuckit, M. A.; Taylor, R.; Todd Webb, B.; Tischfield, J. A.; Porjesz, B.; Foroud, T. *Alcohol. Clin. Exp. Res.* **2010**, *34* (5), 840–852.

(168) Ma, J.; Dempsey, A. A.; Stamatiou, D.; Marshall, K. W.; Liew, C. C. *Atherosclerosis* **2007**, *191* (1), 63–72.

(169) Chung, J.; Torta, F.; Masai, K.; Lucast, L.; Czapla, H.; Tanner, L. B.; Narayanaswamy, P.; Wenk, M. R.; Nakatsu, F.; De Camilli, P. *Science (80-.).* **2015**, *349* (6246), 428–432.

(170) Van Kampen, E.; Beaslas, O.; Hildebrand, R. B.; Lammers, B.; Van Berkel, T. J. C.; Olkkonen, V. M.; Van Eck, M. *PLoS One* **2014**, *9* (10).

(171) Béaslas, O.; Metso, J.; Nissilä, E.; Laurila, P. P.; Kaiharju, E.; Batchu, K. C.; Kaipiainen, L.; Mäyränpää, M. I.; Yan, D.; Gylling, H.; Jauhiainen, M.; Olkkonen, V. M. *PLoS One* **2013**, *8* (3), 1–12.

(172) Guo, X.; Zhang, L.; Fan, Y.; Zhang, D.; Qin, L.; Dong, S.; Li, G. *Oncol. Res. Featur. Preclin. Clin. Cancer Ther.* **2017**, *25* (5), 799–808.

(173) Zhong, W.; Qin, S.; Zhu, B.; Pu, M.; Liu, F.; Wang, L.; Ye, G.; Yi, Q.; Yan, D. *J. Biol. Chem.* **2015**, *290* (14), 8876–8887.

(174) Li, J.; Zheng, X.; Lou, N.; Zhong, W.; Yan, D. *J. Lipid Res.* **2016**, *57* (10), 1845–1853.

(175) Loilome, W.; Yongvanit, P.; Wongkham, C.; Tepsiri, N.; Sripa, B.; Sithithaworn, P.; Hanai, S.; Miwa, M. *Mol. Carcinog.* **2006**, *45* (5), 279–287.

(176) Abdul Aziz, N. A.; Mokhtar, N. M.; Harun, R.; Mollah, M. M. H.; Mohamed Rose, I.; Sagap, I.; Mohd Tamil, A.; Wan Ngah, W. Z.; Jamal, R. *BMC Med. Genomics* **2016**, *9* (1), 58.

(177) Li, L.; Qu, G.; Wang, M.; Huang, Q.; Liu, Y. *Irish J. Med. Sci. (1971 -)* **2014**, *183* (3), 439–448.

(178) Sierra, B.; Triska, P.; Soares, P.; Garcia, G.; Perez, A. B.; Aguirre, E.; Oliveira, M.; Cavadas, B.; Regnault, B.; Alvarez, M.; Ruiz, D.; Samuels, D. C.; Sakuntabhai, A.; Pereira, L.; Guzman, M. G. *PLOS Pathog.* **2017**, *13* (2), e1006220.

(179) Perttilä, J.; Merikanto, K.; Naukkarinen, J.; Surakka, I.; Martin, N. W.; Tanhuanpää, K.; Grimard, V.; Taskinen, M.-R.; Thiele, C.; Salomaa, V.; Jula, A.; Perola, M.; Virtanen, I.; Peltonen, L.; Olkkonen, V. M. *J. Mol. Med.* **2009**, *87* (8), 825–835.

(180) Nissilä, E.; Ohsaki, Y.; Weber-Boyvat, M.; Perttilä, J.; Ikonen, E.; Olkkonen, V. M. *Biochim. Biophys. Acta - Mol. Cell Biol. Lipids* **2012**, *1821* (12), 1472–1484.

(181) Koriyama, H.; Nakagami, H.; Katsuya, T.; Akasaka, H.; Saitoh, S.; Shimamoto, K.; Ogihara, T.; Kaneda, Y.; Morishita, R.; Rakugi, H. *Hypertens. Res.* **2010**, *33* (5), 511–514.

(182) Koriyama, H.; Nakagami, H.; Katsuya, T.; Sugimoto, K.; Yamashita, H.; Takami, Y.; Maeda, S.; Kubo, M.; Takahashi, A.; Nakamura, Y.; Ogihara, T.; Rakugi, H.; Kaneda, Y.; Morishita, R. *J. Atheroscler. Thromb.* **2010**, *17*, 1054–1062.

(183) Stewart, W. C.; Huang, Y.; Greenberg, D. A.; Vieland, V. J. *BMC Proc.* **2014**, *8* (Suppl 1), S111.

(184) Dmitriev, A. A.; Rosenberg, E. E.; Krasnov, G. S.; Gerashchenko, G. V.; Gordiyuk, V. V.; Pavlova, T. V.; Kudryavtseva, A. V.; Beniaminov, A. D.; Belova, A. A.; Bondarenko, Y. N.; Danilets, R. O.; Glukhov, A. I.; Kondratov, A. G.; Alexeyenko, A.; Alekseev, B. Y.; Klein, G.; Senchenko, V. N.; Kashuba, V. I. *Dis. Markers* **2015**, *2015*, 1–13.

(185) Dobashi, A.; Togashi, Y.; Tanaka, N.; Yokoyama, M.; Tsuyama, N.; Baba, S.; Mori, S.; Hatake, K.; Yamaguchi, T.; Noda, T.; Takeuchi, K. *Oncotarget* **2018**, *9* (28), 19555–19568.

(186) Bouchard, L.; Faucher, G.; Tchernof, A.; Deshaies, Y.; Marceau, S.; Lescelleur, O.; Biron, S.; Bouchard, C.; Pérusse, L.; Vohl, M.-C. *Obesity* **2009**, *17* (7), 1466–1472.

(187) Kara, B.; Köroğlu, Ç.; Peltonen, K.; Steinberg, R. C.; Maraş Genç, H.; Hölttä-Vuori, M.; Güven, A.; Kanerva, K.; Kotil, T.; Solakoğlu, S.; Zhou, Y.; Olkkonen, V. M.; Ikonen, E.; Laiho, M.; Tolun, A. *Eur. J. Hum. Genet.* **2017**, *25* (3), 315–323.

(188) Beh, C. T.; Cool, L.; Phillips, J.; Rine, J. *Genetics* **2001**, *157* (3), 1117–1140.

(189) Perry, R. J.; Ridgway, N. D. *Mol. Biol. Cell* **2006**, *17* (June), 2604–2616.

(190) Kaiser, S. E.; Brickner, J. H.; Reilein, A. R.; Fenn, T. D.; Walter, P.; Brunger, A. T. *Structure* **2005**, *13* (7), 1035–1045.

(191) Levine, T. P.; Munro, S. *Curr. Biol.* **2002**, *12* (9), 695–704.

(192) Mesmin, B.; Bigay, J.; Moser von Filseck, J.; Lacas-Gervais, S.; Drin, G.; Antonny, B. *Cell* **2013**, *155* (4), 830–843.

(193) Zewe, J. P.; Wills, R. C.; Sangappa, S.; Goulden, B. D.; Hammond, G. R. V. *Elife* **2018**, *7*.

(194) Prashek, J.; Truong, T.; Yao, X. *PLoS One* **2013**, *8* (11).

(195) Wang, P.-Y.; Weng, J.; Anderson, R. G. W. *Science (80-.).* **2005**, *307* (5714), 1472–1476.

(196) Romeo, G. R.; Kazlauskas, A. *J. Biol. Chem.* **2008**, *283* (15), 9595–9605.

(197) Udagawa, O.; Ito, C.; Ogonuki, N.; Sato, H.; Lee, S.; Tripvanuntakul, P.; Ichi, I.; Uchida, Y.; Nishimura, T.; Murakami, M.; Ogura, A.; Inoue, T.; Toshimori, K.; Arai, H. *Genes to Cells* **2014**, *19* (1), 13–27.

(198) Weber-Boyvat, M.; Kentala, H.; Peränen, J.; Olkkonen, V. M. *Cell. Mol. Life Sci.* **2015**, *72* (10), 1967–1987.

(199) Wang, C.; JeBailey, L.; Ridgway, N. D. *Biochem. J.* **2002**, *361* (Pt 3), 461–472.

(200) Fairn, G. D.; McMaster, C. R. *Biochem. J.* **2005**, *387* (Pt 3), 889–896.

(201) Zhao, K.; Ridgway, N. D. *Cell Rep.* **2017**, *19* (9), 1807–1818.

(202) Rocha, N.; Kuijl, C.; van der Kant, R.; Janssen, L.; Houben, D.; Janssen, H.; Zwart, W.; Neefjes, J. *J. Cell Biol.* **2009**, *185* (7), 1209–1225.

(203) Lee, S.; Wang, P.-Y.; Jeong, Y.; Mangelsdorf, D. J.; Anderson, R. G. W.; Michaely, P. *Exp. Cell Res.* **2012**, *318* (16), 2128–2142.

(204) Hynynen, R.; Suchanek, M.; Spandl, J.; Bäck, N.; Thiele, C.; Olkkonen, V. M. *J. Lipid Res.* **2009**, *50*, 1305–1315.

(205) Escajadillo, T.; Wang, H.; Li, L.; Li, D.; Sewer, M. B. *Mol. Cell. Endocrinol.* **2016**, *427*, 73–85.

(206) Kentala, H.; Koponen, A.; Kivelä, A. M.; Andrews, R.; Li, C.; Zhou, Y.; Olkkonen, V. M. *FASEB J.* **2018**, *32* (3), 1281–1295.

(207) Lehto, M.; Hynynen, R.; Karjalainen, K.; Kuismanen, E.; Hyvärinen, K.; Olkkonen, V. M. *Exp. Cell Res.* **2005**, *310* (2), 445–462.

(208) Cohen, Y. *PLoS One* **2015**, *10* (10), e0140015.

(209) Zhong, W.; Zhou, Y.; Li, S.; Zhou, T.; Ma, H.; Wei, K.; Li, H.; Olkkonen, V. M.; Yan, D. *Exp. Cell Res.* **2011**, *317* (16), 2353–2363.

(210) Galmes, R.; Houcine, A.; van Vliet, A. R.; Agostinis, P.; Jackson, C. L.; Giordano, F. *EMBO Rep.* **2016**, *17* (6), 800–810.

(211) Filges, I.; Manokhina, I.; Peñaherrera, M. S.; McFadden, D. E.; Louie, K.; Nosova, E.; Friedman, J. M.; Robinson, W. P. *MHR Basic Sci. Reprod. Med.* **2015**, *21* (4), 339–346.

(212) Zhou, T.; Li, S.; Zhong, W.; Vihervaara, T.; Béaslas, O.; Perttilä, J.; Luo, W.; Jiang, Y.; Lehto, M.; Olkkonen, V. M.; Yan, D. *PLoS One* **2011**, *6* (6), e21078.

(213) Béaslas, O.; Vihervaara, T.; Li, J.; Laurila, P.-P.; Yan, D.; Olkkonen, V. M. *Exp. Cell Res.* **2012**, *318* (15), 1933–1945.

(214) Zhong, W.; Zhou, Y.; Li, J.; Mysore, R.; Luo, W.; Li, S.; Chang, M.-S.; Olkkonen, V. M.; Yan, D. *Exp. Cell Res.* **2014**, *322* (2), 227–235.

(215) Ngo, M.; Ridgway, N. D. *Mol. Biol. Cell* **2009**, *20* (5), 1388–1399.

(216) Fairn, G. D.; McMaster, C. R. *Biochem. Cell Biol.* **2005**, *83* (5), 631–636.

(217) Lessmann, E.; Ngo, M.; Leitges, M.; Minguet, S.; Ridgway, N. D.; Huber, M. *Cell. Signal.* **2007**, *19* (2), 384–392.

(218) Wyles, J. P.; Ridgway, N. D. *Exp. Cell Res.* **2004**, *297* (2), 533–547.

(219) Zhou, Y.; Li, S.; Mäyränpää, M. I.; Zhong, W.; Bäck, N.; Yan, D.; Olkkonen, V. M. *Exp. Cell Res.* **2010**, *316* (19), 3304–3316.

(220) Goto, a.; Liu, X.; Robinson, C. -a.; Ridgway, N. D. *Mol. Biol. Cell* **2012**, *23* (18), 3624–3635.

(221) Dawson, P. a; Ridgway, N. D.; Slaughter, C. a; Brown, M. S.; Goldstein, J. L. *J. Biol. Chem.* **1989**, *264* (28), 16798–16803.

(222) Wang, P.-Y.; Weng, J.; Lee, S.; Anderson, R. G. W. *J. Biol. Chem.* **2008**, *283* (12), 8034–8045.

(223) Taylor, F. R.; Saucier, S. E.; Shown, E. P.; Parish, E. J.; Kandutsch, a. a. *J. Biol. Chem.* **1984**, *259* (20), 12382–12387.

(224) Suchanek, M.; Hynynen, R.; Wohlfahrt, G.; Lehto, M.; Johansson, M.; Saarinen, H.; Radzikowska, A.; Thiele, C.; Olkkonen, V. M. *Biochem. J.* **2007**, *405* (3), 473–480.

(225) Liu, X.; Ridgway, N. D. *PLoS One* **2014**, *9* (9), e108368.

(226) Mohammadi, a; Perry, R. J.; Storey, M. K.; Cook, H. W.; Byers, D. M.; Ridgway, N. D. *J. Lipid Res.* **2001**, *42* (7), 1062–1071.

(227) Levine, T. P. *Dev. Cell* **2013**, *27* (4), 369–370.

(228) Guo, C.; LaCour, T. G.; Fuchs, P. L. *Bioorganic Med. Chem. Lett.* **1999**, *9* (3), 419–424.

(229) Kandutsch, A. A.; Shown, E. P. *J. Biol. Chem.* **1981**, *256* (24), 13068–13073.

(230) Cenedella, R. J. *Lipids*. June 14, 2009, pp 477–487.

(231) Zhou, Y.; Lingle, C. J. *J. Gen. Physiol.* **2014**, *144* (5), 415–440.

(232) Hofmann, A. F. *Front. Biosci.* **2009**, *Volume* (14), 2584.

(233) Bae, J. W.; Lee, S. H.; Jung, Y. J.; Maing Yoon, C.-O.; Yoon, C. M. *Tetrahedron*

Lett. **2001**, *42* (11), 2137–2139.

(234) Yeh, M. C. P.; Lee, Y. C.; Young, T. C. *Synthesis (Stuttg).* **2006**, *2006* (21), 3621–3624.

(235) Wyles, J. P.; Perry, R. J.; Ridgway, N. D. *Exp. Cell Res.* **2007**, *313* (7), 1426–1437.

Appendix A: Chapter 2 Supplemental Data

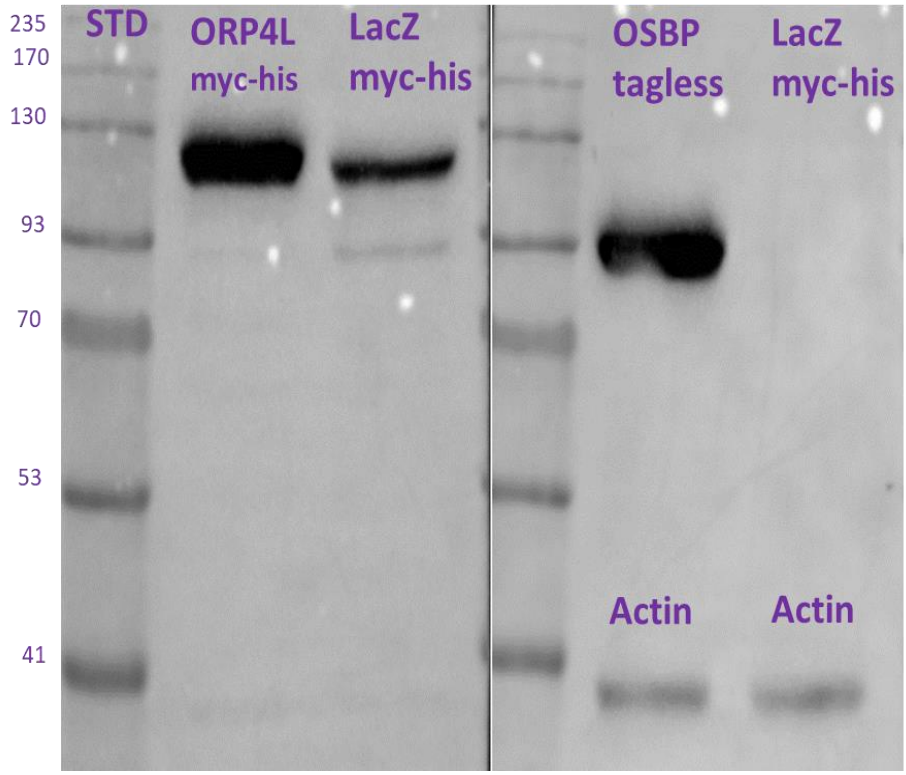

Figure 23: Western Blot of ORP4L-MH, LacZ-MH and OSBP tagless

The western images of ORP4L-myc-His, LacZ-myc-His, and OSBP-tagless transferred from a 7.5% SDS PAGE gel. The image was developed with primary anti-myc antibody or anti-OSBP, and HRP conjugated secondary antibodies. The ladder is True Blue™ Protein Standard (Gold Biotechnology). The membrane was cut in half after transfer because different primary antibodies were used.

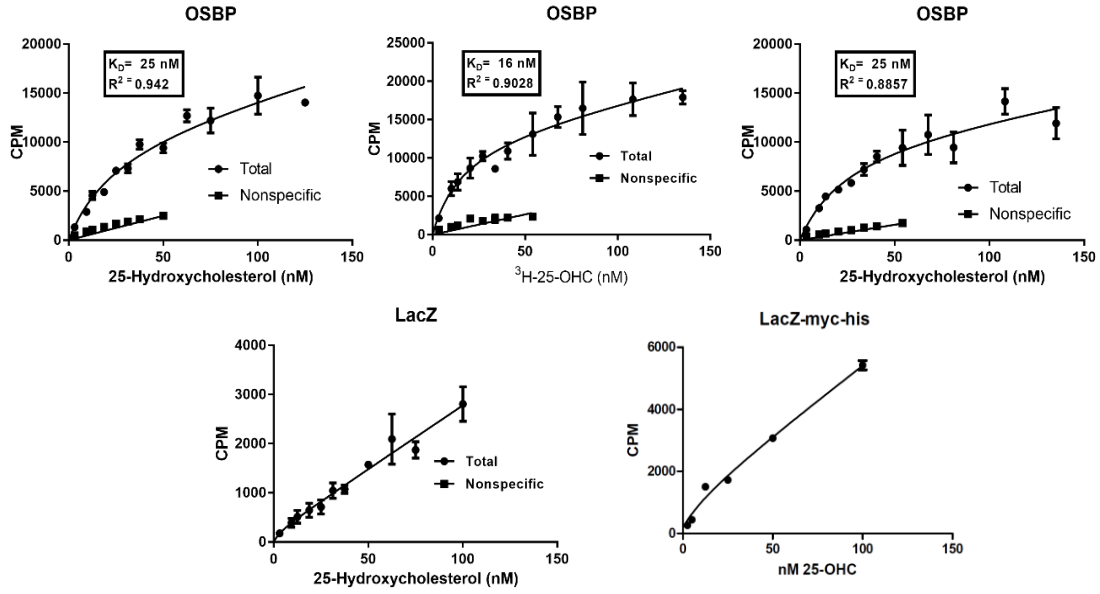

Figure 24: Direct Binding Constant of Human OSBP Tagless and LacZ

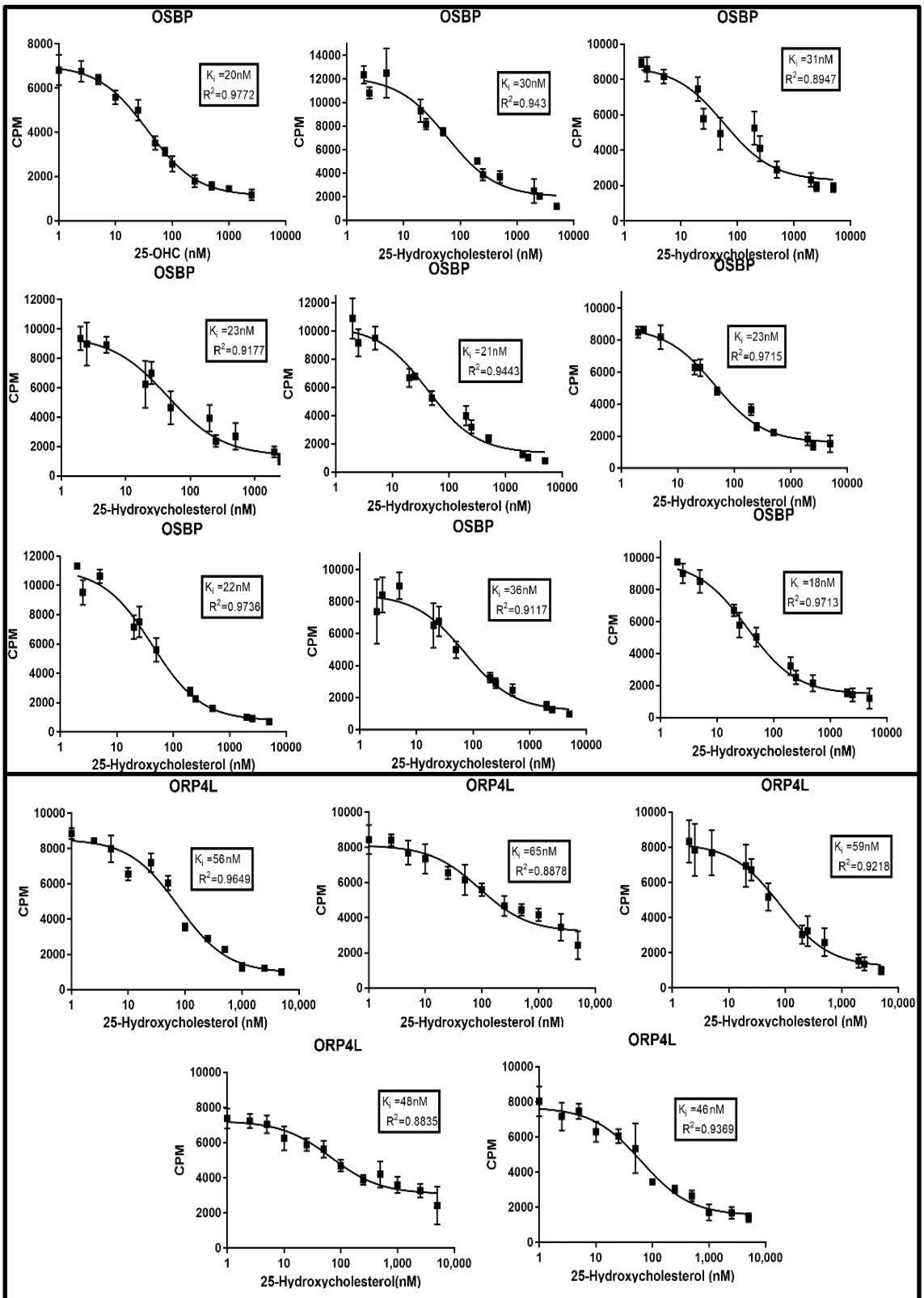

Figure 25: Binding Curves of OSBP (Top) and ORP4L (Bottom) with 25-Hydroxycholesterol

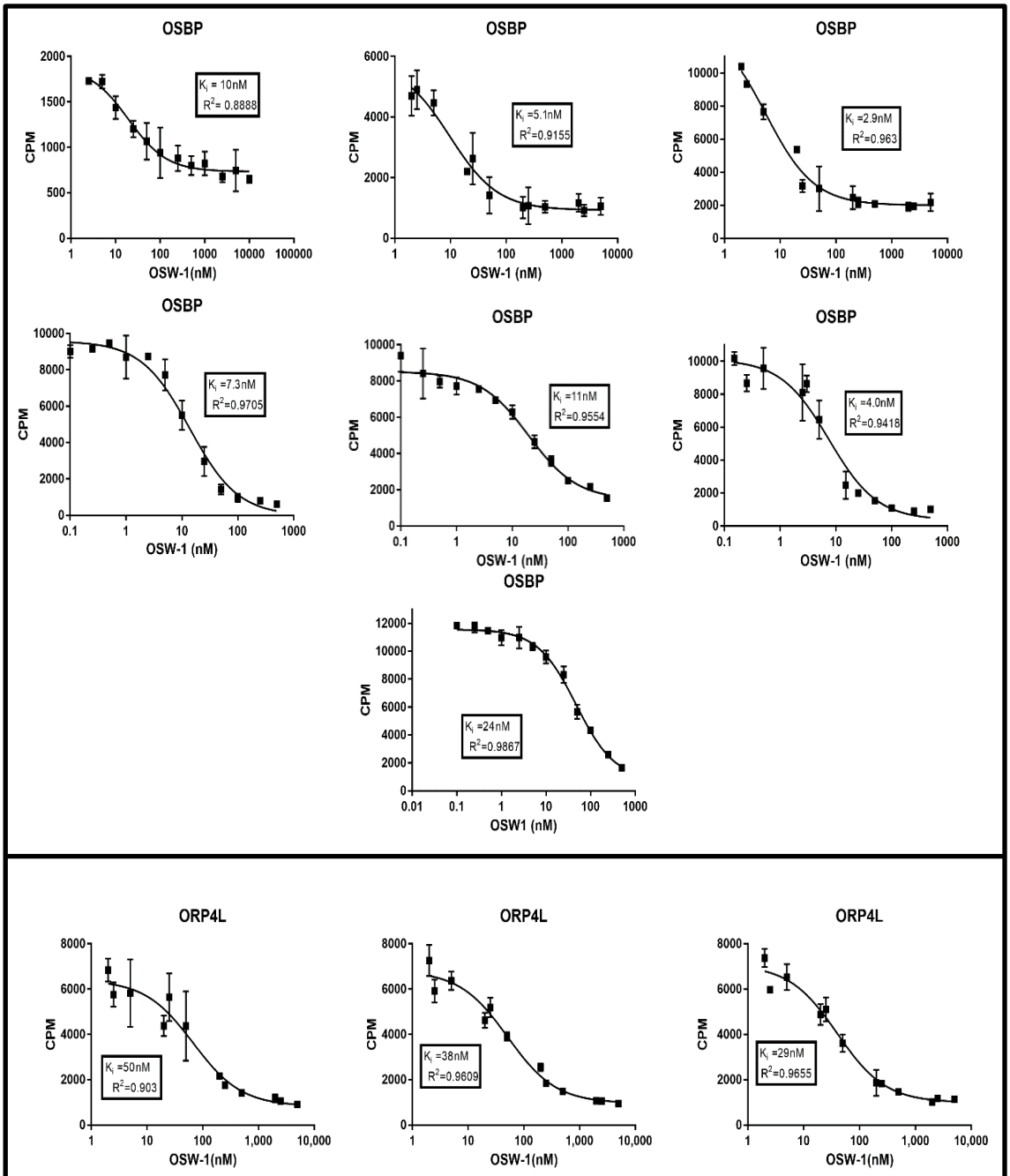

Figure 26: Binding Curves of OSBP (Top) and ORP4L (Bottom) with OSW-1

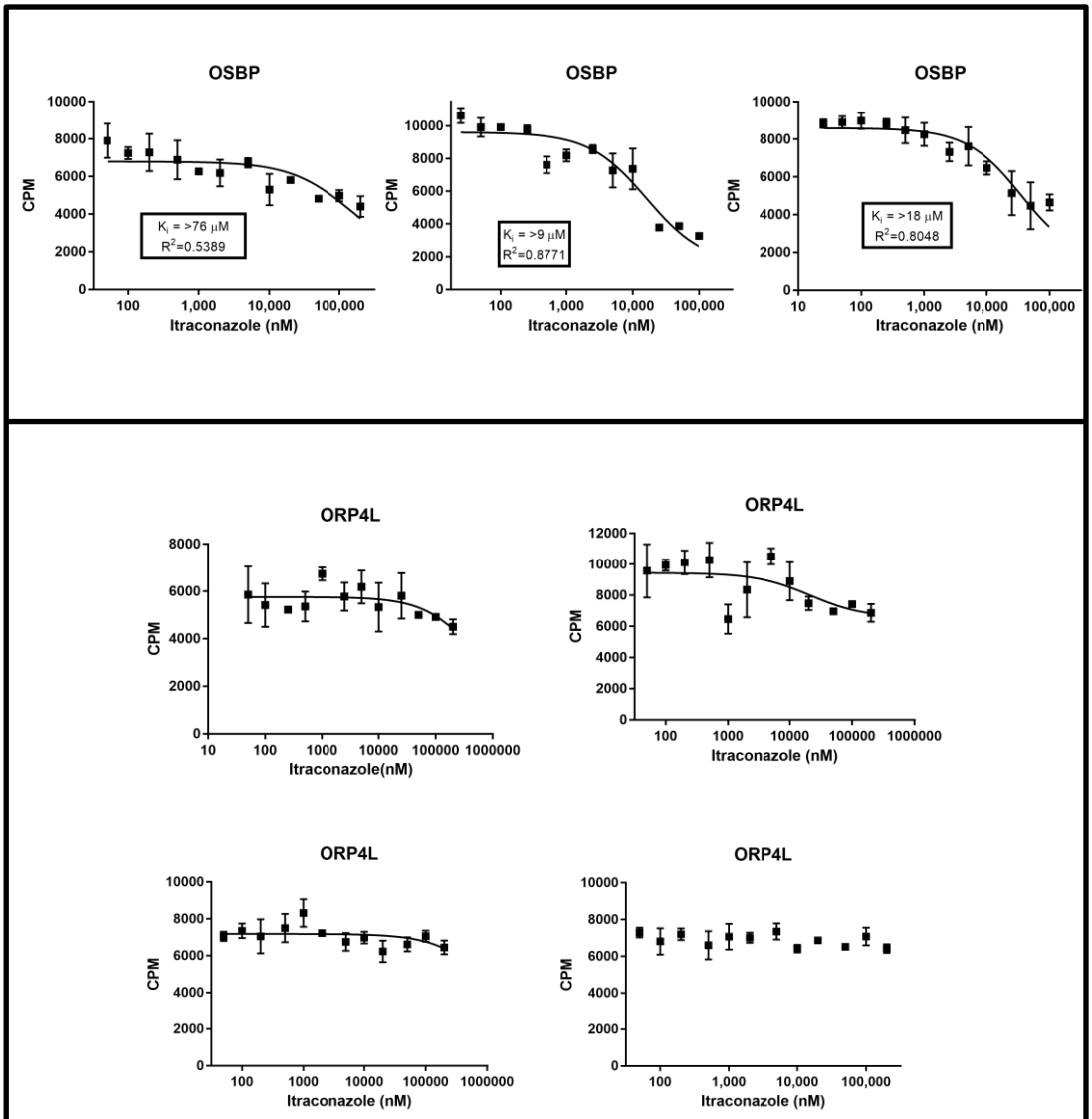

Figure 27: Binding Curves of OSBP (Top) and ORP4L (Bottom) with Itraconazole

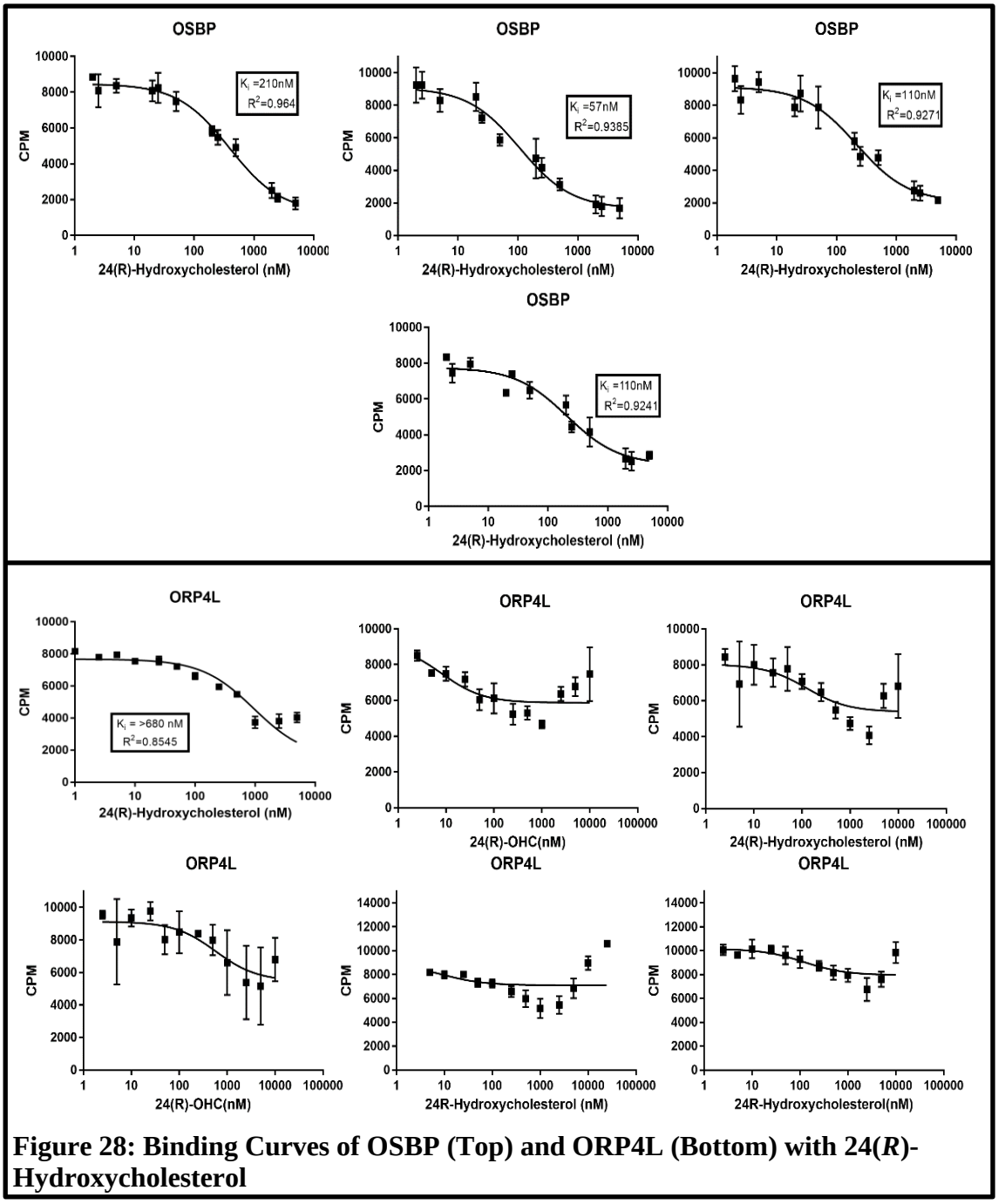

Figure 28: Binding Curves of OSBP (Top) and ORP4L (Bottom) with 24(*R*)-Hydroxycholesterol

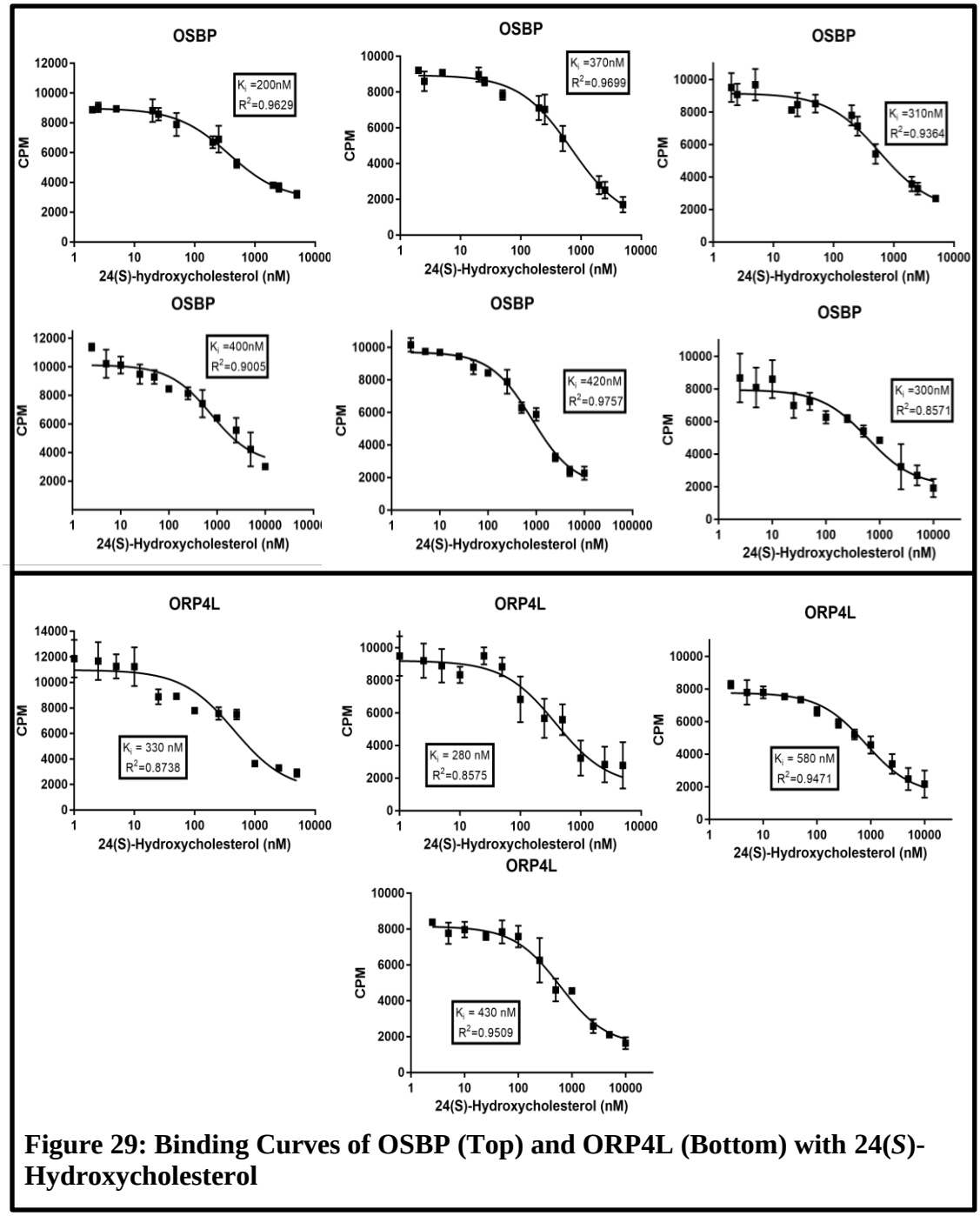

Figure 29: Binding Curves of OSBP (Top) and ORP4L (Bottom) with 24(*S*)-Hydroxycholesterol

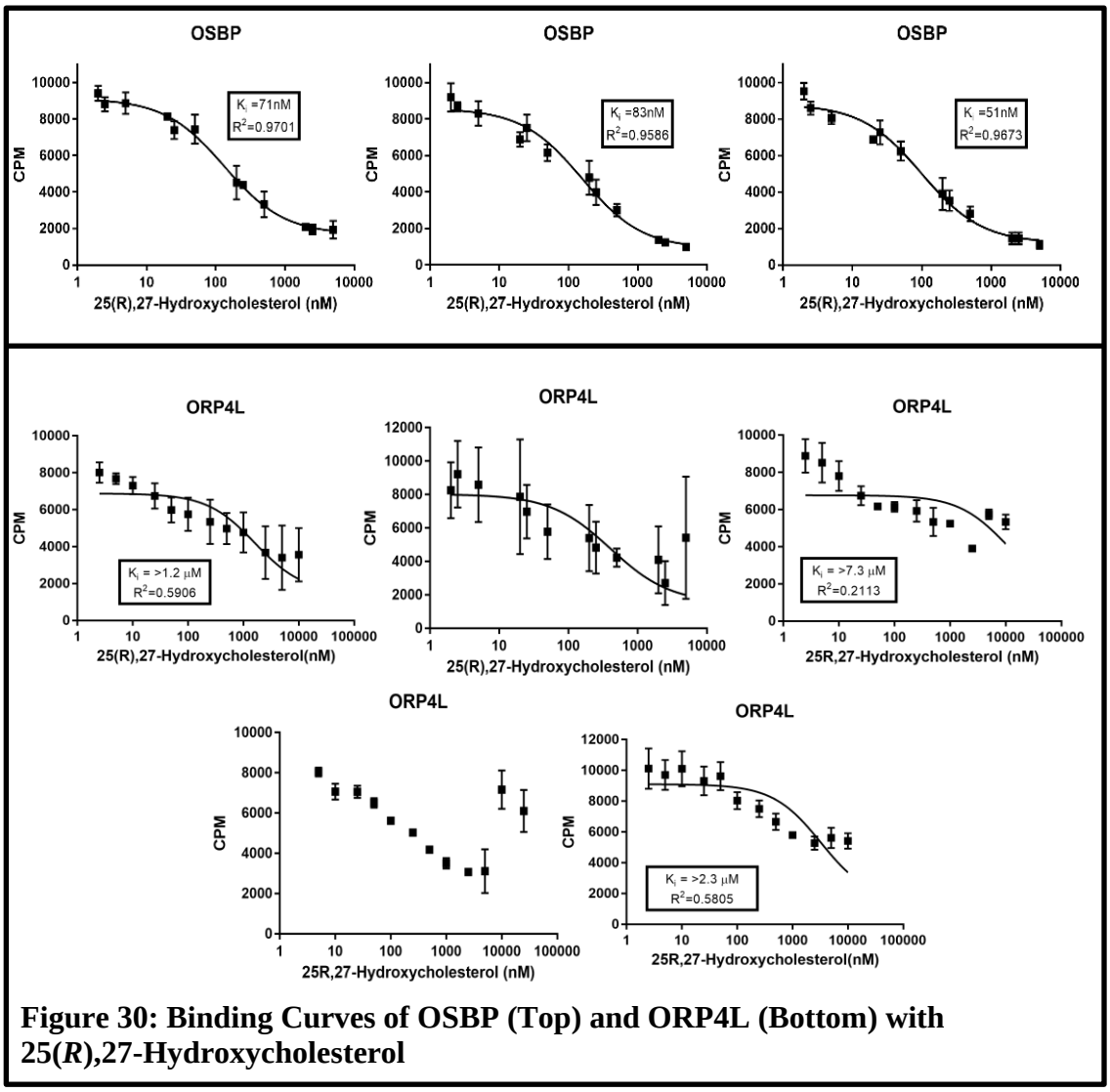

Figure 30: Binding Curves of OSBP (Top) and ORP4L (Bottom) with 25(*R*),27-Hydroxycholesterol

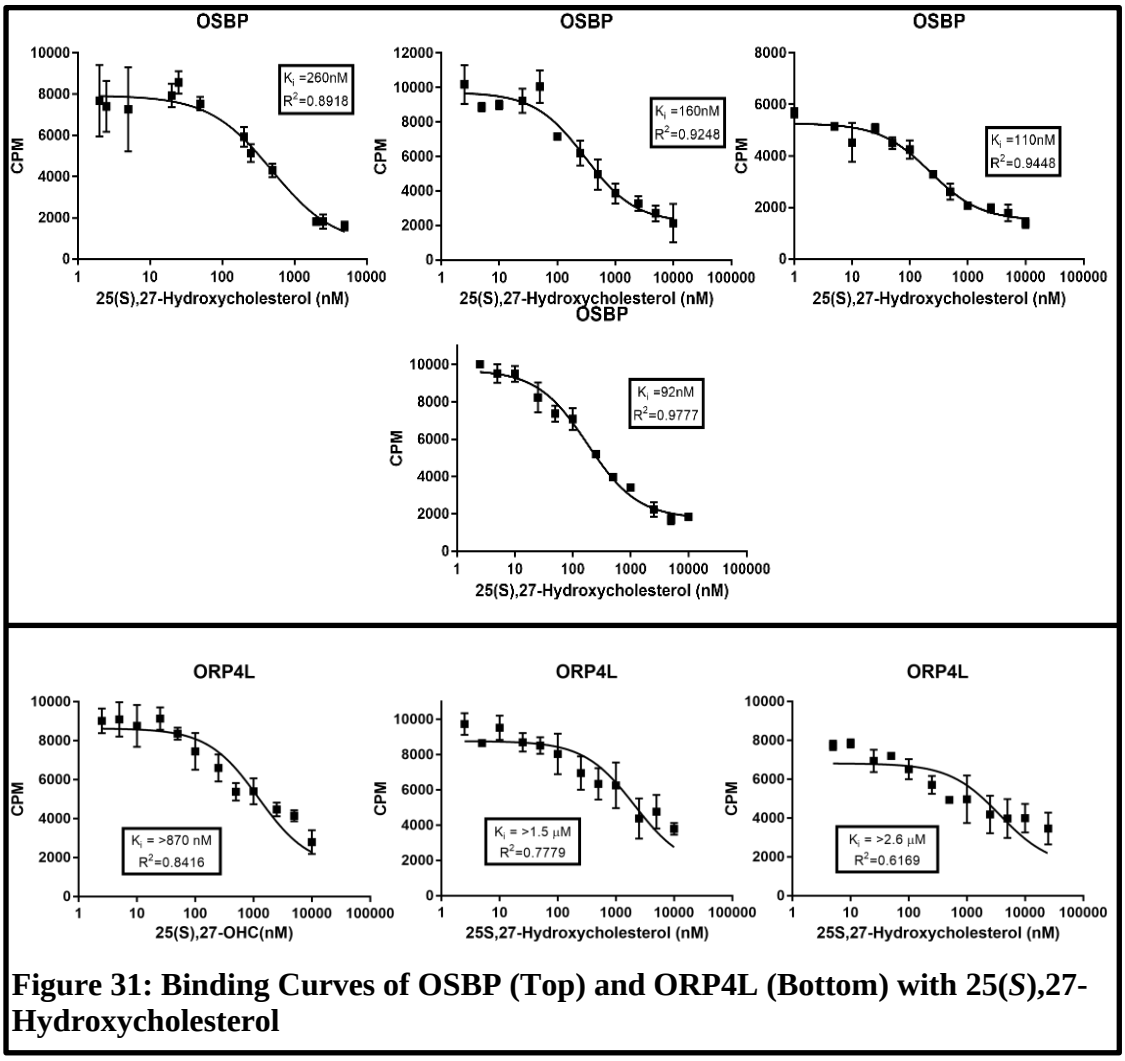

Figure 31: Binding Curves of OSBP (Top) and ORP4L (Bottom) with 25(*S*),27-Hydroxycholesterol

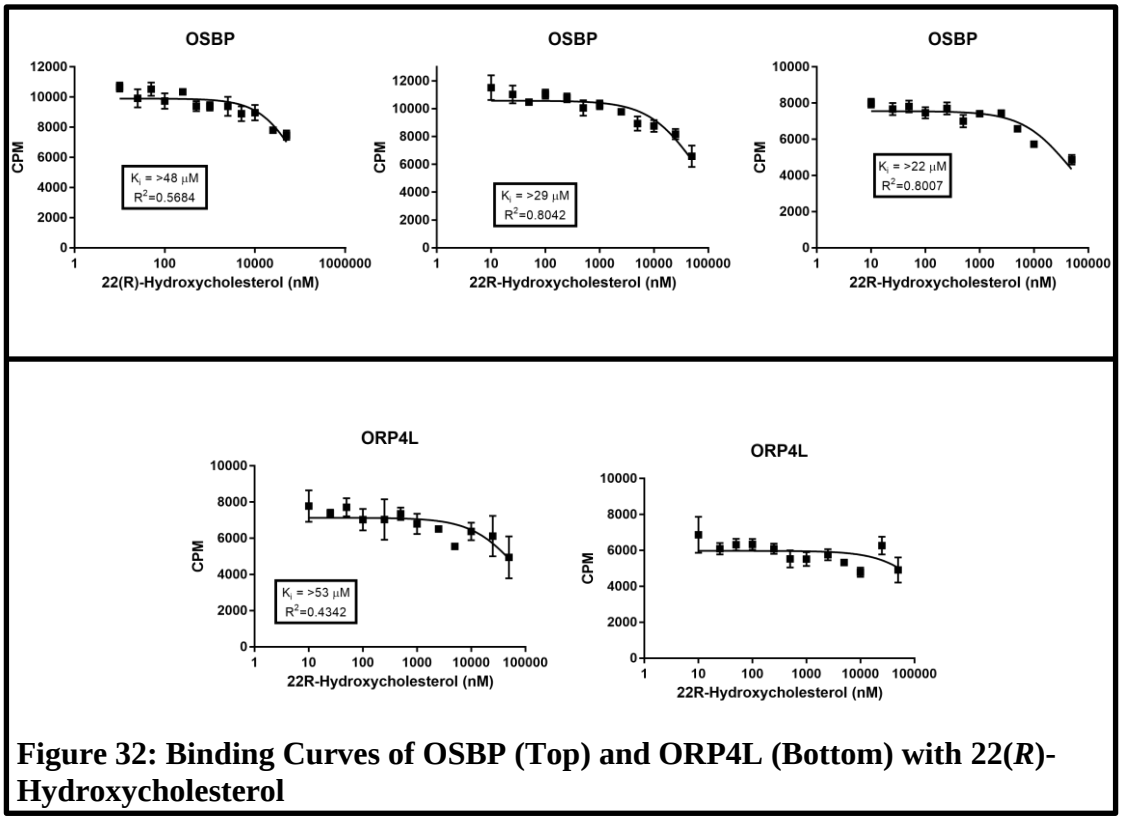

Figure 32: Binding Curves of OSBP (Top) and ORP4L (Bottom) with 22(*R*)-Hydroxycholesterol

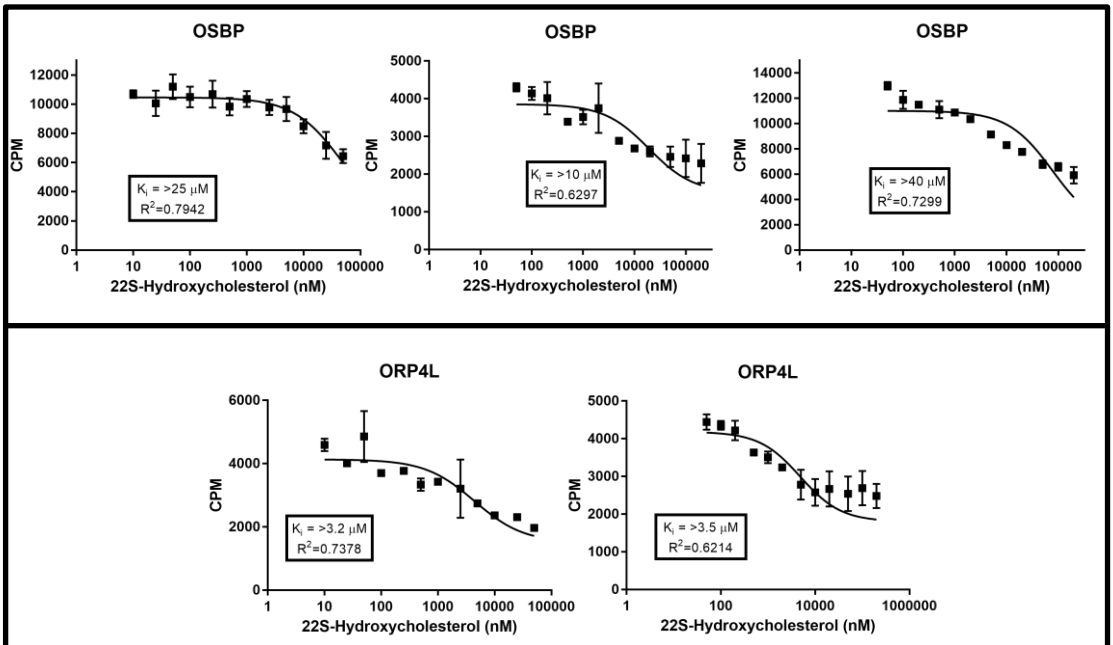

Figure 33: Binding Curves of OSBP (Top) and ORP4L (Bottom) with 22(*S*)-Hydroxycholesterol

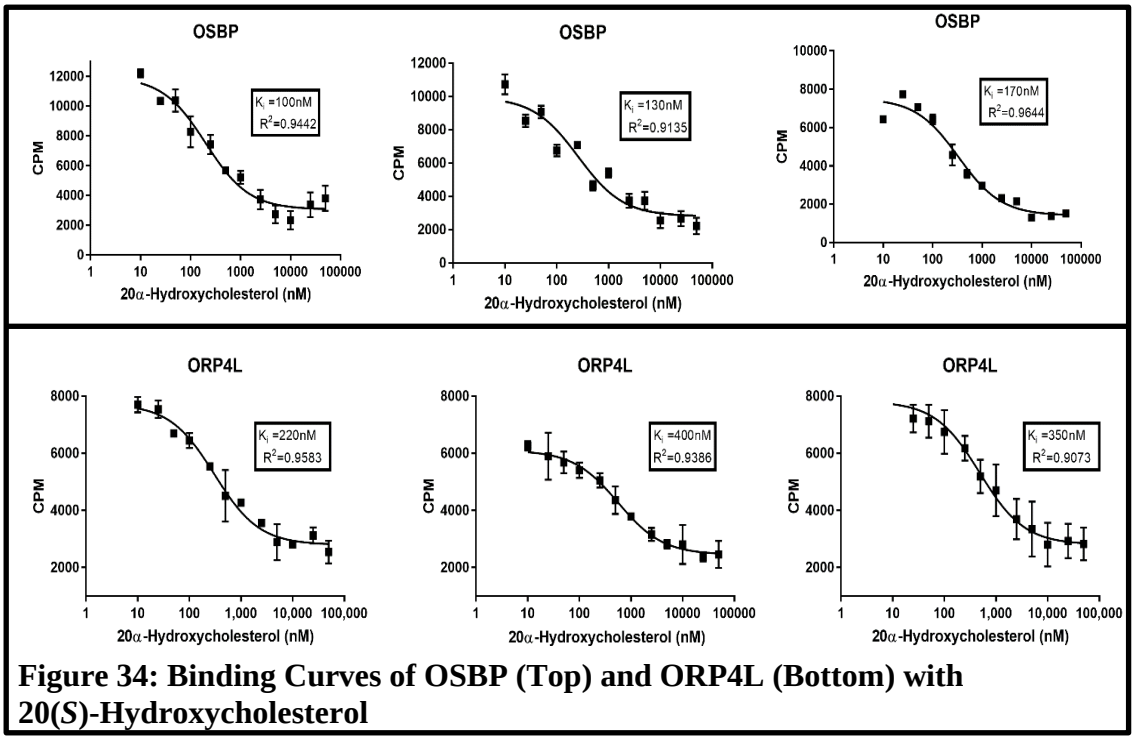

Figure 34: Binding Curves of OSBP (Top) and ORP4L (Bottom) with 20(*S*)-Hydroxycholesterol

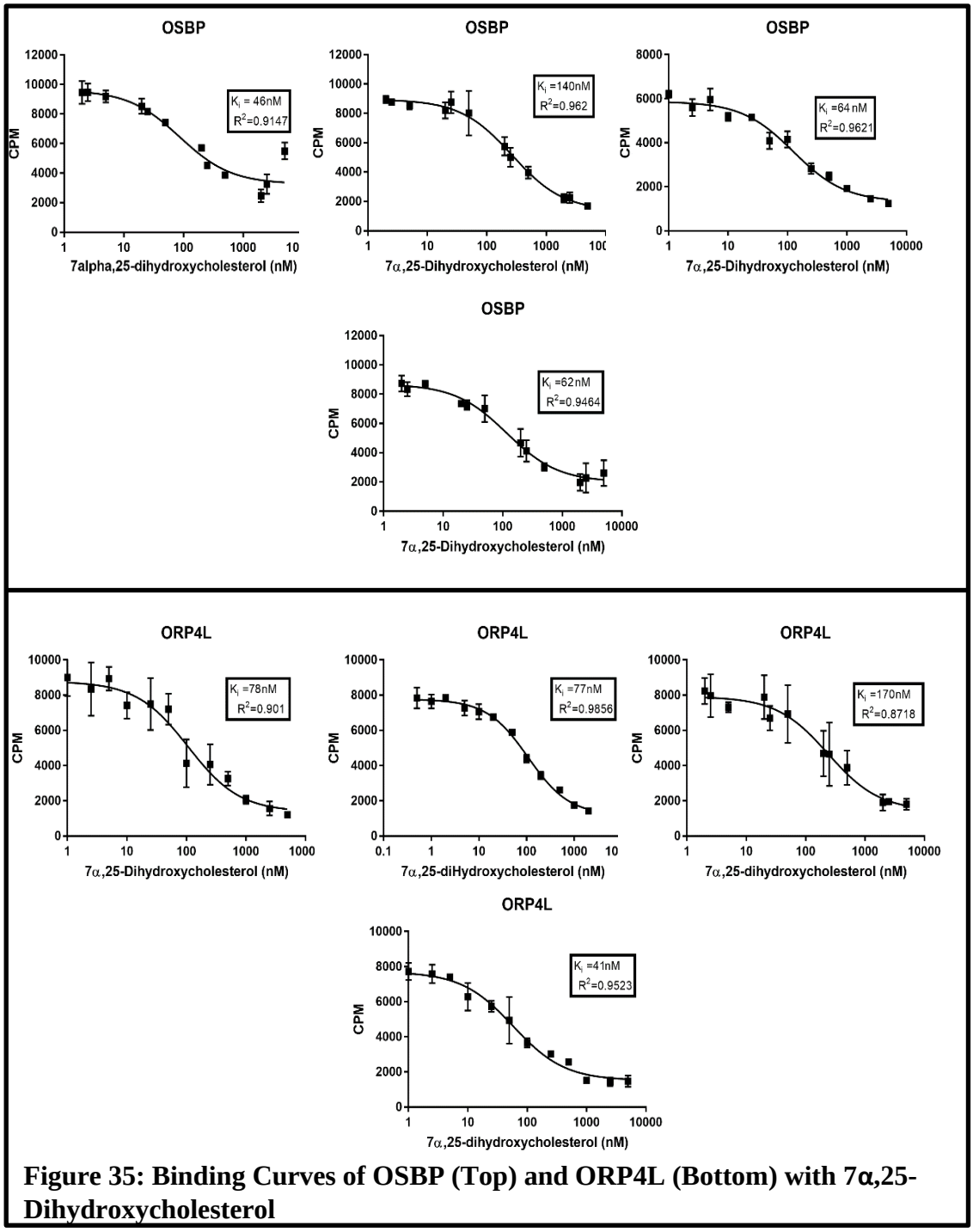

Figure 35: Binding Curves of OSBP (Top) and ORP4L (Bottom) with 7α,25-Dihydroxycholesterol

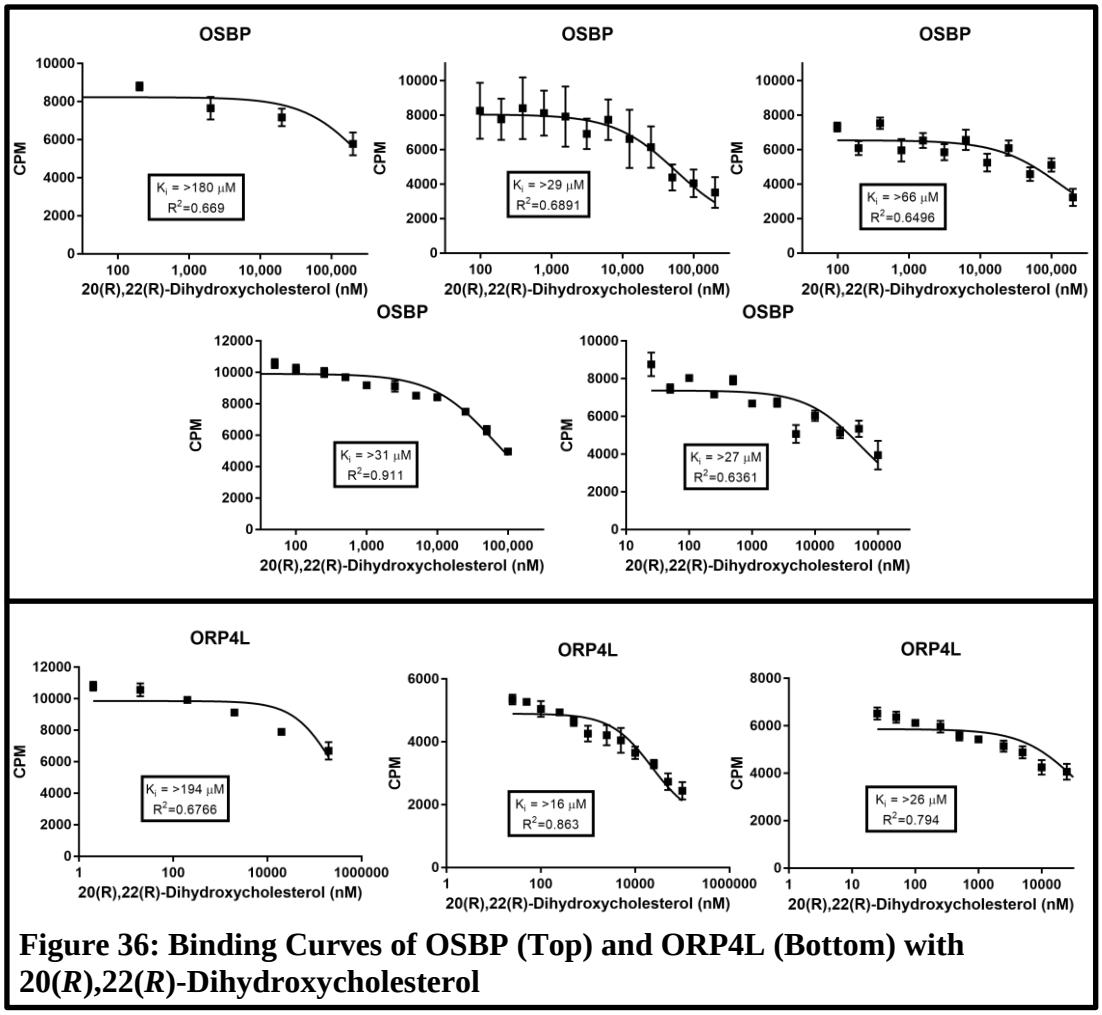

Figure 36: Binding Curves of OSBP (Top) and ORP4L (Bottom) with 20(*R*),22(*R*)-Dihydroxycholesterol

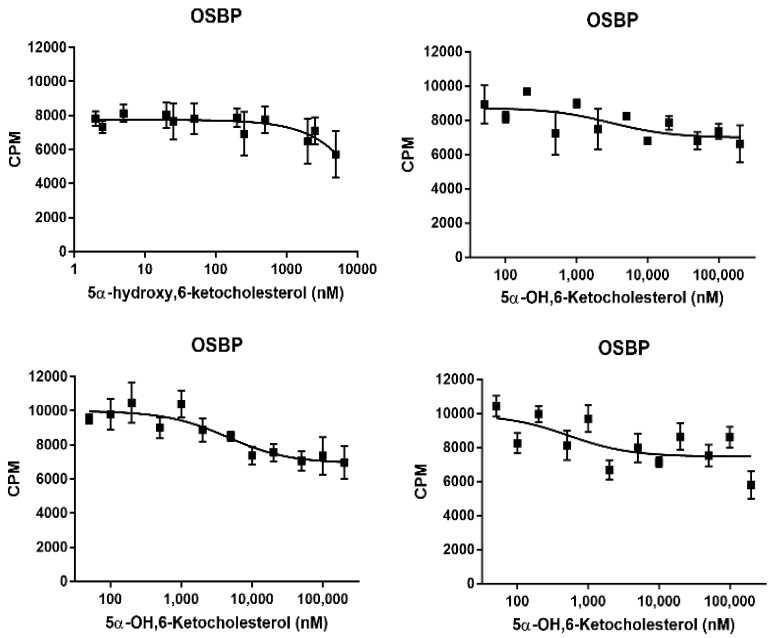

Figure 37: Binding Curves of OSBP with 5α-hydroxy-6-ketocholesterol

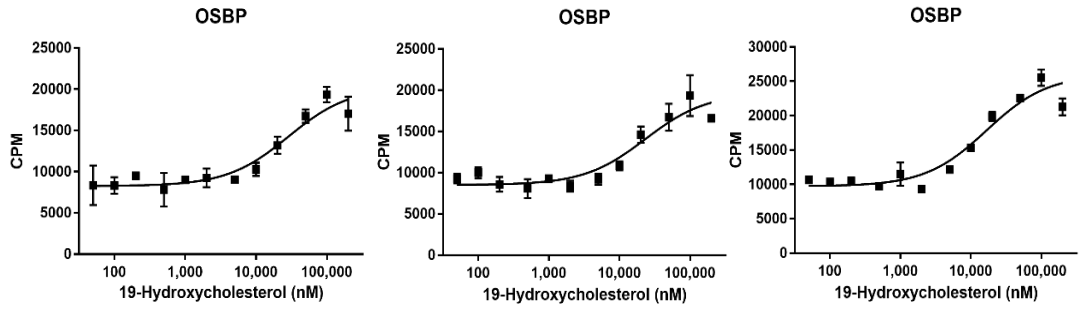

Figure 38: Binding Curves of OSBP with 19-Hydroxycholesterol

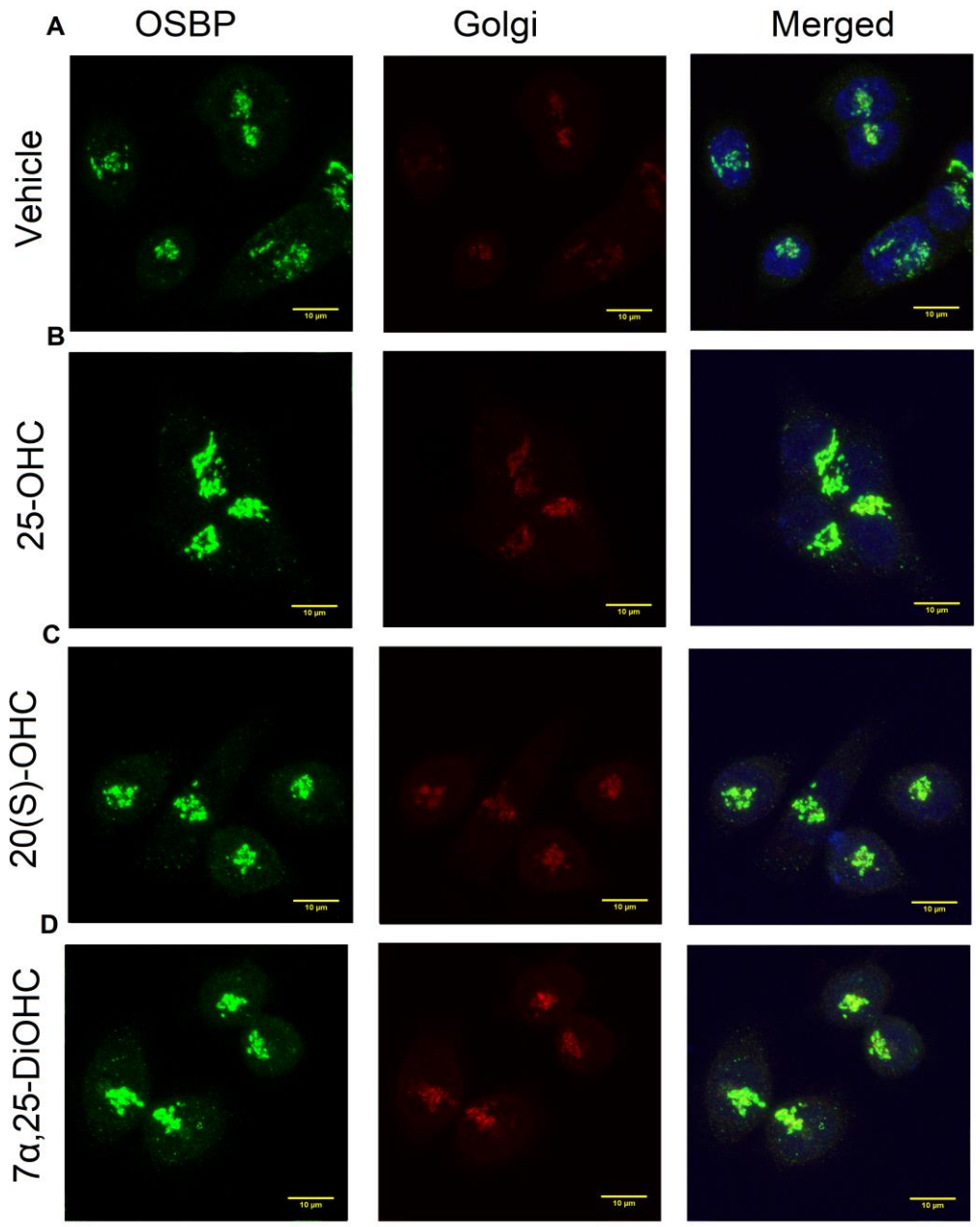

Figure 39: Confocal Immunofluorescence Microscopy Images of HCT-116 Cells

(A-D) OSBP (green) and trans-Golgi (red) were visualized in HCT-116 cells using immunofluorescence microscopy. Cells were treated with vehicle (A), 10μM 25-OHC (B), 10μM 20(*S*)-OHC (C), 10μM 7α,25-DiOHC (D) for 4 hours and then stained using primary antibodies for OSBP (green) and trans-Golgi protein TGN46, followed by secondary staining with fluorescent antibodies. Nuclei (blue) were stained with DAPI. Scale bars are 10 μm.

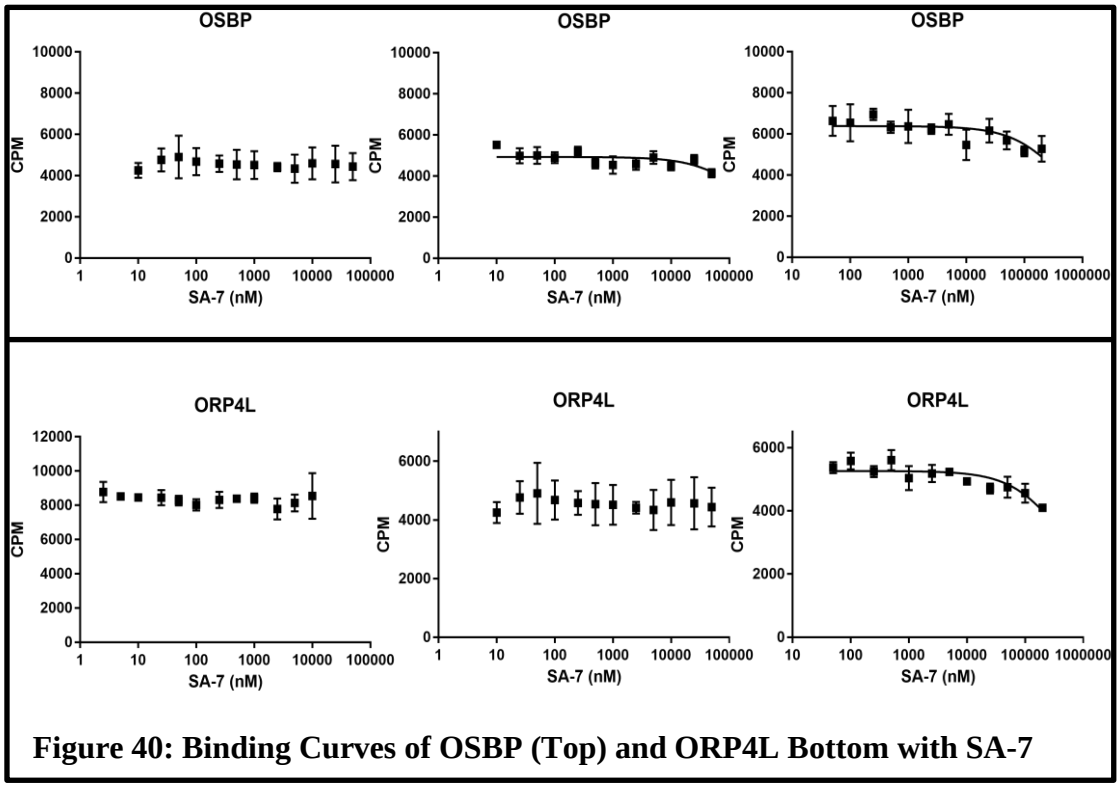

Figure 40: Binding Curves of OSBP (Top) and ORP4L Bottom with SA-7

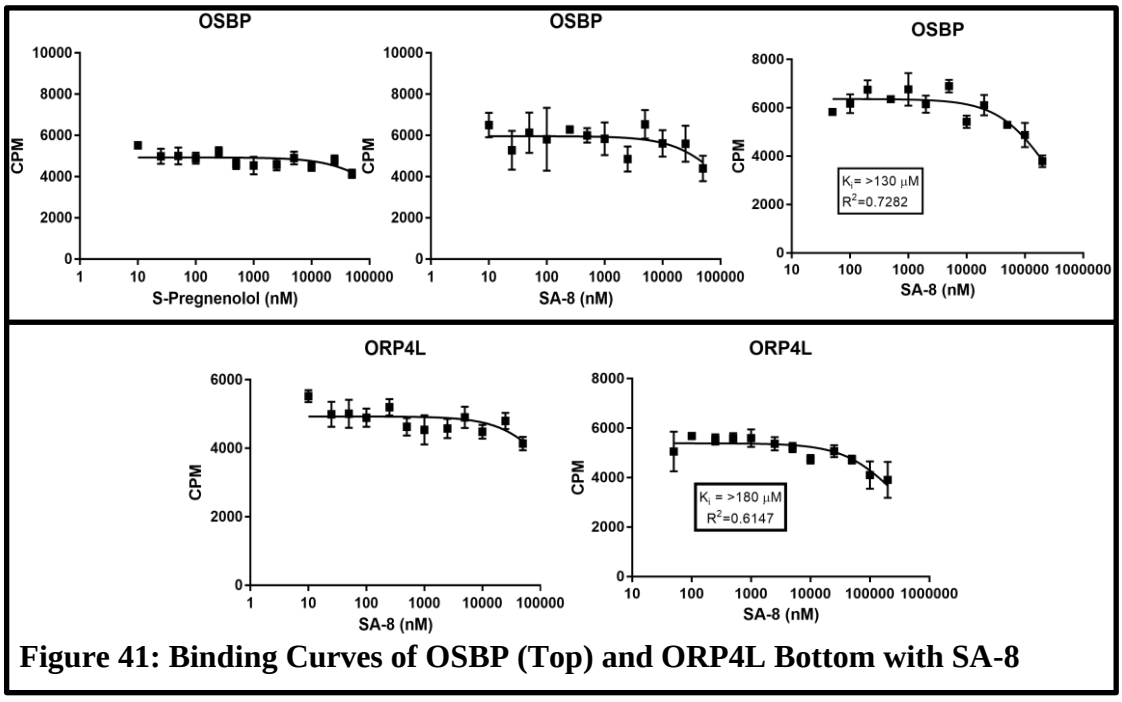

Figure 41: Binding Curves of OSBP (Top) and ORP4L Bottom with SA-8

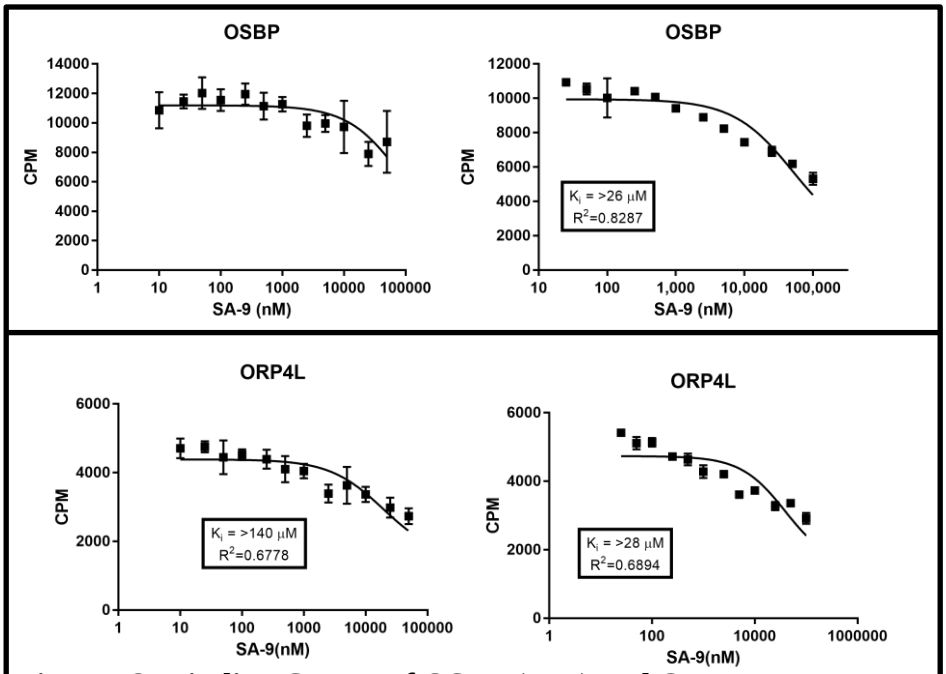

Figure 42: Binding Curves of OSBP (Top) and ORP4L Bottom with SA-9

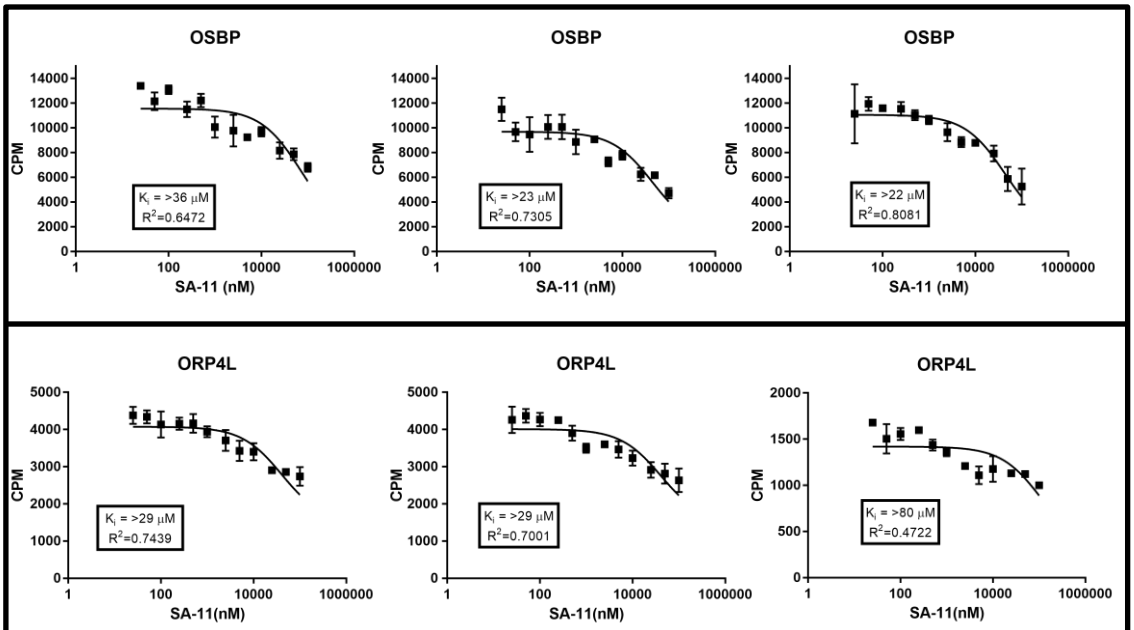

Figure 43: Binding Curves of OSBP (Top) and ORP4L Bottom with SA-11

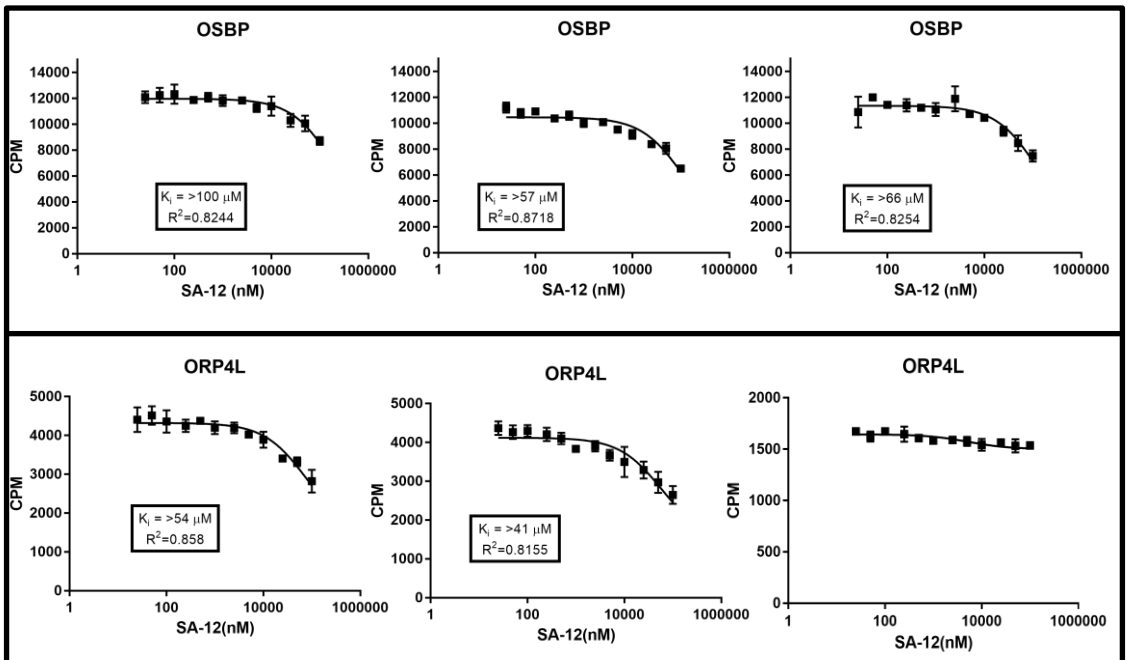

Figure 44: Binding Curves of OSBP (Top) and ORP4L Bottom with SA-12

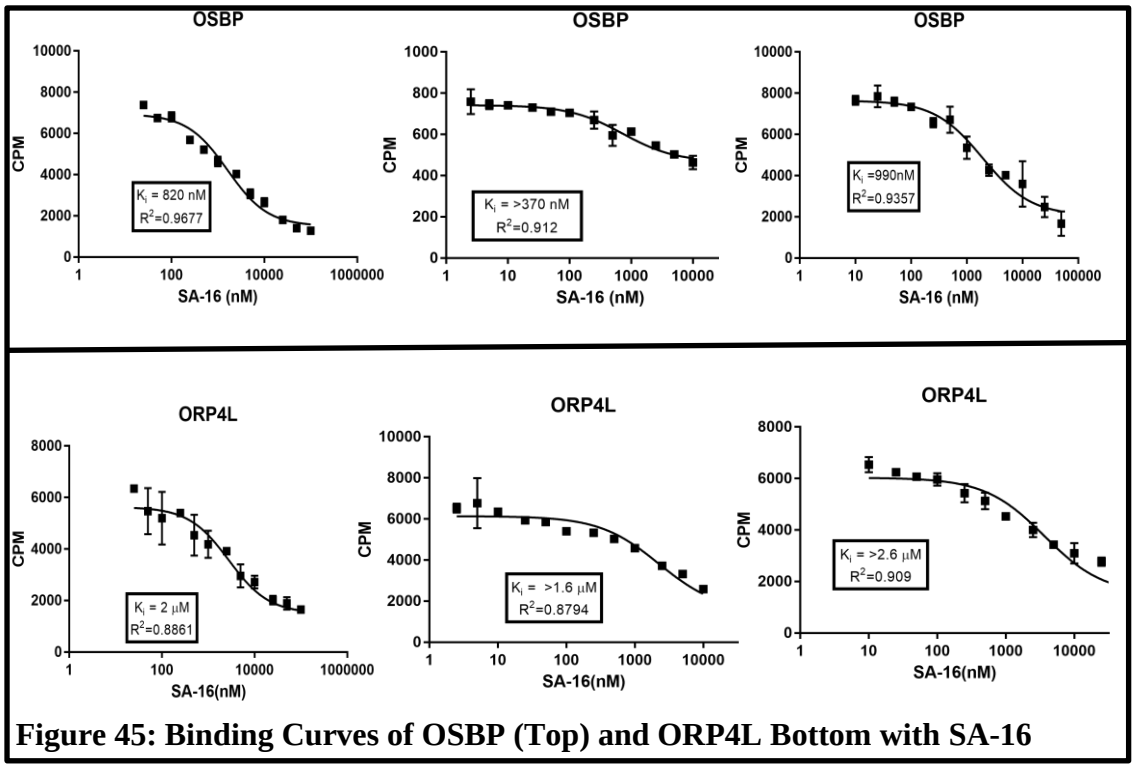

Figure 45: Binding Curves of OSBP (Top) and ORP4L Bottom with SA-16

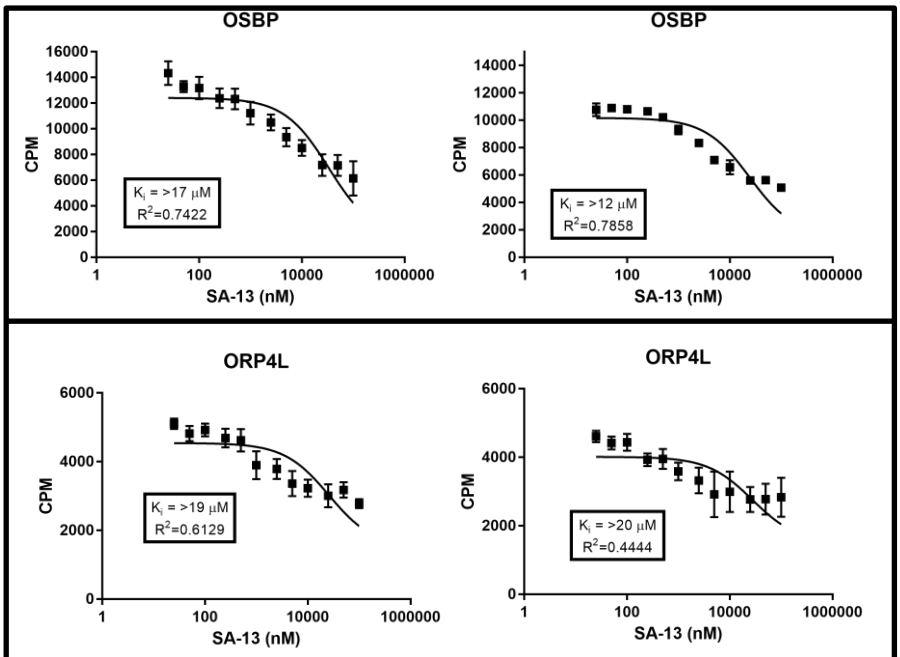

Figure 46: Binding Curves of OSBP (Top) and ORP4L Bottom with SA-13

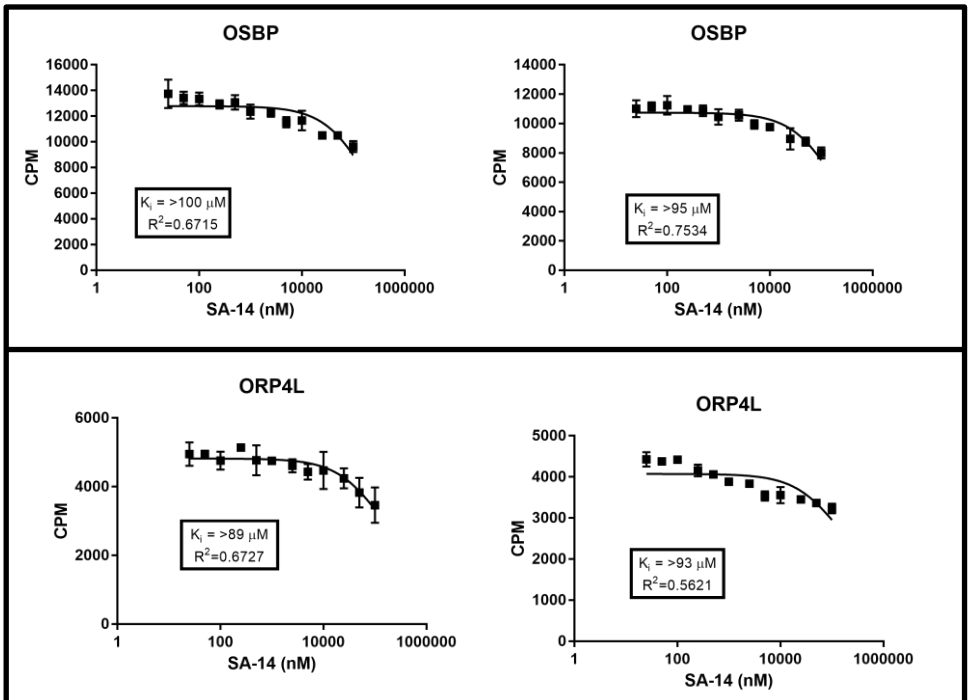

Figure 47: Binding Curves of OSBP (Top) and ORP4L Bottom with SA-14

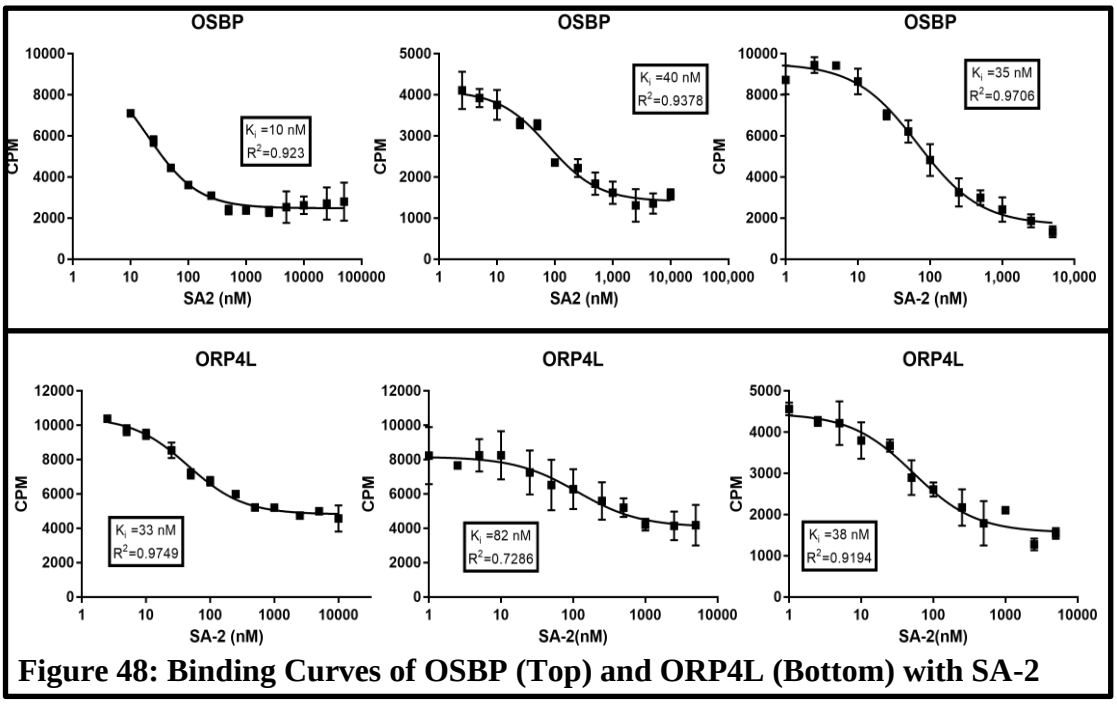

Figure 48: Binding Curves of OSBP (Top) and ORP4L (Bottom) with SA-2

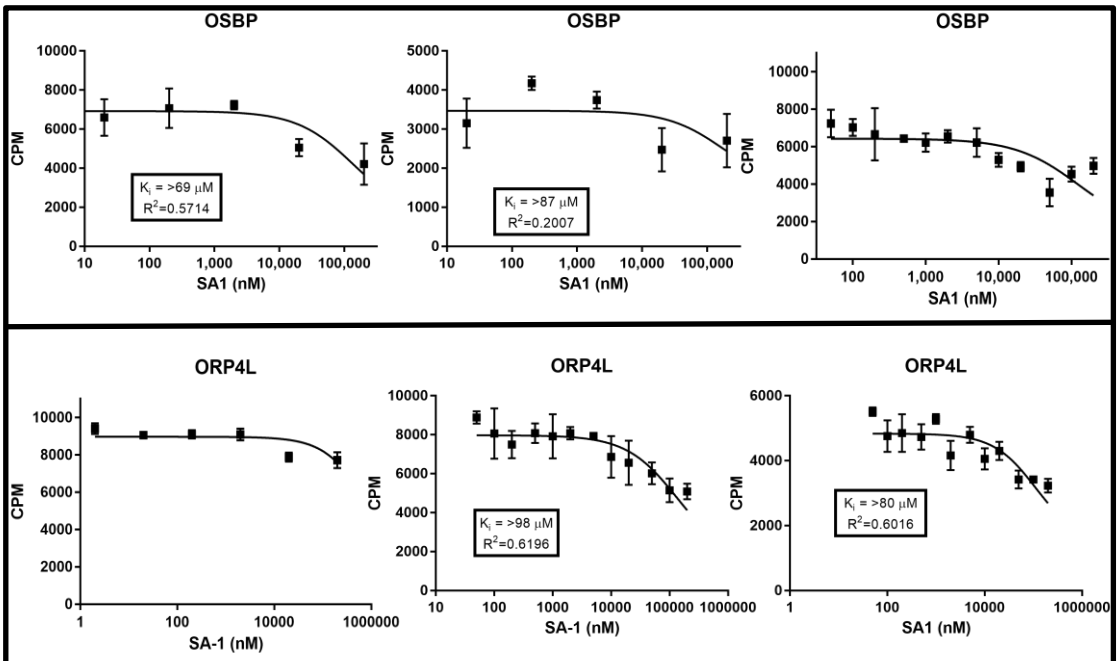

Figure 49: Binding Curves of OSBP (Top) and ORP4L (Bottom) with SA-1

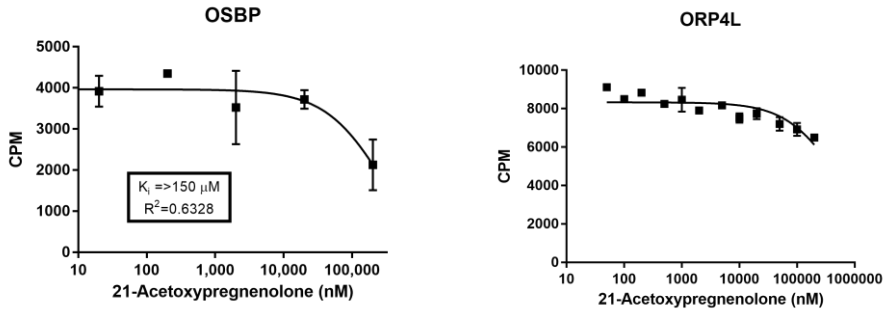

Figure 50: Binding Curves of OSBP and ORP4L to 21-Acetoxypregnenolone

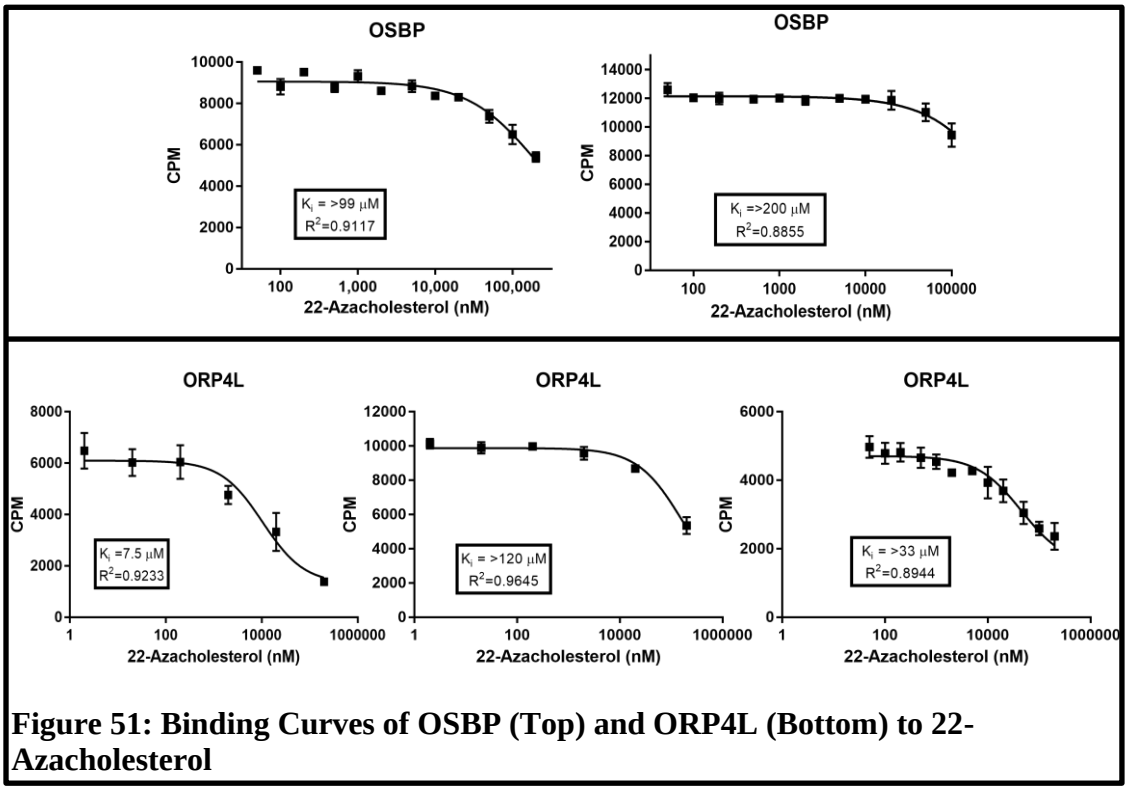

Figure 51: Binding Curves of OSBP (Top) and ORP4L (Bottom) to 22-Azacholesterol

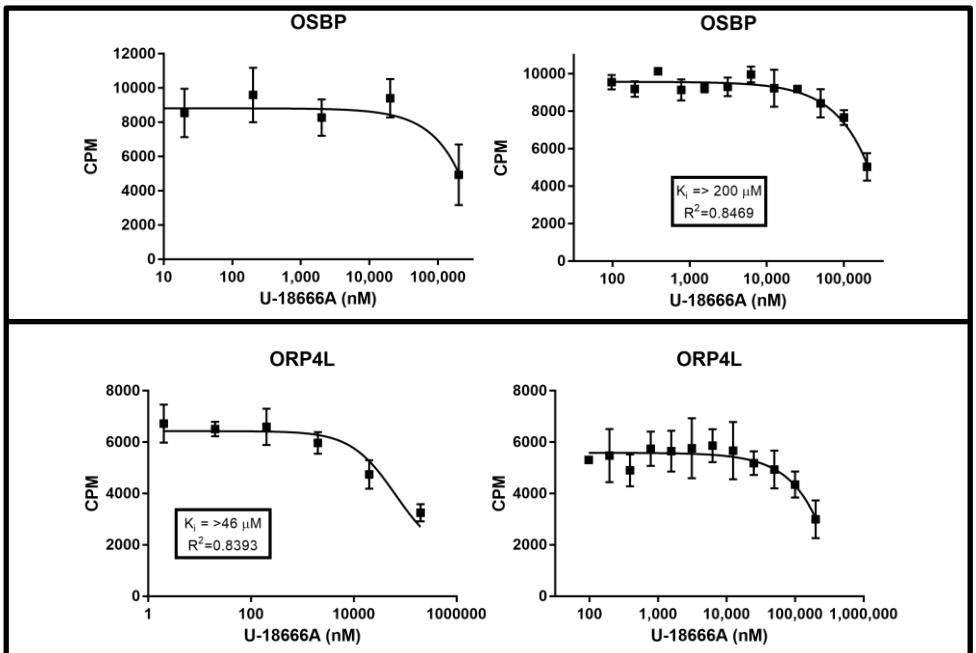

Figure 52: Binding Curves of OSBP (Top) and ORP4L (Bottom) with U-18666A

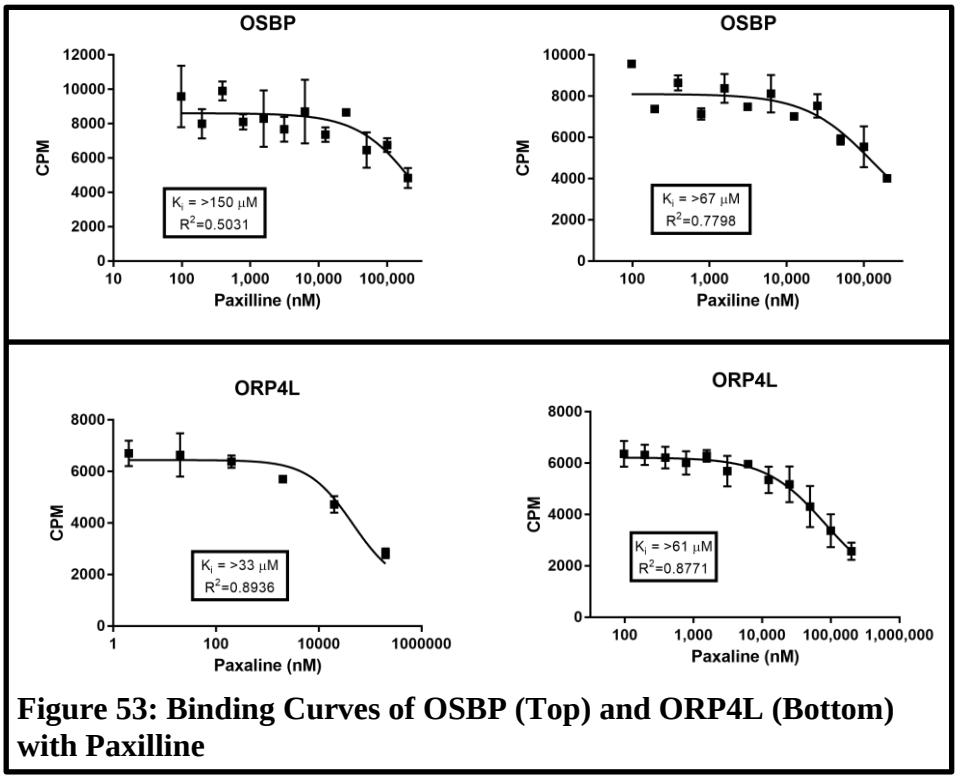

Figure 53: Binding Curves of OSBP (Top) and ORP4L (Bottom) with Paxilline

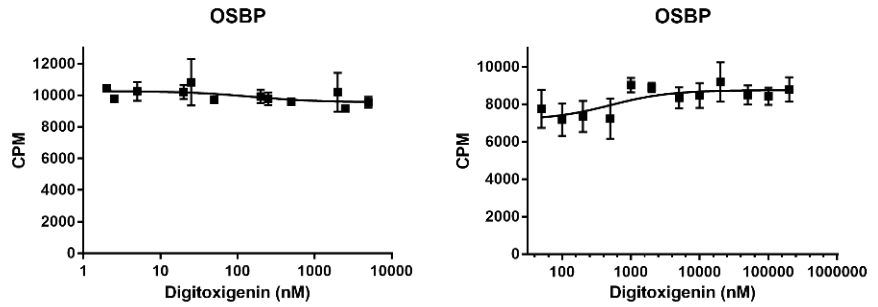

Figure 54: Binding Curves OSBP with Digitoxigenin

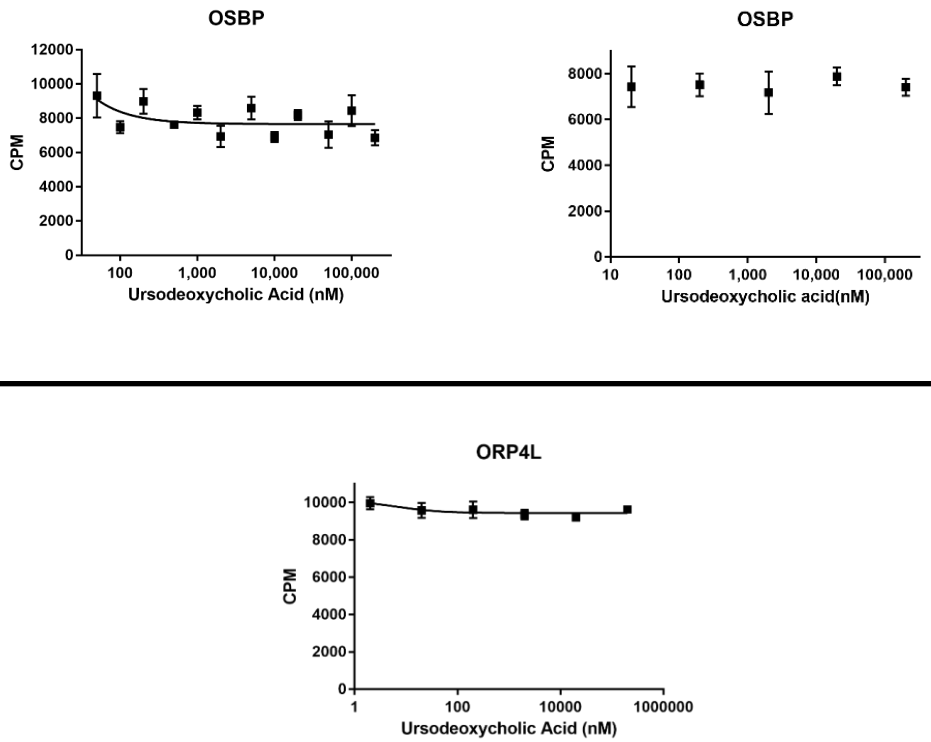

Figure 55: Binding Curves of OSBP (Top) and ORP4L (Bottom) with Ursodeoxycholic Acid

^{1}H NMR (500 MHz, Chloroform-*d*) δ 5.37 (dt, *J* = 5.1, 1.7 Hz, 1H), 4.60 (dddd, *J* = 11.4, 10.2, 6.2, 4.2 Hz, 1H), 2.53 (t, *J* = 8.9 Hz, 1H), 2.37 – 2.27 (m, 2H), 2.24 – 2.14 (m, 1H), 2.12 (s, 3H), 2.03 (s, 3H), 2.02 – 1.96 (m, 0H), 1.91 – 1.83 (m, 2H), 1.73 – 1.53 (m, 5H), 1.53 – 1.40 (m, 3H), 1.28 – 1.10 (m, 3H), 1.01 (s, 3H), 0.63 (s, 3H).

Figure 56: NMR of Pregnenolone Acetate

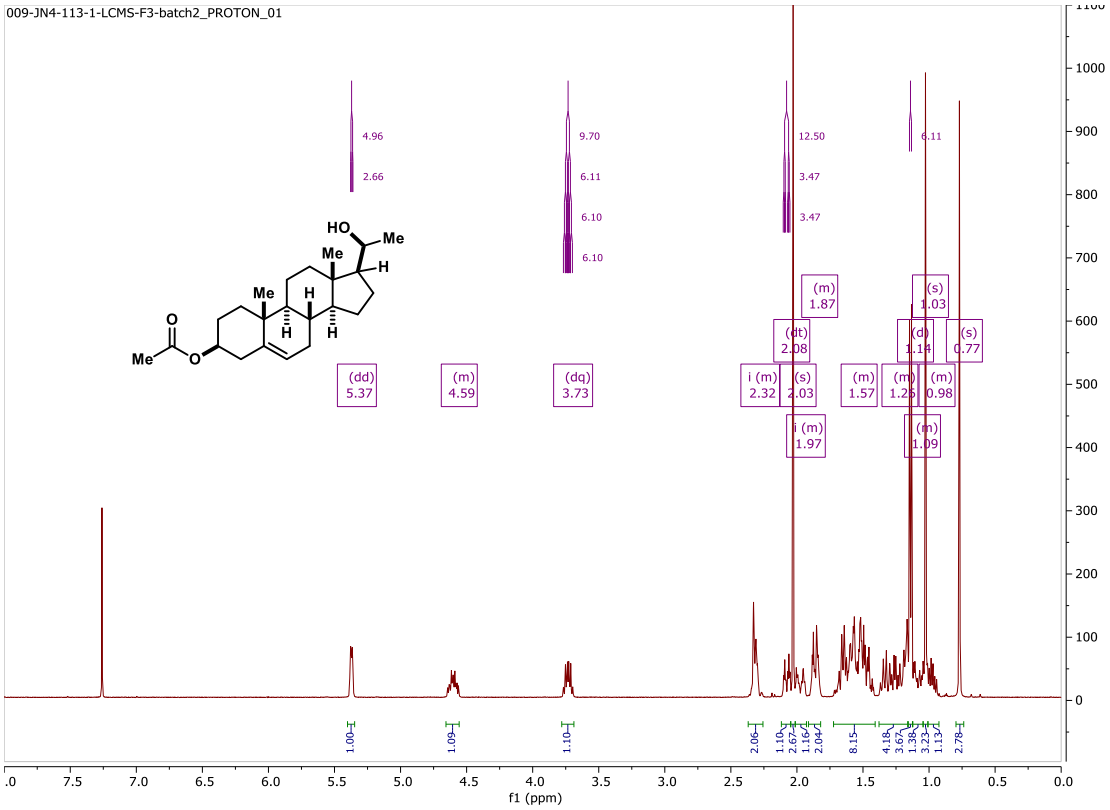

^{1}H NMR (400 MHz, Chloroform-*d*) δ 5.37 (dd, *J* = 5.0, 2.7 Hz, 1H), 4.66 – 4.55 (m, 1H), 3.73 (dq, *J* = 9.7, 6.1 Hz, 1H), 2.38 – 2.25 (m, 2H), 2.08 (dt, *J* = 12.5, 3.5 Hz, 1H), 2.03 (s, 3H), 2.02 – 1.93 (m, 1H), 1.90 – 1.81 (m, 2H), 1.73 – 1.41 (m, 7H), 1.39 – 1.16 (m, 4H), 1.14 (d, *J* = 6.1 Hz, 4H), 1.12 – 1.05 (m, 1H), 1.03 (s, 3H), 1.01 – 0.93 (m, 1H), 0.77 (s, 3H).

Figure 57: NMR of SA-7

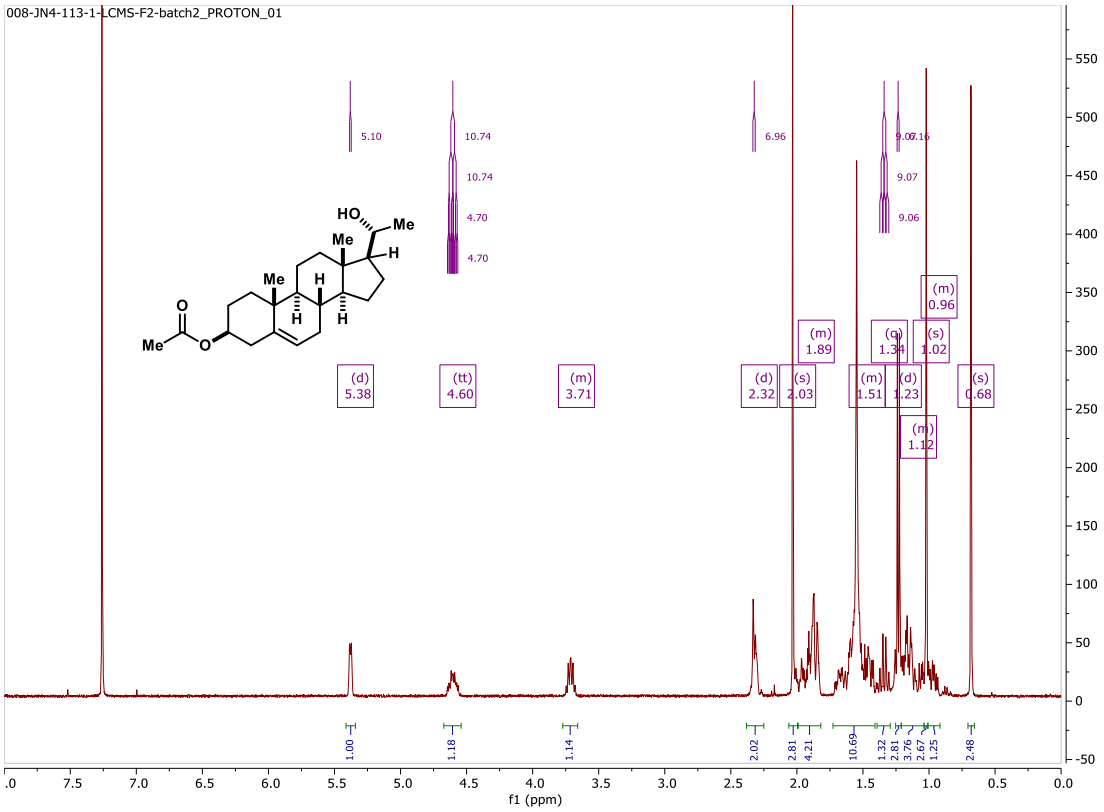

^{1}H NMR (400 MHz, Chloroform-*d*) δ 5.38 (d, *J* = 5.1 Hz, 1H), 4.60 (tt, *J* = 10.7, 4.7 Hz, 1H), 3.78 – 3.66 (m, 1H), 2.32 (d, *J* = 7.0 Hz, 2H), 2.03 (s, 3H), 2.01 – 1.82 (m, 4H), 1.73 – 1.41 (m, 8H), 1.34 (q, *J* = 9.1 Hz, 1H), 1.23 (d, *J* = 6.2 Hz, 4H), 1.20 – 1.04 (m, 3H), 1.02 (s, 3H), 1.00 – 0.92 (m, 1H), 0.68 (s, 3H).

Figure 58: NMR of SA-8